ASSESSMENT OF OXIDATIVE POTENTIAL OF AMBIENT WATER-SOLUBLE AND INSOLUBLE PM2.5

A Dissertation
Presented to
The Academic Faculty

by

Dong Gao

In Partial Fulfillment
of the Requirements for the Degree
Doctor of Philosophy in the
School of Civil & Environmental Engineering

Georgia Institute of Technology
May 2020

ASSESSMENT OF OXIDATIVE POTENTIAL OF AMBIENT WATER-SOLUBLE AND INSOLUBLE PM2.5

Approved by:

Dr. Rodney J. Weber, Thesis Advisor
School of Earth & Atmospheric Sciences
Georgia Institute of Technology

Dr. Nga Lee (Sally) Ng
School of Chemical & Biomolecular Engineering
Georgia Institute of Technology

Dr. James A. Mulholland, Academic Advisor
School of Civil & Environmental Engineering
Georgia Institute of Technology

Dr. Jennifer Kaiser
School of Civil & Environmental Engineering
Georgia Institute of Technology

Dr. Armistead G. Russell
School of Civil & Environmental Engineering
Georgia Institute of Technology

Date Approved: 12/2/2019

ACKNOWLEDGEMENTS

I would like to acknowledge my advisor, Dr. Rodney Weber, for his continuous support and guidance throughout my PhD study. I am truly grateful to him for giving me the opportunity to work in his group. Without his professional, caring, and enthusiastic mentoring, this study would not have been completed. I would also like to thank Dr. James Mulholland for being my academic advisor and helping me successfully fulfill all the degree requirements. I would like to acknowledge my other committee members, Dr. Armistead Russell, Dr. Jennifer Kaiser, and Dr Sally Ng, for serving on my PhD committee and providing invaluable guidance and constructive suggestions for my work.

I would like to thank current and former Weber's group members for their support in my research and their company over the past five years. I appreciate Dr. Ting Fang, Dr. Hongyu Guo, and Linghan Zeng, for their willingness to help whenever I was in trouble. I appreciate Dr. Qian Zhang and Dr. Jenny Wong, for being great meal pals and "agony aunts". I thank Dr. Theo Nah for giving useful career advice. I really appreciate the wonderful moments we have had together.

I'm eternally grateful to my parents and my husband, Chengwei, for standing strong by my side, inspiring and encouraging me to pursue my academic goals. I am so sincerely thankful for their support.

This period of my life was filled with many ups and downs, I want to thank EVERYONE who ever said anything positive to me or taught me something. I heard itall, and it meant something. Finally, thank myself for not giving up and learning to embrace the world bravely.

TABLE OF CONTENTS

LIST OF TABLES

LIST OF FIGURES

LIST OF SYMBOLS AND ABBREVIATIONS

2-VP	2-vinly pyridine
AA	Ascorbic acid
Al	Aluminum
ANOVA	Analysis of Variance
BrC	Brown carbon
Ca	Calcium
COD	Coefficient of divergence
Cr	Chromium
Cu	Copper
CV	Coefficient of variation
DEP	Diesel exhaust particles
DI	Deionized water
DTNB	5,5’- dithiobis-(2-nitrobenzoic acid)
DTT	Dithiothreitol
EC	Elemental carbon
EDTA	Ethylenediaminetetraacetate
EPR	Electron paramagnetic resonance
ESR	Electron spin resonance
Fe	Iron
GR	Glutathione reductase
GSH	Reduced glutathione
GSSG	Oxidized glutathione

GSx	Total glutathione
GT	Georgia Tech
H_2O_2	hydrogen peroxide
HCl	hydrochloric acid
HiVol	High-volume sampler
HULIS	HUmic-Like Substances
HNO_3	nitric acid
IC	Ion Chromatograph
ICP-MS	Inductively Coupled Plasma-Mass Spectrometry
K	potassium
LOD	limit of detection
LWCC	Liquid Wave-guide Capillary Cell
Mg	magnesium
Mn	manganese
Na_2CO_3	sodium carbonate
$NaHCO_3$	sodium bicarbonate
NH_4^+	ammonium ion
NO_3^-	nitrate ion
OC	organic carbon
OM	organic matter
OP	oxidative potential
OP^{AA}	oxidative potential measured by depletion of ascorbic acid
OP^{DTT}	oxidative potential measured by depletion of dithiothreitol
OP^{GSH}	oxidative potential measured by depletion of reduced glutathione
OPm	mass-normalized oxidative potential

$OP^{Total\text{-}DTT}$	total oxidative potential measured by depletion of dithiothreitol
OPv	volume-normalized oxidative potential
$OP^{WI\text{-}DTT}$	water-insoluble oxidative potential measured by depletion of dithiothreitol
$OP^{WS\text{-}DTT}$	water-soluble oxidative potential measured by depletion of dithiothreitol
PAHs	polycyclic aromatic hydrocarbons
PM	particulate matter
$PM_{2.5}$	particulate matter with aerodynamic diameters less than 2.5 µm
PP	polypropylene
PQN	9,10-phenanthrenequinone
ROS	reactive oxygen species
r	Pearson's r
R^2	coefficient of determination
RS	roadside
RTLF	respiratory tract lining fluid
SCAPE	Southeastern Center for Air Pollution and Epidemiology
SEARCH	Southeastern Aerosol Research and Characterization
SO_4^{2-}	sulfate ion
TCA	trichloroacetic acid
TEOM	Tapered Element Oscillating Microbalance
TNB	2-nitro-5-thiobenzoic acid
TOC	total organic carbon
Total-Al	total aluminum
Total-Ca	total calcium
Total-Cu	total copper
Total-Fe	total iron

Total-K	total potassium
Total-Mg	total magnesium
Total-Mn	total manganese
Total-Zn	total zinc
UA	uric acid
WIOC	water-insoluble organic carbon
WIOM	water-insoluble organic matter
WS-Cu	water-soluble copper
WS-Fe	water-soluble iron
WS-K	water-soluble potassium
WS-Mn	water-soluble manganese
WSOC	water-soluble organic carbon
WSOM	water-soluble organic matter
WS-Zn	water-soluble zinc
Zn	zinc

SUMMARY

Oxidative stress has been proposed as a possible mechanism responsible for adverse health effects associated with particulate matter (PM) pollution. Various methods have been developed to measure PM oxidative potential (OP), the potential for particles to generate reactive oxygen species and elicit oxidative stress. But no consensus has been reached as to the best OP assay. Both water-soluble and insoluble PM components contribute to PM OP, but the water-insoluble OP fraction has been less studied. This dissertation aims to characterize water-soluble PM OP measured by different OP assays and water-insoluble OP in terms of temporal variability and chemical determinants. This dissertation provides a direct inter-comparison between two health-relevant OP assays for quantifying OP of ambient particles: the synthetic respiratory tract lining fluid (RTLF) assay and the dithiothreitol (DTT) assay. These assays were used to measure the water-soluble OP of ambient fine PM collected in urban Atlanta over a year-long period. The results show that these assays were driven by different groups of aerosol species. The DTT assay and the ascorbic acid depletion in RTLF were associated with organic species, transition metal ions and the antagonistic interactions between species. The glutathione depletion in RTLF was strongly dependent on water-soluble copper. The OP responses in the RTLF assay were affected by the composition of synthetic lung fluid, which emphasizes the importance of developing a "standard" technique for OP assays.

To develop a method for quantifying total PM OP, we compared three commonly used methods for total OP assessment, involving methanol extraction (1) with or (2) without filtering the extracts, followed by solvent removal and reconstitution with water, and (3)

water extraction without removing the particle-laden filter. The results indicate that performing the OP assay directly on water extracts that still contained the particle-laden filter is a more effective way to capture water-insoluble OP compared to organic solvent extraction. An automated system using programmable syringe pumps was developed based on the DTT assay, facilitating the total OP^{DTT} analysis. The OP analyses clearly demonstrated a measurable OP contribution from water-insoluble PM, which accounted for 20–35 % of total OP. No significant spatial difference in water-insoluble OP fraction was observed between an urban site and a roadside site, suggesting that the insoluble OP contributors were largely secondary. Seasonal trends were found for total and water-insoluble OP^{DTT}, with higher levels in winter than in summer. Correlation analysis shows associations of $OP^{Total\text{-}DTT}$ and $OP^{WI\text{-}DTT}$ with brown carbon (BrC) and total metals, especially total crustal elements. A multivariate regression model was derived for $OP^{Total\text{-}DTT}$, showing that the variability of $OP^{Total\text{-}DTT}$ was primarily affected by BrC, followed by EC, total Cu and the antagonistic interaction between BrC and total Cu. By comparing with $OP^{WS\text{-}DTT}$ model, it was found $OP^{WI\text{-}DTT}$ was related to products of incomplete combustion (e.g., biomass burning) and surface properties of soot and water-insoluble metals.

CHAPTER 1. INTRODUCTION

Increasing concern exists over the adverse effects of air pollution on human health. Air pollution is now considered to be the largest contributor to the global burden of disease from the environment. In accordance with recent estimates by the World Health Organization (WHO), air pollution accounts for 7 million premature deaths every year, and is associated with a number of diseases, ranging from asthma to cancer, pulmonary illnesses and heart disease.

Among the main substances affecting health is ambient particulate matter (PM). PM is a complex, heterogeneous mixture of solids and liquids suspended in the air. It is composed of a variety of chemical components such as black carbon, organic compounds, and trace metals (US Environmental Protection Agency). PM originates from both natural and anthropogenic sources and may be directly emitted (primary particles) or subsequently formed within the atmosphere as a result of chemical reactions (secondary particles). PM has been shown to be associated with human diseases (Anderson et al., 2012).

1.1 Health effects of fine PM

The size of particles is directly linked to their potential for causing health problems. Particles less than 2.5 μm ($PM_{2.5}$ or fine PM) in aerodynamic diameter are of particular concern, as these fine particles can penetrate deep into the lungs, affecting both the respiratory and vascular systems. Epidemiological studies have consistently reported associations between $PM_{2.5}$ and adverse health effects, increased morbidity and mortality (Lippmann, 2014; Norris et al., 1999; Pope et al., 2004; Samet et al., 2000; Sun et al.,

2010). A recent Global Burden of Disease study (Cohen et al., 2017) found that ambient $PM_{2.5}$ was the fifth-ranking mortality risk factor in 2015.

To date, most evidence of health effects of particles has been based on $PM_{2.5}$ mass concentration. While the association between health outcomes and ambient $PM_{2.5}$ concentrations appears robust, the strength of the relationship differs markedly in different studies. It is highlighted in the 2005 WHO Air Quality Guidelines that the excess risk estimates across 38 studies published in the US and Canada ranged from no effect to 7% for a 25 $\mu g/m^3$ $PM_{2.5}$ mass concentration increment (Samet et al., 2005). This heterogeneity was hypothesized to arise from the use of bulk PM mass concentration as an exposure metric.

PM mass is likely to be a crude surrogate for the true harmful entities responsible for adverse effects. This argument is based on the evidence that much of particle mass consists of low-toxicity components, such as sulfate and nitrate (Harrison et al., 2003); in contrast, relatively tiny masses of transition metals and organic species may make a major contribution to PM toxicity (Donaldson et al., 2005). Other than chemical components, some PM physical characteristics including size, surface area and solubility are potential contributors to toxicity (Kelly and Fussell, 2012), which cannot be characterized by PM mass. Moreover, PM mass concentration is insensitive to variation in PM physicochemical characteristics attributable to varying source contributions at a given location (Kunzli et al., 2006). Therefore, there is a need for a more refined metric used in epidemiological and toxicological research to represent the integrated effects of PM.

1.2 Oxidative stress and oxidative potential (OP)

Superoxide radicals (O_2•-), hydrogen peroxide (H_2O_2), hydroxyl radicals (•OH), and singlet oxygen ($^1O_2$) are commonly defined reactive oxygen species (ROS); they are highly reactive due to unpaired electron(s). In biological systems, ROS is generated as metabolic by-products and normally can be neutralized by natural antioxidant defenses. When the presence and formation of ROS or free radicals overwhelms the antioxidant defenses, oxidative stress occurs. Oxidative stress causes damages to cellular structures, such as membranes, lipids, and DNA, and can be responsible for the induction of both chronic and degenerative diseases (Das, 2016; Halliwell, 1994; Pizzino et al., 2017).

The capacity of inhaled PM to elicit oxidative stress has emerged as a hypothesis to explain adverse health effects induced by PM exposure. ROS can be either transported on inhaled particles to the air-lung interface or generated *in vivo* by interaction between deposited redox-active PM components and physiological antioxidants (Lakey et al., 2016). The ability of PM to generate ROS, referred to as oxidative potential (OP), integrates various biologically relevant properties of particles, including size, surface and chemical composition, which may better reflect the biological response to PM exposure and consequently be more informative regarding health effects than PM mass, or specific PM chemical species.

1.3 Acellular assays for OP measurement

Both cellular and acellular assays are available to quantify PM OP (Ayres et al., 2008). Cellular assays generally involve the use of fluorescent probes (such as 2',7'-dichlorodihydrofluorescein diacetate, DCFH-DA) for measuring the PM-induced

intracellular ROS in alveolar macrophages or other cell lines (Landreman et al., 2008; Tuet et al., 2016). The cellular assays may be health-relevant and predictive as they reflect the oxidant-generating properties of PM within a biological microenvironment. However, these assays are laborious, complex, and require long analysis time. Acellular assays, on the other hand, are easier to perform and provide a rapid readout of PM OP. The commonly used acellular assays and their working principles are summarized below.

Depletion of antioxidants: The PM OP is determined by measuring the depletion of antioxidants within a synthetic respiratory tract lining fluid (RTLF), specifically the major low-molecular-weight antioxidants, ascorbic acid (AA), uric acid (UA), and reduced glutathione (GSH) (Kelly et al., 1996; Mudway et al., 2004; Zielinski et al., 1999). RTLF forms an interface between the underlying cells and external environment, and thus constitutes an important defense against PM-induced oxidative damage. The extent to which these antioxidants are depleted by PM with time reflects a direct measure of PM oxidative activity, expressed as OP^{AA}, OP^{UA} and OP^{GSH}.

There is a simplified alternative to AA analysis in RTFL, where only single antioxidant AA is contained in the solution.

Consumption of cellular reductant surrogate: Dithiothreitol (DTT) acts as a chemical surrogate of cellular reductants, such as NADH or NADPH. The redox-active compounds in PM catalyzes the transfer of electrons from the DTT to oxygen, leading to DTT consumption and ROS generation. When this reaction is monitored under conditions of excess DTT, the DTT consumption over time is proportional to the concentration of PM

redox-active species, and thus can be used to assess PM OP (OP^{DTT}) (Cho et al., 2005; Kumagai et al., 2002).

Fluorescent probes: This assay is based on the principle that a fluorescent product is generated when a non-fluorescent probe reacts with ROS. PM OP is quantified by measuring the fluorescence intensity. The common probes used include DCFH probe and chemiluminescent reductive acridinium triggering (CRAT) probe (Venkatachari et al., 2005; Zomer et al., 2011).

ROS generation: Electron paramagnetic/spin resonance (EPR/ESR) with 5,5-dimethylpyrroline-N-oxide as spin trap, measures the ability of PM to induce •OH radicals in the presence of H_2O_2 (Shi et al., 2003a; Shi et al., 2003b).

1.4 Linkage between OP and biological end points

Many epidemiological and clinical studies investigated the associations between OP measures and various biological end points, including biomarkers of oxidative stress and inflammation, pulmonary disease, cardiovascular disease, and mortality. Detailed reviews on the relationships between OP and adverse health effects are given by Bates et al. and Ovrevik et al. (Bates et al., 2019; Ovrevik, 2019). The DTT assay has been shown to be associated with airway inflammation (Janssen et al., 2015; Yang et al., 2016), lung function, cardiovascular disease (Bates et al., 2015; Fang et al., 2016), and asthma/wheeze (Abrams et al., 2017; Bates et al., 2015; Fang et al., 2016; Yang et al., 2016). Mixed associations have been reported for OP^{GSH}. A series of studies conducted in Canada have shown that OP^{GSH} modified the impact of respiratory illness, myocardial infarctions and birth outcomes (Weichenthal et al., 2016a; Weichenthal et al., 2016b; Weichenthal et al.,

2016c). A study in London, however, found no association between OP^{GSH} and all-cause, respiratory, or cardiovascular mortality in all-age adults (Atkinson et al., 2016). By contrast, studies using AA depletion to measure PM OP have almost consistently failed to find associations between OP^{AA} and any health outcomes (Fang et al., 2016; Weichenthal et al., 2016a; Weichenthal et al., 2016b; Weichenthal et al., 2016c). Based on current literature, OP^{DTT} and OP^{GSH} in the RTLF assay are the OP measures most relevant to health.

1.5 Contribution of PM chemical composition to OP

Toxicological studies suggest that PM compounds that are both soluble and insoluble in lung fluids can induce oxidative stress and cause inflammation (Calas et al., 2017).

1.5.1 Water-soluble contribution

OP of water-soluble PM fraction is the focus of most studies applying OP assays since the soluble PM components are considered more bioavailable than the water-insoluble compounds (Calas et al., 2017). Several studies have found that transition metals, especially the water-soluble fractions, are associated with health-response indicators (Campen et al., 2002; Frampton et al., 1999). Transition metals (e.g., copper (Cu), iron (Fe), manganese (Mn), nickel (Ni) etc.) are the group of elements which have unpaired electrons in their valance d-orbital, and they can generate free radical species via redox cycling mechanisms with biological reductants. These metals have been shown to have associations with OP, among which Fe and Cu are considered important in PM-induced formation of ROS through the Fenton reaction (Schwarze et al., 2006; Vidrio et al., 2008).

Some organic compounds in PM, especially quinones and semiquinones, are highly redox-active species that are capable of generating ROS and redox cycling with biological reductants (Kumagai et al., 2002). In general, the semiquinone radical can reduce oxygen to form superoxide. Biological reductants, such as AA, NAD(P)H, and GSH, are able to reduce the oxidized quinoid back the reduced state, enabling the reaction to cycle (Squadrito et al., 2001).

Various studies using many types of OP assays indicate different relationships of the chemical composition with water-soluble PM OP. OP^{DTT} has been found to be sensitive to organic species, such as oxygenated quinones (Cho et al., 2005; Kumagai et al., 2002) and HUmic-Like Substances (HULIS) (Lin and Yu, 2011; Verma et al., 2012), and transition metals (Charrier et al., 2016; Fang et al., 2016; Verma et al., 2015a). OP^{ESR} and OP^{AA} are mostly responsive to metals (Fang et al., 2016; Yang et al., 2014). Antioxidants within the synthetic RTLF appear sensitive to oxidation by different metals. For example, OP^{AA} reacts to iron and OP^{GSH} reacts to aluminum (Godri et al., 2010). But both OP^{AA} and OP^{GSH} are sensitive to copper (Ayres et al., 2008).

1.5.2 Water-insoluble contribution

Studies have shown that water-insoluble fraction of PM also plays an important role in generating oxidative stress (Knaapen et al., 2002; Yi et al., 2014), and the associations between insoluble constituents and OP measures were reported (Daher et al., 2011; Li et al., 2013b; McWhinney et al., 2013; Verma et al., 2012; Yang et al., 2014). Evidence is accumulating to suggest that organic components carried on the soot surface, such as quinones, mediated the toxic effect of insoluble particles (Antinolo et al., 2015). Including

the contributing of water-insoluble species in OP assessment would be closer to actual PM exposure, and thus may better explain the health effects related to PM exposure.

1.6 Motivation and scope of this work

Several assays are available for quantifying OP, but it is not clear which assay is the most suitable as specific assays respond preferentially to different components. There remains a need to compare different assays on identical particle samples. **Chapter 2** presents a comparison of two commonly used acellular OP assays that track the depletion of antioxidants, DTT assay vs. RTLF assay. These assays were used to assess the water-soluble OP of ambient particles collected from urban Atlanta over a one-year period based on daily filter samples. The relationship between the OP metrics and various PM components was investigated using univariate and multivariate regression, which advances our understanding of the major chemical characteristics driving these assays. Previous studies have shown significant associations of these two assays with adverse health outcomes, and thus the comparison is also helpful in explaining the health results and further the understanding of the association between PM and health.

Chapter 3 and **4** focus on assessment and characterization of water-insoluble OP. **Chapter 3** presents a semi-automated system for measuring the total PM OP with the DTT assay. Three approaches for extracting water-insoluble PM fraction were compared, including methanol extraction (1) with or (2) without filtering the extracts, followed by solvent removal and reconstitution with water, and (3) water extraction without removing the particle-laden filter. The water extraction method with the filter remaining in the vial was found to be a more effective way to capture water-insoluble OP and was employed along

with the automated system in the following study (**Chapter 4**) for total OP assessment. In **Chapter 4**, a large data set of water-soluble and total OP^{DTT} were obtained from an urban site, with water-insoluble OP^{DTT} determined by difference. The temporal variations in these OP measures and their associations with PM species were investigated.

CHAPTER 2. CHARACTERIZATION AND COMPARISON OF PM2.5 OXIDATIVE POTENTIAL ASSESSED BY TWO ACELLULAR ASSAYS

Dong Gao, Krystal J. Godri Pollitt, James A. Mulholland, Armistead G. Russell, Rodney J. Weber

Atmos. Chem. Phys. Discuss., in review, 2019

http://doi.org/10.5194/acp-2019-941

2.1 Abstract

The capability of ambient particles to generate *in vivo* reactive oxygen species (ROS), called the oxidative potential (OP), is a potential metric for relating particulate matter (PM) to health effects and is supported by several recent epidemiological investigations. However, studies using various types of OP assays differ in their sensitivities to varying PM chemical components. In this study, we systematically compared two health-relevant acellular OP assays that track the depletion of antioxidants or reductant surrogates: the synthetic respiratory tract lining fluid (RTLF) assay that tracks the depletion of ascorbic acid (AA) and glutathione (GSH), and the dithiothreitol (DTT) assay that tracks the depletion of DTT. Year-long daily samples were collected at an urban site (Jefferson Street) in Atlanta during 2017 and both DTT and RTLF assays were applied to measure the OP of water-soluble $PM_{2.5}$ components. $PM_{2.5}$ mass and major chemical components, including metals, ions, and organic and elemental carbon were also analyzed. Correlation

analysis found that OP as measured by the DTT and AA depletion (OP^{DTT} and OP^{AA}, respectively) were correlated with both organics and some water-soluble metal species, whereas that from the GSH depletion (OP^{GSH}) was exclusively sensitive to water-soluble Cu. These OP assays were moderately correlated with each other due to the common contribution from metal ions. OP^{DTT} and OP^{AA} were moderately correlated with $PM_{2.5}$ mass, with Pearson's r = 0.55 and 0.56, respectively, whereas OP^{GSH} had a significantly lower correlation (r = 0.24). There was little seasonal variation in the OP levels for all assays due to the weak seasonality of OP-associated species. Multivariate linear regression models were developed to predict OP measures from the particle composition data. The models indicated that the variabilities in OP^{DTT} and OP^{AA} were attributed to not only the concentrations of metal ions (mainly Fe and Cu) and organic compounds, but also antagonistic metal–organic and metal–metal interactions. OP^{GSH} was sensitive to the change in water-soluble Cu and brown carbon (BrC), a proxy for ambient humic-like substances.

2.2 Introduction

Epidemiological studies have consistently reported associations between fine particulate matter ($PM_{2.5}$) and increased morbidity and mortality (Brunekreef and Holgate, 2002; Cohen et al., 2017; Lippmann, 2014; Norris et al., 1999; Pope et al., 2004; Samet et al., 2000; Sun et al., 2010; Thurston et al., 2017). The capacity of inhaled particulate matter (PM) to elicit oxidative stress has emerged as a hypothesis to explain PM-induced adverse health effects. Inhaled PM can directly introduce PM-bound reactive oxygen species (ROS) to the surface of the lung where they react with and deplete lung lining fluid antioxidants, or introduce redox-active PM species which can react with biological reductants and

generate ROS *in vivo* (Lakey et al., 2016). The latter can occur in organs beyond the lungs by particles or chemical species being translocated from the lungs throughout the body. Oxidative stress arises when the presence and production of ROS overwhelms the antioxidant defenses, and can lead to cell and tissue damage and induction of chronic and degenerative diseases (Das, 2016; Halliwell, 1994; Pizzino et al., 2017). The ability of PM to generate ROS *in vivo*, referred to as the oxidative potential (OP) of particles, has gained increasing attention as possibly a more integrative health-relevant measure of ambient PM toxicity than $PM_{2.5}$ mass which may contain a mix of highly toxic (e.g. polycyclic aromatic hydrocarbons (PAHs), quinones, and transition metals) to relatively benign (e.g. sulfate and ammonium nitrate) PM components (Frampton et al., 1999; Lippmann, 2014).

A variety of acellular assays have been developed to assess PM OP (Ayres et al., 2008; Bates et al., 2019). In general, these assays involve the incubation of PM extracts or suspension with chemical reagents/probes, and the response is recorded over time or after incubation. The responses recorded include the depletion of reductant surrogate, such as the dithiothreitol (DTT) assay (Cho et al., 2005), and depletion of specific antioxidants in a composite solution, such as a synthetic respiratory tract lining fluid (RTLF) model (Godri et al., 2011; Mudway et al., 2004; Zielinski et al., 1999). In contrast, other assays measure ROS generation (e.g., the dichlorofluorescein assay (Huang et al., 2016; Venkatachari et al., 2005)), or hydroxyl radical formation in the presence of H_2O_2 (e.g., electron paramagnetic/spin resonance (EPR/ESR) (Shi et al., 2003a; Shi et al., 2003b)). The assays based on exposing PM species to antioxidants are currently more commonly used. The DTT assay (Cho et al., 2005) is a chemical system that mimics the *in vivo* PM-catalyzed electron transfer process. In this assay, DTT acts as a surrogate of the cellular reductant

(NADH or NADPH), donating electrons to oxygen and producing ROS with the catalytic assistance of PM redox-active species. PM OP (i.e., OP^{DTT} in this case) is determined by measuring the depletion of DTT over time, which is assumed to be proportional to the concentration of redox-active compounds in PM. For the RTLF assay, RTLF is constructed to simulate the aqueous environment that particles first encounter when inhaled into the lungs and deposited. The antioxidants in RTLF, specifically the major low-molecular-weight antioxidants, ascorbic acid (AA), uric acid (UA), and reduced glutathione (GSH), provide protective defenses against PM-induced oxidative damage. The extent to which they are depleted by PM over time reflects a direct measure of PM oxidative activity by this assay, expressed as OP^{AA}, OP^{UA}, and OP^{GSH} (Kelly et al., 1996; Mudway et al., 2004; Zielinski et al., 1999). Some studies (DiStefano et al., 2009; Fang et al., 2016; Janssen et al., 2015) have used a simplified alternative approach to AA analysis in RTFL, where only the single antioxidant AA is contained in the solution. If not explicitly stated, OP^{AA} in this paper represents OP^{AA} obtained from the RTLF model.

Recently, a number of epidemiological studies have used some of these OP assays to examine the linkage between particle OP and adverse health outcomes. OP^{DTT} of ambient fine particles has been found to be more strongly associated with multiple cardiorespiratory outcomes, such as airway inflammation (Delfino et al., 2013; Janssen et al., 2015; Yang et al., 2016), asthma (Abrams et al., 2017; Bates et al., 2015; Fang et al., 2016; Yang et al., 2016) and congestive heart failure (Bates et al., 2015; Fang et al., 2016), than PM mass. Multiple population-scale studies conducted in Canada employed the RTLF assay to assess OP of $PM_{2.5}$, and found that OP^{GSH} was associated with lung cancer, cardiometabolic mortality (Weichenthal et al., 2016a), emergency room visits for respiratory illness

(Weichenthal et al., 2016c), and myocardial infarction (Weichenthal et al., 2016b). The association between airway inflammation in asthmatic children and OP^{GSH} of $PM_{2.5}$ personal exposure was also reported (Maikawa et al., 2016). However, a human exposure study in the Netherlands did not find an association between OP^{GSH} and acute airway inflammation after 5 h of exposure (Strak et al., 2012). A population-scale study in London found no association between OP^{GSH} and mortality and hospital admission (Atkinson et al., 2016). For the AA depletion by PM assay, either in the composite RTLF model or in a simplified AA-only model, no association with adverse health end points has been found, including cause-specific mortality and cardiorespiratory emergency department visits (Fang et al., 2016; Weichenthal et al., 2016a; Weichenthal et al., 2016b; Weichenthal et al., 2016c). Bates et al. (Bates et al., 2019) provide a review of the relationships of various OP assays with adverse health effects.

The differences in observed health effects may be due to the different sensitivity of OP assays to various PM species. Past studies have shown that specific assays are correlated with different PM components. OP^{DTT} has been found to be sensitive to transition metals (Charrier and Anastasio, 2012; Fang et al., 2016; Verma et al., 2015a) and organic species, especially more oxygenated aromatic organics, such as quinones and hydroxyquinones (Cho et al., 2005; Kumagai et al., 2002; McWhinney et al., 2011; Verma et al., 2015b). OP^{AA} obtained from the simplified AA-only model are mostly responsive to the metal content of PM (Fang et al., 2016; Yang et al., 2014). Antioxidants (AA and GSH) within the synthetic RTLF are responsive to a slightly different group of metals. For example, OP^{AA} responds to iron and OP^{GSH} is related to aluminum (Godri et al., 2010). But both OP^{AA} and OP^{GSH} are sensitive to copper (Ayres et al., 2008). Studies performed on real PM

samples or standard solutions indicate that quinones also drive the oxidative losses of both antioxidants (Ayres et al., 2008; Calas et al., 2018; Kelly et al., 2011; Pietrogrande et al., 2019).

Since different assays capture different chemical fractions of the oxidative activity of PM, it is challenging to synthesize the findings from OP-health studies. There remains a need to compare different assays on identical particle samples to advance our understanding of the effects of PM species on OP measures, and in turn assess the results of the health studies that use OP. In this study, we used two acellular OP assays, DTT and RTLF, to measure the water-soluble OP of ambient $PM_{2.5}$ collected from urban Atlanta over one-year period. These two assays were chosen since they are currently most commonly used and have shown significant associations with adverse health outcomes in some studies. A suite of chemical components was also measured on these samples and univariate and multivariate linear regression analyses were performed to identify and evaluate the contribution of major chemical components to each of these OP metrics.

2.3 Methods

2.3.1 Sampling

Year-long sampling was conducted in 2017 from 1 January to 30 December at the Jefferson Street SEARCH (Southeastern Aerosol Research and Characterization) site (Edgerton et al., 2006, 2005). Jefferson Street is situated roughly 4.2 km northwest of downtown Atlanta and 2.3 km from a major interstate highway and is representative of urban Atlanta region. The site has been extensively used in past studies characterizing urban-Atlanta air quality

(Hansen et al., 2006) and the data used in OP and epidemiological studies (Abrams et al., 2017; Bates et al., 2015; Fang et al., 2016; Sarnat, 2008; Verma et al., 2014).

Ambient fine particles were collected daily (from midnight to midnight, 24 h integrated samples) onto pre-baked 8×10 in. quartz filters (Pallflex Tissuquartz, Pall Life Sciences) using high-volume samplers (HiVol, Thermo Anderson, nominal flow rate 1.13 m^3 min^{-1}, $PM_{2.5}$ impactor). A total of 349 filter samples were collected for analysis; missing days were due to instrumentation issues. The HiVol quartz filters were wrapped in pre-baked aluminum foil after collection and stored at -18 °C until analyses. $PM_{2.5}$ mass concentration was monitored continuously by a tapered element oscillating microbalance (TEOM, Thermo Scientific TEOM 1400a), the sample stream dried at 30 °C using a Sample Equilibration System (Meyer et al., 2000). A Sunset semi-continuous OCEC analyzer (Sunset Laboratory) was used to provide in situ measurements of organic and elemental carbon (OC/EC) content of fine PM. The data were obtained hourly by using 1 h cycles in which the instrument sampled ambient air through an activated carbon denuder for 45 min and analyzed the particles collected on the quartz filter for 15 min using NIOSH 5040 analysis protocol (Birch and Cary, 1996).

2.3.2 Oxidative potential measurements

Two acellular assays, DTT and RTLF assays, were performed to measure the oxidative potential of water-soluble $PM_{2.5}$. The DTT analysis was completed at Georgia Institute of Technology, and all filters were analyzed within one month after collection. The RTLF assay was conducted at Yale University during Oct. 2018. Prior to the OP analyses, a fraction of each HiVol filter (5.07 cm^2 for DTT and 4.5 cm^2 for RTLF) was punched out,

placed in a sterile polypropylene centrifuge vial (VWR International LLC, Suwanee, GA, USA) and then extracted in 5 mL of deionized water (DI, >18 MΩ cm^{-1}) via 30 min sonication. The water extract was filtered through a 0.45 μm PTFE syringe filter (Fisherbrand, Fisher Scientific) and then used for OP analysis.

2.3.2.1 DTT assay

The DTT assay was performed with a semi-automated system developed by Fang et al. (Fang et al., 2015b), following the protocol described by Cho et al. (Cho et al., 2005). In brief, the PM extract (3.5 mL) was incubated with DTT solution (0.5 mL; 1 mM) and potassium phosphate buffer (1 mL; pH~7.4, Chelex-resin treated) at 37 °C. A small aliquot (100 μL) of the mixture was withdrawn at designated times (0, 4, 13, 23, 31 and 41 min) and mixed with trichloroacetic acid (TCA, 1 % w/v) to quench the DTT reactions. After addition of Tris buffer (pH ~8.9), the remaining DTT was reacted with 5,5'-dithiobis-(2-nitrobenzoic acid) (DTNB) to form a colored product which absorbs light at 412 nm. The final mixture was pushed through a 10 cm path length liquid waveguide capillary cell (LWCC; World Precision Instruments, Inc., FL, USA), and the light absorption was recorded by an online spectrometer, which included a UV-Vis light source (DT-mini-2, Ocean Optics, Inc., Dunedin, FL, USA) and a multi-wavelength light detector (USB4000 Miniature Fiber Optic Spectrometer). The DTT consumption rate, used as a measure of OP, was determined from the slope of the linear regression of DTT residual vs. time. Good linearity was found for all samples with correlation coefficients (R^2) larger than 0.98. In parallel with all sample batches, at least one field blank and one positive control (9,10-phenanthraquinone) was analyzed, and their OP values remained constant throughout the analysis. The PM OP measured by this assay (i.e., OP^{DTT}) was blank-corrected and

normalized by the air volume that passed through the extracted filter fraction, expressed as nmol DTT min^{-1} per m^3. This approach did not involve the use of PM samples with constant mass, which is sometimes employed to limit nonlinear DTT response to certain metal ions (Charrier et al., 2016).

2.3.2.2 RTLF assay

The RTLF assay is based on the protocol adopted by Maikawa et al. (Maikawa et al., 2016). PM water extracts were transferred into a 96-well microplate with 180 µL of sample liquid in each well. 20 µL of synthetic RTLF (pH ~7.0) containing equimolar concentrations (2 mM) of AA, UA and GSH was added into each well, resulting in a final starting concentration of 200 µM of antioxidants. The PM-RTLF mixture was incubated in a plate reader (SpectraMax190, Molecular Devices, LLC, San Jose, CA, USA) for 4 hours at 37 °C with gentle mixing. Following incubation, the concentrations of AA and GSH were analyzed immediately. UA concentration was not measured since studies have consistently suggested that no depletion of UA was observed in the presence of PM (Kunzli et al., 2006; Mudway et al., 2004; Zielinski et al., 1999).

AA concentration was determined with the plate reader by measuring the light absorbance at 260 nm. The GSH concentration was indirectly quantified by measuring total glutathione (GSx) and oxidized glutathione (GSSG) concentrations, both compounds determined using the enzymatic recycling method (Baker et al., 1990). The incubated PM-RTLF mixture was diluted 49-fold with 100 mM sodium phosphate buffer (pH ~7.5) containing ethylenediaminetetraacetic acid (EDTA). To measure the GSx concentration, 50 µL of each diluted sample was dispensed onto a microplate. 100 µL of reaction mixture (0.15

mM DTNB, 0.2 mM NADPH and 1 U glutathione reductase (GR)) was added to each well. In the mixture, GSH reacted with DTNB, forming a yellow colored product 5-thio-2-nitrobenzoic acid (TNB) and the mixed disulfide GS-TNB. In the presence of NAPDH and GR, GSSG and GS-TNB were reduced back to GSH, leading to more TNB production. The plate was analyzed on the plate reader for two minutes under constant mixing to continuously monitor the formation of TNB. The TNB formation rate, which is proportional to the GSH concentration, was measured at an absorbance of 405 nm. For GSSG measurement, 5 µL of 2-vinly pyridine (2-VP) was added to 130 µL of the diluted sample to conjugate GSH. The solution was incubated at room temperature for 1 hour, followed by similar procedures performed for the GSx measurement. The GSH concentration was calculated by subtracting two times the GSSG concentration from the measured GSx concentration.

Field blanks and known controls (e.g. positive controls: H_2O_2 and Cu; negative control: Zn) were run in parallel with all sample batches. All samples and controls were measured in triplicate. The percentage of AA and GSH depletion after 4 h incubation for each PM sample was calculated relative to the field blank. PM OP obtained from this assay, i.e., OP^{AA} and OP^{GSH}, was determined by normalizing the percentage loss with the sampled air volume, in unit of % depletion per m^3.

2.3.3 Chemical analysis on PM filters

2.3.3.1 Elemental analysis

Both total and water-soluble trace metals were determined by inductively coupled plasma-mass spectrometry (ICP-MS) (Agilent 7500a series, Agilent Technologies, Inc., CA,

USA), including magnesium (Mg), aluminum (Al), potassium (K), calcium (Ca), chromium (Cr), manganese (Mn), iron (Fe), copper (Cu) and zinc (Zn). For the determination of concentrations of total metals, a 1.5 cm^2 filter punch from the HiVol quartz filter was acid-digested for 20 min using aqua regia (HNO_3+3HCl). The acid-digested sample was then diluted in DI water to 10 mL, filtered with a 0.45 µm PTFE syringe filter. For the analysis of water-soluble metals, no digestion was required. In this case, one circular punch (1 in. diameter) was extracted in 5 mL of DI via 30 min sonication. The extract was filtered using a 0.45 µm PTFE syringe filter, and then acid-preserved by adding concentrated nitric acid (70 %) to a final concentration of 2 % (v/v).

2.3.3.2 Water-soluble organic carbon (WSOC) and brown carbon (BrC)

Two 1.5 cm^2 filter punches from the HiVol filter were extracted in 15 mL DI in a pre-baked glass centrifuge vial (DWK Life Sciences, Rockwood, TN, USA) by 30 min sonication. The extracts filtered with 0.45 µm PTFE syringe filters were used to measure water-soluble organic carbon (WSOC) and its light absorption properties (BrC, used as a source tracer). A fraction (~6 mL) of filter extract was injected by a syringe pump (Kloehn, Inc., NV, USA) into a 2.5 m path length LWCC (World Precision Instruments, Inc., FL, USA), with an internal volume of 500 µL. The absorbance at 365 nm wavelength (BrC) was measured by an online spectrophotometer. The remaining liquid extract was drawn into Sievers total organic carbon (TOC) analyzer (Model 900, GE Analytical Instruments, Boulder, CO, USA) for determination of WSOC concentration. The TOC was calibrated with a series of prepared sucrose standards.

2.3.3.3 Water-soluble ionic species

One 1.5 cm^2 filter punch from the HiVol filter was extracted in 10 mL DI via sonication. The inorganic ions (SO_4^{2-}, NO_3^- , and NH_4^+) in the filtered water extracts were measured by ion-exchange chromatography (IC) with conductivity detection (Anion: Metrosep A Supp 5–150/4.0 anion separation column; eluent: 3.2 mM Na_2CO_3, 1.0 mM $NaHCO_3$, eluent flow rate 0.78 mL/min. Cation: Metrosep C 4–150/4.0 cation separation column; eluent: 1.7 mM HNO_3, 0.7 mM dipicolinic acid, eluent flow rate 0.9 mL/min) with an automated sampler (Dionex AS40, Thermo Fisher Scientific, Waltham, MA).

2.3.4 Multivariate regression models

Multivariate linear regression models were developed to predict OPs based on PM speciation data and investigate the relative importance of species on different OPs. Prior to the regression analysis, the boxplots were used to identify the outliers and test the normality of data. The extreme values (a total of around 3 % of the OP measurements) were removed from the data set. Linear regression was performed between PM components and the various OPs. To simplify the analysis, PM components correlated with OP ($r>0.4$, $p<0.05$) were selected as the independent variables of the models. A stepwise regression was applied to the data set using Matlab R2016a to form the multivariate regression models. To evaluate the performance of the final models, 5-fold cross validation was employed and repeated 50 times. For each OP measure, the average mean-squared error over 50 iterations was within 25 % of the mean OP value (23.4 %, 17.9 % and 12.2 % for OP^{DTT}, OP^{AA} and OP^{GSH}, respectively).

2.4 Results and discussion

2.4.1 Ambient PM composition

Figure 2-1 shows the time series of $PM_{2.5}$ mass concentration and the averaged chemical composition of ambient particles collected at the site. A factor of 1.6 was applied to convert organic carbon to organic matter (Turpin and Lim, 2001; Weber, 2003). Reconstituted mass from measured chemical species agreed well with $PM_{2.5}$ mass measured by the TEOM with Pearson's r=0.84, and accounted for more than 80 % of the $PM_{2.5}$ mass. The missing mass may result from other species not measured, semi-volatile material lost from the filter, and the uncertainty in converting measured carbon mass to organic matter (factor of 1.6 used).

Fractions of various chemical components in $PM_{2.5}$ are consistent with previous observations (Edgerton et al., 2005; Verma et al., 2014). In general, PM mass was dominated by organic compounds (WSOM+WIOM~50 %), followed by inorganic ions (10 % SO_4^{2-}, 4–7 % NH_4^+, and 1–8 % NO_3^-). Metals constituted 6–13 % of the PM mass, among which water-soluble metals were at trace amounts (1–2 %). EC accounted for a small fraction of the PM mass (5–6 %). NH_4^+, and NO_3^-, which are semi-volatile, accounted for a larger fraction of fine particle mass during the cold season. The metal fraction also increased in winter, whereas the fractions of other PM components did not vary significantly during the sampling period.

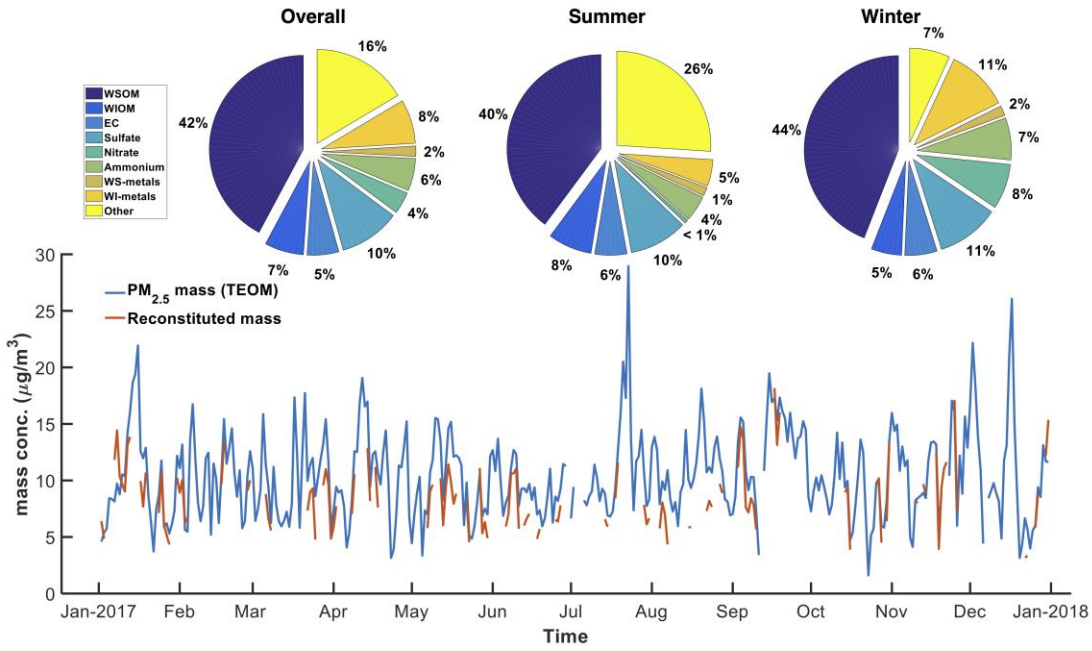

Figure 2-1. Time series of $PM_{2.5}$ mass concentration. The pie charts show the average aerosol composition based on $PM_{2.5}$ mass measured by the TEOM during the whole sampling year, summer and winter. WSOM: water-soluble organic matter (=WSOC*1.6); WIOM: water-insoluble organic matter (=OM-WSOM); WS-metals: sum of water-soluble metals, including Al, Mg, Ca, K, Fe, Cu, Mn, Zn; WI-metals: water-insoluble metals (=total_metals-WS_metals). Summer: Jun–Aug; winter: Jan–Feb and Nov–Dec.

Although insoluble PM components also play an important role in OP (Gao et al., 2017; Verma et al., 2012), this study solely focus on water-soluble OP measurements, and thus the water-soluble PM components are the primary focus in this study.

2.4.2 Association of OP with PM components

Pearson's correlation coefficients for the linear regression between OP and select chemical components are shown in Table 2-1. The detailed correlation matrices for different seasonal periods are given in Table A-1–A-3. We defined the strength of the absolute correlation

coefficient value as strong for values ≥ 0.65, moderate from 0.40 to 0.65, and weak for values < 0.4. The OP assays were moderately inter-correlated over the sampling year. In all cases (whole year and summer or winter), OP^{AA} and OP^{GSH} had the highest correlations, which may in part be due to these measurements being conducted on the same sample extracts. As for OP^{DTT}, the correlations with OP^{AA} and OP^{GSH} varied, but were largely similar. The correlations between the OP measures and various PM components varied, highlighting the different sensitivities of OP assays to various PM components. Note these correlations do not imply that the compounds are responsible for the OP as some of them are not redox active compounds. However, they could be considered as indicators of other compounds simultaneously produced by the same source.

As shown in Table 2-1, OP^{DTT} was correlated with OC and WSOC, indicating a contribution from PM organic compounds. The correlations between OP^{DTT} and certain water-soluble metals, such as Fe, Cu and Mn, were also observed. A moderate correlation of EC with OP^{DTT} (r=0.51) and somewhat with metals and OC (r=0.55, 0.43 and 0.83 for Fe, Mn and OC, respectively; Table A-1) suggests that incomplete combustion could be one of their common sources. The associations of OP^{DTT} with PM species are consistent with a number of previous studies (Fang et al., 2016; Fang et al., 2015b; Verma et al., 2014; Yang et al., 2014), though the correlations in our work were weaker (r > 0.5 compared with r>0.65 in other studies).

Table 2-1. Pearson's r between OP and PM composition

	Overall			Summer			Winter		
	OP^{AA}	OP^{GSH}	OP^{DTT}	OP^{AA}	OP^{GSH}	OP^{DTT}	OP^{AA}	OP^{GSH}	OP^{DTT}
OP^{GSH}	**0.67****			**0.78****			0.62**		
OP^{DTT}	0.61**	0.45**		**0.66****	**0.70****		0.53**	0.50**	
$PM_{2.5}$ mass	0.56**	0.24**	0.55**	0.23*	0.19	0.49**	**0.70****	0.36**	0.54**
OC	0.50**	0.10	0.55**	0.16	0.03	0.40**	0.61**	0.26**	0.50**
EC	0.49**	0.13*	0.51**	0.11	0.01	0.39**	0.60**	0.28**	0.44**
WSOC	0.55**	0.19**	0.52**	0.24*	0.20	0.41**	**0.66****	0.38**	0.54**
BrC	0.36**	0.04	0.41**	0.33**	0.14	0.51**	0.51**	0.33**	**0.69****
SO_4^{2-}	0.41**	0.37**	0.34**	0.42**	0.35**	0.48**	0.33**	0.27**	0.18*
WS-K	0.49**	0.30**	0.50**	0.32**	0.08	0.46**	0.52**	0.33**	0.56**
WS-Fe	0.47**	0.17**	0.50**	0.43**	0.21	0.59**	0.52**	0.24**	0.48**
WS-Cu	0.50**	**0.74****	0.36**	0.51**	**0.79****	**0.65****	0.60**	**0.78****	0.31**
WS-Mn	0.38**	0.19**	0.37**	0.34**	0.13	0.61**	0.49**	0.28**	0.37**
WS-Zn	0.31**	0.31**	0.34**	0.32**	0.11	0.46**	0.41**	0.14	0.31**

Note: **p-value<0.01; *p-value<0.05. Correlations not statistically significant (p>0.05) are in grey, r>0.65 are bold. All metals listed are water-soluble metals.

Similar to OP^{DTT}, OP^{AA} was moderately correlated with OC, WSOC and water-soluble metals, mainly Fe and Cu (r=0.47–0.55). The results are compared with a previous study conducted in the same Atlanta region by Fang et al. (Fang et al., 2016) wherein a simplified AA assay was applied to assess water-soluble OP of $PM_{2.5}$. The AA depletion in the AA-only model was found to be strongly correlated with water-soluble Cu with Pearson's r >0.65, and associations with WSOC (or BrC) and metals were also observed. The weaker sensitivity of AA to water-soluble Cu observed in our study is possibly due to the reactivity hierarchy existing within the antioxidant model with GSH>AA>> UA (Zielinski et al., 1999). This is further supported by other studies. In the study of Charrier et al. (Charrier and Anastasio, 2011), ligand speciation modeling indicated that GSH was a stronger ligand compared to AA and caused a dramatic shift in Cu speciation by forming Cu–GSH

complexes. The experimental results in the study of Pietrogrande et al. (Pietrogrande et al., 2019) showed that the response of the acellular AA assay was strongly dependent on the composition of synthetic RTLF used and the presence of GSH and UA would lower the sensitivity of AA response to Cu. The correlations of organics and EC which comprised a large fraction of PM mass (Fig. 2-1), with OP^{DTT} and OP^{AA}, likely account for the OP^{DTT} and OP^{AA} correlations with PM mass.

In contrast to OP^{DTT} and OP^{AA}, OP^{GSH} was found to be exclusively correlated with water-soluble Cu with Pearson's r >0.7. The consistent lower correlation of OP^{AA} with water-soluble Cu than OP^{GSH} with Cu, is consistent with GSH outcompeting AA in the RTLF in forming Cu complexes. The results are also consistent with other studies (Aliaga et al., 2010; Ayres et al., 2008; Godri et al., 2011).

The correlations differed by seasons. In winter, OP^{AA} and OP^{DTT} were more correlated with organic species, with stronger associations with WSOC, BrC and K, indicating biomass burning as a common source of OP^{AA} and OP^{DTT}. In summer, all OP assays tended to be metal-driven. OP^{AA} and OP^{DTT} were more correlated with Cu, along with SO_4^{2-}, suggesting possible influence of secondary processing on metal mobilization (Fang et al., 2017a; Ghio et al., 1999) and resulting in a strong inter-correlation between different OP metrics.

2.4.3 Temporal variation

The time series of the monthly averages of different OP measures are shown in Fig. 2-2. Significant seasonal variability in these OP measures was not evident; only a subtle seasonal variation observed for OP^{DTT} and no variations for OP^{AA} and OP^{GSH}. OP^{DTT} was slightly higher during the cold period (Jan–Feb and Nov–Dec) with an average level of

0.24±0.08 nmol min^{-1} m^{-3} compared to 0.20±0.04 nmol min^{-1} m^{-3} in the warm period (May–Aug) and a median OP^{DTT} ratio between two periods of 1.20. However, OP^{AA} and OP^{GSH} had more similar levels across seasons, with median ratios between cold and warm periods of 1.10 and 0.97, respectively.

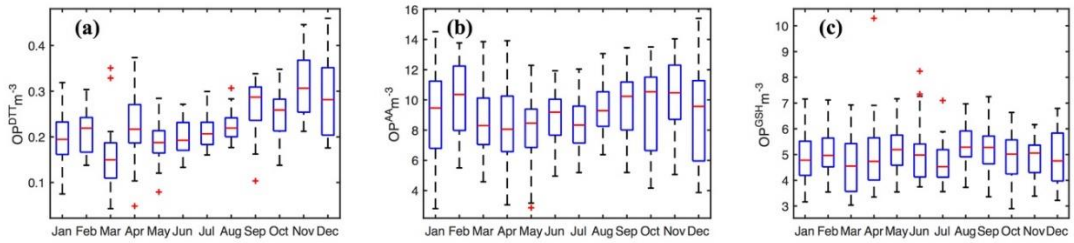

Figure 2-2. Temporal variation for (a) OP^{DTT} m^{-3} (nmol min^{-1} m^{-3}), (b) OP^{AA} m^{-3} (% depletion of AA m^{-3}), and (c) OP^{GSH} m^{-3} (% depletion of GSH m^{-3}).

The seasonality in OP measures should result from the temporal variations in PM species driving the various OP. From the temporal variation of the OP-associated species shown in Fig. 2-3, BrC had an obvious seasonality, higher in winter and lower in summer, which is due to the stronger influence of biomass burning in winter. The variation in BrC may lead to the small variation in OP^{DTT}, considering the good correlation between OP^{DTT} and BrC in winter. Water-soluble Cu is slightly higher in mid-summer and water-soluble Fe is slightly higher in fall, but these trends are not seen in the various measures of OP.

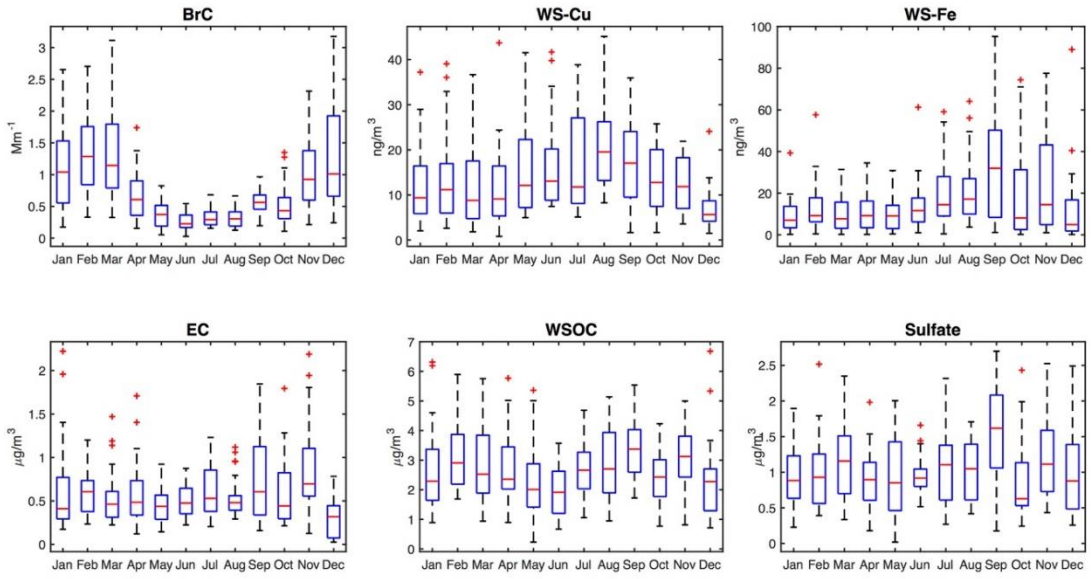

Figure 2-3. Temporal variation for select PM species.

2.4.4 Multivariate model

Given that one or more PM components contributed to these measures of OP, multivariate linear regression analysis was conducted to identify the main water-soluble PM components that drive the variability in OP and provide a contrast between the assays. Water-soluble organic species (WSOC or BrC) and metals, mainly Fe, Cu, Mn, were selected as the independent variables to form multivariate linear regression models for OP^{DTT} and OP^{AA}, based on their high correlations, as noted above. For OP^{GSH}, WSOC and BrC were used as input in addition to water-soluble Cu to include the possible influence of organic species on OP^{GSH}. The resulting linear relationships between different OP measures and PM components are shown in Table 2-2. The time series of measured and predicted OPs and the contributions of model variables to each OP measure are given in

Fig. A-1. Overall, the multivariate models explained variability in OP measures reasonably well with the coefficients of determination between modeled and measured OPs (R^2) greater than 0.4, with the models better capturing the OP^{AA} and OP^{GSH} variability. In the regression results for OP^{DTT} and OP^{AA}, components including water-soluble Fe, Cu and BrC (or WSOC) and interaction terms between metal–organic and metal–metal were included, suggesting that the variability of OP^{DTT} or OP^{AA} is dependent upon not only bulk concentrations of PM components but also interactions between species. The regression model for OP^{GSH} captured the contributions from Cu and BrC but had no interaction terms. The intercept in each regression model, though large and accounting for over 50 % of the mean of OP measures (Fig. A-1), is practically meaningless, because the regression models are applicable only when the PM components are at ambient concentrations.

Table 2-2. Multivariate linear regression models for OP metrics.

	Fe	Cu	WSOC	BrC	metal–organic		metal–metal		intercept	R^2
OP^{DTT}	2.28E-3	2.69E-3		5.75E-2	-1.36E-3	Cu*BrC	-4.09E-5	Fe*Cu	0.13	0.40
OP^{AA}	1.17E-1	1.07E-1	9.32E-1		-1.30E-2	Fe*WSOC	-2.05E-3	Fe*Cu	4.38	0.54
OP^{GSH}		7.41E-2		2.77E-1					3.65	0.56

Note: All metals are water-soluble metals. The values represent the coefficients for variables. Cell is left blank where the corresponding variable is not included in the equation. As an example, the linear equation of OP^{DTT} is as follows: OP^{DTT} = 2.28E-3*Fe +2.69E-3*Cu +5.75E-2*BrC-1.36E-3*(Cu*BrC)-4.09E-5*(Fe*Cu)+0.13. The concentrations of water-soluble metals are in units of ng m^{-3}, whereas the units for WSOC and BrC are μg m^{-3} and Mm^{-1}, respectively.

Note that BrC and WSOC are present in different models. Although they were correlated with each other (Table A-1–A-3), and both represent the contribution from organic species, there is a difference between these two parameters. It has been found that BrC predominantly represents the hydrophobic organic fraction (i.e., the humic-like substances (HULIS) fraction) in PM (Verma et al., 2012) and is largely from incomplete combustion (mainly biomass burning) (Hecobian et al., 2010). For example, quinones, as a subset of the HULIS fraction (Verma et al., 2015b), can be estimated better with BrC than with WSOC. WSOC also includes organic compounds present in the hydrophilic fraction, e.g., levoglucosan, (Zhang et al., 2011) and low molecular weight organic acids (Sullivan and Weber, 2006) and thus is a more integrative measure of organic compounds compared to BrC. The difference between BrC and WSOC is also supported by the different seasonal variation observed in BrC and WSOC (Fig. 2-3).

For OP^{DTT} results, the presence of Cu and BrC in the equation is as expected, since Cu and organic species have been found active in DTT oxidation (Charrier and Anastasio, 2012; Cho et al., 2005). However, Fe, which has a low intrinsic DTT activity (Charrier and Anastasio, 2012), was found to be predictive of OP^{DTT}, likely suggesting that Fe represents surrogate measures of constituents with intrinsic redox active properties which were not quantified. This is also supported by the evidence that Fe had correlations with other PM constituents such as OC and EC (Table A-1–A-3) which may suggest that Fe in the PM water extracts is solubilized by forming complexes with combustion-derived organic species. The interaction terms, along with their negative coefficients, suggest antagonistic interactions between Cu and organic compounds and between Cu and Fe. The interaction between metal and organics, though not taken into account when applying multivariate

regression analysis in previous studies (Calas et al., 2018; Verma et al., 2015a), is consistent with experimental results (Yu et al., 2018) wherein antagonistic interactions between Cu and ambient HULIS were observed in the DTT consumption. However, the interaction between metals contrasts with experiments which showed additive effects for metal mixtures (Yu et al., 2018). But it should be noted that the interactions among metals were usually tested with mixtures of individual species, which can poorly represent the complex chemistry of ambient PM.

For RTLF assay, the variability of OP^{AA} was attributed to the concentrations of Fe, Cu and WSOC, antagonistic metal–organic interaction between Fe and organic compounds and metal–metal competition between Fe and Cu. Even though the RTLF assay in previous studies was generally used to measure the OP of methanol-extracted PM suspension, the contributions from metals and organics observed in our water-soluble OP are in agreement with previous results (Ayres et al., 2008; Kelly et al., 2011; Pietrogrande et al., 2019). The presence of interaction terms is novel and is supported by little empirical evidence. The antagonistic interaction between Fe and WSOC is reasonable. Fe in the water extracts has been found largely complexed with organic compounds (Wei et al., 2019). Since AA is not a strong ligand for Fe (Charrier and Anastasio, 2011), the complexation between Fe and organic compounds can prevent Fe from reacting with AA. For OP^{GSH}, despite weak correlation of OP^{GSH} with BrC, BrC still accounted for the variability in OP^{GSH}, consistent with previous findings that OP^{GSH} is responsive to quinones (Ayres et al., 2008; Calas et al., 2018).

It is noteworthy that the multivariate regression models do not account for the possible nonlinear behavior of species with OP responses. For example, nonlinear concentration–

response curves have been found for DTT oxidation by dissolved Cu and Mn (Charrier and Anastasio, 2012), which may not be characterized in the multivariate regression model, potentially affecting the accuracy of the OP^{DTT} model. We note that the variables in the models not only represent the contribution from individual species, but also show a possible influence from co-emitted unquantified components. There are also interactions existing among PM species, affecting the relationships between PM compounds and OP metrics.

To further investigate the sensitivity of different OP assays to PM species, standardized regression was applied to rescale the variables measured in different units and make the coefficients in the regression equations comparable. It is also an effective way to reduce collinearity induced by the inter-correlated nature of PM species and the existence of interaction terms. The standardized coefficient of a specific component indicates the estimated change in an OP measure for every one-unit increase in component. The higher the absolute value of the standardized coefficient, the stronger the effect of the PM species on the OP measure.

Figure 2-4 shows the relative importance of each PM component to OP metrics based on the calculation of standardized coefficients. As shown in Fig. 2-4, water-soluble Fe was the most important variable in the model of OP^{DTT}, followed by BrC, Cu and antagonistic interactions. Even though OP^{DTT} is not responsive to water-soluble Fe, Fe may be a surrogate measure of compounds co-emitted with Fe from brake/tire wear and secondary formation which have been identified as two major sources of Fe in the southeastern US (Fang et al., 2015a). For OP^{AA}, the strength of the effects of Fe, Cu and WSOC on OP^{AA} was similar. OP^{GSH} was approximately four times more sensitive to Cu than to BrC, with

standardized coefficients of 0.70 and 0.18 for Cu and BrC, respectively. These results show clear contrasts between the assays, where OP^{DTT} and OP^{AA} are more similar and both have significant contrasts to OP^{GSH}.

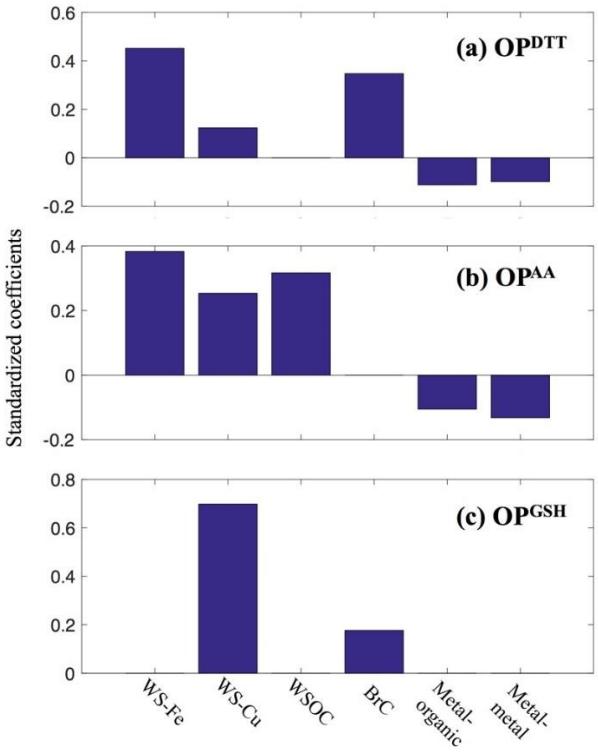

Figure 2-4. Standardized regression coefficients for different OP measures with selected PM components.

In all these cases, it must also be kept in mind that the measurements were performed on the PM water extracts, which are not the conditions that are found in the ambient aerosol. Thus, inferring associations between species in the extracts and applying to ambient conditions is not straightforward, however, this analysis is useful for interpreting and

contrasting the possible causes for associations between these types of assays and any health effects.

Water-soluble Fe, as the most important determinant of OP^{DTT}, has shown the strongest estimated effect on cardiovascular outcomes in the Atlanta metropolitan region (Ye et al., 2018), which may account for associations between OP^{DTT} and health outcomes observed in this region. OP^{GSH} is strongly dependent on a limited number of PM components, and thus associations between OP^{GSH} and health outcomes may vary more significantly by regions than other assays do and associations could be expected if the PM toxicity in a region is mainly driven by specific species, such as water-soluble Cu. OP^{AA} is affected by the composition of synthetic lung fluid, and thus the AA responses obtained from RTLF and AA-only model are not comparable and should be distinguished from each other. In the RTLF model, the response of OP^{AA} metric to PM samples is diminished due to the presence of GSH, possibly leading to weaker associations between OP^{AA} and health endpoints.

2.5 Conclusions

In this study, a comparison was made between two of the most common techniques used for the assessment of PM oxidative potential based on antioxidant depletion from a complex synthetic RTLF (OP^{AA} and OP^{GSH}) and DTT oxidation (OP^{DTT}). These two assays were used to quantify the water-soluble OP of ambient $PM_{2.5}$ collected in urban Atlanta over a one-year period based on daily filter samples. We observed moderate correlations among the OP assays, suggesting different sensitivities of OP measures to PM species. Univariate and multivariate regression analyses indicated that OP^{DTT} and OP^{AA} were

correlated to organic species and water-soluble metals (Fe and Cu) and were negatively affected by the interactions among species. At a more detailed level, for organic components, OP^{DTT} was associated specifically with HULIS and incomplete combustion products identified by BrC, whereas OP^{AA} was associated to a more general measure of organic components, WSOC. OP^{GSH}, though also affected by organic species, was predominantly sensitive to water-soluble Cu. Subtle temporal variation in OP^{DTT} and no seasonal variations in OP^{AA} and OP^{GSH} were observed, which appears to be due to little seasonality in the combined PM constituents affecting each assay. A small OP^{DTT} variation was associated with variation in BrC that was higher in the cold seasons.

This study suggests that all three OP metrics are associated with transition metal ions. However, OP^{DTT} and OP^{AA} are more chemically integrative OP measures compared to OP^{GSH}, and thus may be more informative when try to find linkage between OP and health end points. The multivariate regression models for different OP measures indicate the degree to which OP variability in the PM water extracts is predicted by PM constituents.

CHAPTER 3. A METHOD FOR MEASURING TOTAL AEROSOL OXIDATIVE POTENTIAL (OP) WITH THE DITHIOTHREITOL (DTT) ASSAY AND COMPARISION BETWEEN AN URBAN AND ROADSIDE SITE OF WATER-SOLUBLE AND TOTAL OP

Dong Gao, Ting Fang, Vishal Verma, Linghan Zeng, Rodney J. Weber

Atmos Meas Tech, 10, 2821-2835, 2017

https://doi.org/10.5194/amt-10-2821-2017

3.1 Abstract

An automated analytical system was developed for measuring the oxidative potential (OP) with the dithiothreitol (DTT) assay of filter extracts that include both water-soluble and water-insoluble (solid) aerosol species. Three approaches for measuring total oxidative potential were compared. These include using methanol as the solvent with (1) and without (2) filtering the extract, followed by removing the solvent and reconstituting with water, and (3) extraction in pure water and performing the OP analysis in the extraction vial with the filter. The water extraction method (the third approach, with filter remaining in the vial) generally yielded highest DTT responses with better precision (coefficient of variation of 1–5 %), and was correlated with a greater number of other aerosol components. Because no organic solvents were used, which must be mostly eliminated prior to DTT analysis, it was the easiest to automate by modifying an automated analytical system for measuring

water-soluble OP developed by Fang et al. (2015). Therefore, the third method was applied to the field study for the determination of total OP. Daily 23h filter samples were collected simultaneously at a roadside (RS) and a representative urban (GT) site for two one-month study periods, and both water-soluble ($OP^{WS\text{-}DTT}$) and total ($OP^{Total\text{-}DTT}$) OP were measured. Using $PM_{2.5}$ (aerodynamic diameter < 2.5 μm) high-volume samplers with quartz filters, the $OP^{WS\text{-}DTT}$ to $OP^{Total\text{-}DTT}$ ratio at the urban site was 65 % with a correlation coefficient (r) of 0.71 (N=35; p-value<0.01), compared to a ratio of 62 % and r=0.56 (N=31; p-value<0.01) at the roadside site. Same DTT analyses were performed and similar results were found using particle composition monitors (flow rate of 16.7 L min^{-1}) with Teflon filters. Comparison of measurements between sites showed only slightly higher levels of both $OP^{WS\text{-}DTT}$ and $OP^{Total\text{-}DTT}$ at the RS site, indicating both $OP^{WS\text{-}DTT}$ and $OP^{Total\text{-}DTT}$ were largely spatially homogeneous. These results are consistent with roadway emissions as sources of DTT-quantified $PM_{2.5}$ OP and that both soluble and insoluble aerosol components contributing to OP are largely secondary.

3.2 Introduction

Exposure to ambient particulate matter (PM) is associated with adverse health effects (Atkinson et al., 2001; Li et al., 2003a; Lim et al., 2013; Pope, 1995; Pope and Dockery, 2006). The mechanisms of PM toxicity are complex and not completely understood. One view is that PM toxicity occurs through inducement of oxidative stress (Delfino et al., 2005; Delfino et al., 2013; Nel, 2005); a state of biochemical imbalance in which the presence and formation of reactive oxygen species (ROS) in the human body overwhelms antioxidant defenses, eventually leading to various adverse health outcomes (Delfino et al., 2011; Donaldson et al., 2001; Li et al., 2003a). ROS can be either transported on inhaled

particles to the air–lung interface or generated in vivo by interaction between deposited PM and physiological chemical components (Lakey et al., 2016). The ability of PM to generate ROS is defined as the oxidative potential (OP) of PM. OP integrates various biologically relevant properties of particles, including size, surface and chemical composition, which may better reflect the biological response to PM exposure and consequently be more informative than PM mass, or specific PM chemical species, when attempting to link aerosols to adverse health effects.

Various methods have been developed to assess PM OP (Ayres et al., 2008; Cho et al., 2005; King and Weber, 2013; Mudway et al., 2004; Shi et al., 2003b; Wang et al., 2011). The dithiothreitol (DTT) assay is used in this study to measure the OP of fine particles (i.e., OP^{DTT}). DTT acts as a surrogate of cellular reductants, such as NADH/NADPH. The goal is to mimic interactions between physiological reductants and aerosol components through a purely chemical analysis. Various aerosol components can react directly with antioxidants (reducing agents), or transfer electrons from the antioxidants to dissolved oxygen, leading to antioxidant depletion in the first case and both antioxidant depletion and ROS generation in the second. In the DTT assay, physiological reductants are represented by DTT. When this reaction is monitored under conditions of excess DTT, the DTT consumption over time is proportional to the concentration of PM redox-active species, quantified as OP^{DTT}. OP^{DTT} per volume of air sampled has been found to correlate with biological markers, such as cellular hemeoxygenase (HO-1) expression (Li et al., 2003b) and fractional exhaled nitric oxide (FE_{NO}) in human subjects (Delfino et al., 2013; Janssen et al., 2015). Epidemiological studies have linked OP^{DTT} to adverse health outcomes, such as asthma, rhinitis (Yang et al., 2016) and asthma or wheezing and

congestive heart failure (Bates et al., 2015; Fang et al., 2016). Utilizing different measures of OP (e.g., ascorbic acid, AA; glutathione, GSH; uric acid, UA), some other studies, however, have not found links between OP and adverse health effects (Atkinson et al., 2016; Canova et al., 2014).

OP^{DTT} of water-soluble PM components (referred to as $OP^{WS\text{-}DTT}$) is the common focus of OP studies. Researchers have identified DTT-active water-soluble PM components, including HUmic-Like Substances (HULIS) (Lin and Yu, 2011; Verma et al., 2012; Verma et al., 2015a), oxygenated quinones (a subset of HULIS) (Cho et al., 2005; Kumagai et al., 2002), and transition metals (Charrier and Anastasio, 2012; Fang et al., 2016; Verma et al., 2015a). Water-insoluble species can also be an important fraction of the overall PM redox activity. Li et al. (2013b) found that the solid particle phase was a dominant factor in the DTT-based redox activity of soot particles. Akhtar et al. (2010) found that redox-active substances could be strongly bound to solid particles and not be easily extracted by water. McWhinney et al. (2013) reported that 89 %–99 % of the redox activity of diesel exhaust particles (DEP) were water-insoluble and not extractable by moderately polar (methanol) and nonpolar (dichloromethane) organic solvents. Daher et al. (2011) reported the highest intrinsic OP^{DTT} for particle collection with a Biosampler, which was considered most efficient in capturing both the soluble and insoluble PM species. Including the contribution of water-insoluble species in the OP assessment would be closer to actual PM exposure. A measure of both water-soluble and water-insoluble OP would be useful to elucidate the relative risks of water-soluble versus water-insoluble OP-induced health risks for specific health endpoints, such as respiratory versus cardiovascular dysfunction.

Several PM extraction methods have been used to assess the OP of water-insoluble PM. A common approach is to extract water-insoluble species in organic solvents, such as methanol and dichloromethane. Verma et al. (2012) found OP^{DTT} (expressed per μg of PM mass) of filtered methanol extracts to be correlated with water-insoluble organic carbon and elemental carbon (N=8). The DTT assay response for the methanol extracts was significantly higher than that for the water extracts with methanol-to-water OP^{DTT} ratio of 1.6 ± 0.4. Yang et al. (2014) compared OP^{DTT} of ambient PM with two extraction methods for Teflon filters: methanol extraction without filtering and water extraction. They found that the methanol extracts were more DTT-reactive (expressed per m^3 of sampled volume) than the water extracts. In this method, removal of organic solvent by evaporation was necessary prior to the DTT assay, which can result in the loss of labile redox-active PM species, such as semi-volatile organic compounds. Instead of attempting to dissolve water-insoluble species in various solvents, other studies perform the assay in the extraction liquid without filtration, retaining the insoluble particles in the DTT reaction solution. McWhinney et al. (2013) measured total redox activity of DEP using particle suspensions that were obtained by a water-extraction procedure with the filter removed after extraction. Whereas Charrier et al. (2016) performed the DTT assay on the extraction liquid that still contained the filter. Daher et al. (2011) collected particles directly into water with a BioSampler and performed the DTT analysis without filtration.

In this study, we assess techniques for quantifying the overall oxidative potential of ambient particles and determine the relative contribution from water-soluble and water-insoluble components to PM OP by contrasting measurements from different sites. This was accomplished by conducting the DTT assay on samples extracted by three different

methods. The goal was to develop a system for measuring both soluble and total OP^{DTT} (insoluble OP^{DTT} by difference) fractions to allow studies on the health effects of soluble (Bates et al., 2015) versus insoluble PM OP.

3.3 Experimental methods

3.3.1 Sampling methods and locations

Measurements were made at two contrasting sampling sites: Georgia Tech and Roadside. The Georgia Tech (GT) site was situated on the rooftop of the Ford ES&T building on the campus of Georgia Tech about 30 m above ground level and approximately 420 m from the roadside site. (A map of the sites is provided in Supplement Fig. B-1.) The GT site is assumed to be representative of the urban Atlanta environment. The Roadside (RS) site is adjacent (within 3 m) to a heavily trafficked interstate freeway (I-85/75) with an annual average daily traffic count of 382,000 vehicles in 2015 (Georgia Department of Transportation (GDOT) traffic data, station ID 1215482). Heavy-duty trucks are restricted, resulting in predominantly light-duty gasoline vehicle traffic (non-heavy duty truck traffic nominally 95 %, GDOT 2013 data).

Measurements were undertaken during two different periods using different particle filter collection systems. A high-volume (HiVol) sampler (Thermo Anderson, nominal flow rate 1.13 m^3 min^{-1}, $PM_{2.5}$ impactor) was set up at each site to collect ambient fine particles simultaneously from 21 April 2016 to 30 May 2016. Fine particles were collected with prebaked 8×10 in. quartz filters (Pallflex Tissuquartz, Pall Life Sciences) for 23 h (11:00 am–10:00 am the next day). The HiVol quartz filters were wrapped in prebaked aluminum foil immediately after collection and stored at -18 ℃ until analyses. The bias between the

two High Volume samplers was assessed by running them side-by-side at GT for 9 days. The measurements were within 10 % for both water-soluble OP^{DTT} ($OP^{WS\text{-}DTT}$) and total OP^{DTT} ($OP^{Total\text{-}DTT}$) (obtained by method 3, described below) (Supplement Fig. B-2). In Sect. 3.4, OP data from HiVol 1 were adjusted to match HiVol 2 based on the orthogonal linear regression from this comparison. The factors used to convert OP from HiVol 1 to HiVol 2 were 1.00 and 1.10 for $OP^{WS\text{-}DTT}$ and $OP^{Total\text{-}DTT}$, respectively.

Zefluor PTFE membrane filters (diameter 47 mm, 2 μm pore size, Pall Life Sciences) were used as well for simultaneous $PM_{2.5}$ sample collection from 26 July 2016 to 21 August 2016 using particle composition monitors (PCM, 16.7 L min^{-1}, $PM_{2.5}$ URG cyclone, un-denuded). Two PCMs were installed at each site to obtain two Teflon samples, one was used for $OP^{WS\text{-}DTT}$ and the other for $OP^{Total\text{-}DTT}$ analysis. Similar to the HiVol filter sampling, after 23 h collection, the PCM Teflon filters were placed into Petri dishes and stored at -18 ℃.

3.3.2 Measurements of PM oxidative potential

OP analyses were performed on both HiVol quartz and PCM Teflon filters. The DTT assay followed the protocol developed by Cho et al. (2005). All OP analyses on HiVol quartz filters were done immediately after collection; OP measurements on Teflon filters were completed within one month after collection.

3.3.2.1 $OP^{WS\text{-}DTT}$ analysis

One circular punch (diameter of 1 in.) from the HiVol quartz filter was extracted in 4.9 mL of deionized water (DI, >18 MΩ cm^{-1}) in a sterile polypropylene centrifuge tube (VWR

International LLC, Suwanee, GA, USA) via 30-min sonication. Considering the potential for radical formation during the sonication process (Miljevic et al., 2014), experiments using sonication versus shaking were done. Little difference observed in OP for sonication versus shaking indicated negligible bias in $OP^{WS\text{-}DTT}$ measurement due to sonication, see Supplementary Material Fig. B-3. The extract was then filtered through 0.45 μm PTFE syringe filters (Fisherbrand, Fisher Scientific) to remove insoluble material. The filtered PM water-extract was analyzed using a semi-automated system ($OP^{WS\text{-}DTT}$ system) developed by Fang et al. (2015) where all chemical reagents and reaction mixtures were mixed and transferred by two programmable syringe pumps. Briefly, 3.5 mL water extract is incubated with 0.5 mL of 1 mM DTT and 1 mL potassium phosphate buffer (K-buffer; pH=7.4) in a single incubation vial (IV) at 37 ℃. At designated time points (0, 4, 13, 23, 32, 41 min), an aliquot (100 μL) of this mixture is transferred to another vial (reaction vial, RV) and mixed with trichloroacetic acid (TCA) to quench the reaction. Tris buffer (pH=8.9) and 5,5'-dithiobis-(2-nitrobenzoic acid) (DTNB) are then added to form a colored product which absorbs light at 412 nm. The final mixture is pushed through a 10cm path length liquid waveguide capillary cell (LWCC), and the absorbance at 412 nm is detected and recorded by an online UV–visible spectrophotometer. The DTT concentration at each time point is quantified based on the absorbance calibration curve, which had previously been determined from standard DTT solutions also containing TCA, Tris buffer, and DTNB. The DTT consumption rates are then determined by applying linear regression to the observed DTT concentration versus time. The final OP results are calculated by subtracting a blank value from the sample and normalized by the volume of air that passed through the filter (of 1-inch diameter punch size), expressed as nmol DTT min^{-1} per

sampled air volume ($OP^{WS\text{-}DTT}$ m^{-3}; if not explicitly stated, $OP^{WS\text{-}DTT}$ is $OP^{WS\text{-}DTT}$ m^{-3}) to provide a measure of atmospheric levels of water-soluble aerosol OP. The DTT consumption rate of multiple blanks for quartz filters (N=42) was stable with a mean ± 1σ of 0.33 ± 0.07 nmol min^{-1}. Since DTT is a relatively unstable compound, it can react with dissolved oxygen in the liquid in the absence of particles (Kumagai et al., 2002), resulting in OP response in blanks. The blank OP values are also due to trace levels of contaminants on the filter, in the DI-water, and introduced during sample preparation. 9,10-phenanthrenequinone (PQN) is used as positive control throughout the analysis to evaluate the stability of the analytical system.

Water extraction was also performed on the PCM Teflon filters. Each of the two Teflon filters collected simultaneously at each site was cut in half. One half of each filter was combined and immersed in 4.9 mL DI in a beaker and sonicated for 30 minutes. The water extract was then filtered and $OP^{WS\text{-}DTT}$ determined using the automated system. DTT analytical processing was exactly the same as that for quartz filters described above. The other filter halves were stored in a freezer until $OP^{Total\text{-}DTT}$ analysis. This analysis approach removed any potential biases associated with the separate filter collection systems at each site. Sample flow rates were measured at the beginning and end of sampling for each filter system and the overall average was used to calculate $OP^{WS\text{-}DTT}$ m^{-3}. Field blanks were also tested in the same manner and had an average slope plus or minus standard deviation of 0.35 ± 0.08 nmol min^{-1} (mean ± 1σ, N=18).

3.3.2.2 $OP^{Total\text{-}DTT}$ analysis

Sample extraction and preparation: To assess methods for characterizing $OP^{Total\text{-}DTT}$, we used three different methods of sample preparation using the HiVol quartz filters. Sample preparation schemes are illustrated in Fig. 3-1. Multiple method analysis was done only on HiVol filters since there was insufficient mass collected to compare different methodologies using the PCM Teflon samples.

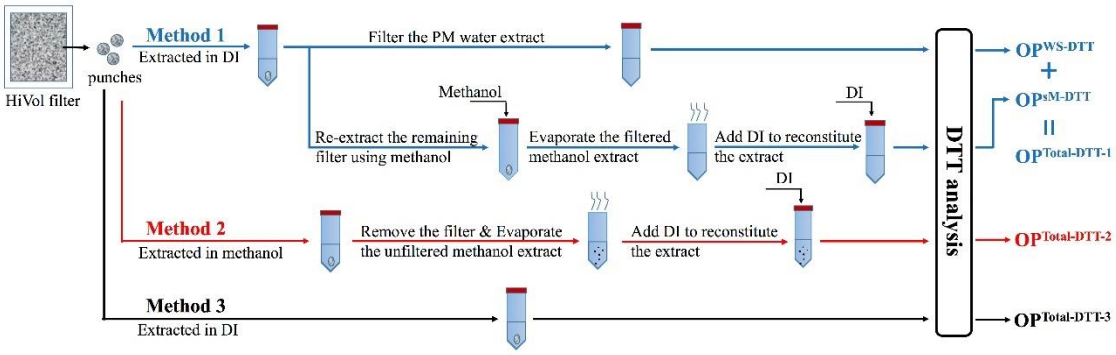

Figure 3-1. Analytical scheme for three sample extraction methods to determine total OP with the DTT assay ($OP^{Total\text{-}DTT}$).

Method 1 consisted of two steps, water extraction and sequential methanol extraction. A 1-inch circular punch taken from the HiVol quartz filter was extracted in 4.9 mL DI via 30-minute sonication. The water extract was then filtered using a 0.45 μm PTFE syringe filter. This step was the same as the measurement of $OP^{WS\text{-}DTT}$. The water-extracted filter punch was retained in the vial, dried in room air and re-extracted using methanol (HPLC grade) via 30-minute sonication. The methanol extract was also filtered through a syringe filter (0.45 μm PTFE) and then concentrated to about 200 μL using high purity nitrogen

gently blown into the vial above the liquid surface. DI was added into the vial to reconstitute the small aliquot of remaining methanol liquid to 4.9 mL of solution. The reconstituted extract was stirred using a vortex mixer (VWR® Analog Vortex Mixer, 300–3200 rpm) for 10 seconds to re-suspend any particles deposited on the walls of the vial during methanol blow-down. The purpose of the sequential and filtered methanol extraction was to assess if water-insoluble species could be dissolved by methanol as a way of quantifying the water-insoluble OP^{DTT} through a contrast to methods that retained solid particles (discussed next). As methanol is less polar than water, it may dissolve most of the water-insoluble organic species in addition to some water-soluble compounds. However, since the solid-phase material in the extract may have been removed by filtering the extract, this method will not include DTT-active species that cannot be separated from a solid particle and is therefore removed by the syringe filter. The determination of OP^{DTT} for both water extract ($OP^{WS\text{-}DTT}$) and sequential DI-reconstituted methanol extract ($OP^{sM\text{-}DTT}$) was conducted using the $OP^{WS\text{-}DTT}$ analytical system since all extracts had been filtered, avoiding any plugging or contamination issues in the analytical system by solid particles. The sum of $OP^{WS\text{-}DTT}$ and $OP^{sM\text{-}DTT}$ is the total redox activity obtained by method 1, which will be denoted as $OP^{Total\text{-}DTT\text{-}1}$. Blank filters were also similarly processed and analyzed for OP^{DTT}, producing blank values of 0.33 ± 0.07 nmol min^{-1} (mean $\pm 1\sigma$, N=42) for $OP^{WS\text{-}DTT}$ and 0.43 ± 0.09 nmol min^{-1} (mean $\pm 1\sigma$, N=18) for $OP^{sM\text{-}DTT}$. This method was used in the Southeastern Center for Air Pollution and Epidemiology (SCAPE) study and so a substantial data set (N=198) exists on $OP^{sM\text{-}DTT}$.

Method 2 is similar to the methanol extraction by Yang et al. (2014). The filter punch was extracted in methanol via 30-minute sonication. After extraction, the filter punch was

removed from the vial. The methanol extract was not filtered so that the methanol-insoluble components were also retained and would possibly participate in the subsequent DTT reaction. The methanol suspension was blown down to nominally 200 μL using nitrogen gas and reconstituted to 4.9 mL with DI. The reconstituted extract was stirred for 10 seconds using a vortex mixer in an attempt to re-suspend particles deposited on vial walls. Due to the presence of solid material in the extract, such as quartz filter fibers released by sonication, the $OP^{WS\text{-}DTT}$ system could not be utilized. Instead, a modified automated system was needed to measure the OP of this aqueous suspension, discussed below. The OP^{DTT} of PM sample extracted in this manner is referred to as $OP^{Total\text{-}DTT\text{-}2}$. The blank value for this method was 0.42 ± 0.13 nmol min^{-1} (mean ± 1σ, N=18).

Method 3 is the easiest to perform among the three methods in terms of sample preparation (Fig. 3-1). In this case the circular filter punch was immersed in the mixture of 4.9 mL DI and 1.4 mL K-buffer in a sterile polypropylene centrifuge tube, followed by 30min sonication. The DTT assay was then performed directly in the vial with the filter punch present using the modified automated system discussed below. Some DTT-active species may be strongly absorbed to the filter surface so that they are not extractable into water. But in method 3, since the whole filter is suspended in DTT solution, these DTT-active species may participate in the reaction with DTT. In the study of Charrier et al. (2016), where DTT was also directly incubated with the PM filter, an alcohol, 2,2,2-Trifluoroethanol, was added to the extraction solvent to facilitate removal of particles from the filter substrate. We tested adding small amounts of methanol (up to 10 % of total extraction volume) into the extraction solvent to investigate if methanol would expose more solid aerosol for reaction with DTT, which would be observed as an increase in DTT

response. The test results are given in Supplement Fig. B-4 and show that the added methanol had negligible effects on the final OP^{DTT} measured, therefore, only DI was used for extraction in this method. The OP^{DTT} obtained in this way is referred to as $OP^{Total\text{-}DTT\text{-}3}$. Sonication versus shaking tests were also performed on method 3, and the results (Supplement Fig. B-5) show little effects of sonication on $OP^{Total\text{-}DTT\text{-}3}$ measurements. Only method 3 was used for the $OP^{Total\text{-}DTT}$ determination of Teflon filters. Multiple blanks were processed similarly with DTT consumption rates of 0.37 ± 0.06 nmol min^{-1} (mean ± 1σ, N=18) for quartz filters and 0.43 ± 0.04 nmol min^{-1} (mean ± 1σ, N=18) for Teflon filters.

Automated system for $OP^{Total\text{-}DTT}$ measurements: A modified automated analytical system for $OP^{Total\text{-}DTT}$ was developed by modifying the $OP^{WS\text{-}DTT}$ system of Fang et al. (2015) for analysis of filters extracted using methods 2 and 3. A schematic is shown in Fig. 3-2. In this approach the sample extraction vial containing the suspension or suspension plus filter that had gone through method 2 or 3 extraction is placed in the thermal mixer, prior to which 1.4 mL K-buffer had been loaded manually. In this case, each sample vial is used as an incubation vial directly, continuously shaken and maintained at 37 ℃ via a Thermo-mixer (VWR® Cooling Thermal Shake Touch; rotational frequency of 400 rpm, temperature of (37 ± 0.5) °C). Two peek tubes (PEEK Tubing Green 1/16 inch OD × 0.030 inch ID), which are connected to a 14-port multi-position valve (VICI Valco Instrument Co. Inc., USA), are inserted into each incubation vial, with one tube having an in-line syringe filter (0.45 μm Polypropylene (PP) filter media, Whatman) and the other not. For each run, 0.7 mL DTT (1 mM) is loaded into the incubation vial through the tubing without in-line filter via the programmable syringe pump A (see Fig. 3-2). Air is then pumped into the incubation vial to thoroughly mix. In the mixture, DTT is presumably oxidized with

the catalytic assistance of both water-soluble and water-insoluble DTT-active species associated with the PM collected on the HiVol quartz or PCM Teflon filter. After mixing, the multi-position valve is switched so that the syringe can withdraw an aliquot of sample through the filter, at a low speed so as not to form air bubbles by cavitation. At designated time intervals (13, 30, 48, 65, 82 min), the aliquot is withdrawn through the in-line filter, transferred to the reaction vial (RV) and mixed with TCA preloaded in the vial by pump B. The DTT concentration is then determined following the same steps as that for the OP^{WS-DTT} system (Fang et al., 2015). A total of five data points of remaining DTT concentrations versus time is generated and used for the final OP^{DTT} determination. After finishing the DTT analysis of each sample, the system is thoroughly cleaned by flushing with DI to remove the residual liquid left in the various tubing, reaction vial, pump syringes and LWCC. Following the flushing, the 14-port multi-position valve is switched to the next sample for analysis. Due to the slow piston motions in liquid transfer from IV to RV, it generally takes 1.5 hours for $OP^{Total-DTT}$ system to analyze one sample, compared with 1 hour of analysis time of OP^{WS-DTT}. The $OP^{Total-DTT}$ system, like the OP^{WS-DTT} system, can operate unattended and be monitored remotely to analyze, at least, seven filters. (This is limited by the 14-channels of the multi-position valve in Fig. 3-2). To avoid contamination from the insoluble material captured in the in-line syringe filter, the syringe filter is replaced after each sample run. The automated system is cleaned every 4 weeks of continued operation by flushing at least three times with methanol, followed by four times with DI.

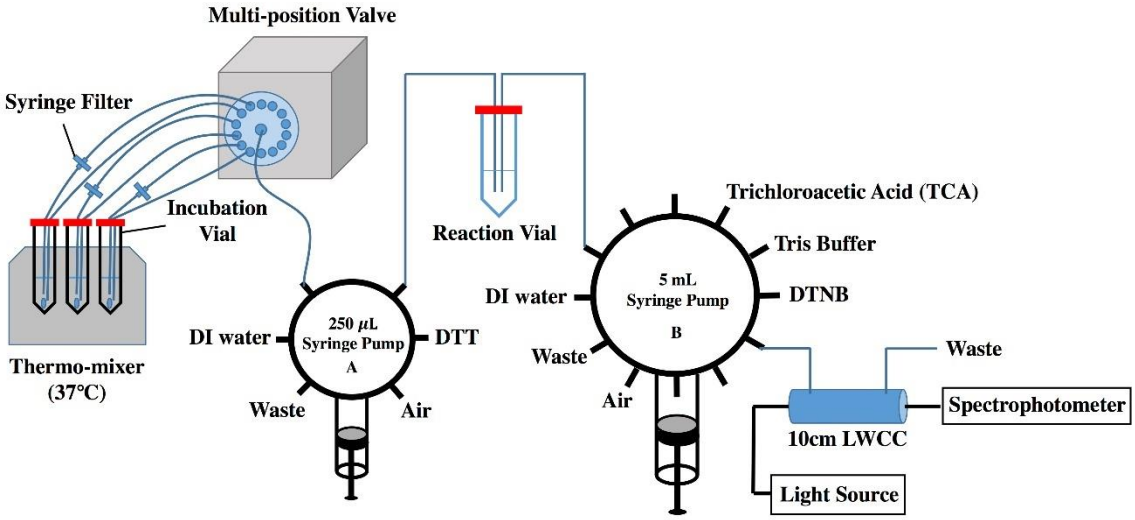

Figure 3-2. Automated system setup for measuring $OP^{Total\text{-}DTT}$. The assay is performed in the vial containing the filter sample and extraction water, which had been sonicated. The assay is filtered just prior to analysis in the liquid wave guide capillary cell (LWCC).

3.3.3 Other chemical analysis

A number of other aerosol components were analyzed on the HiVol quartz filters for assessing the various methods of measuring $OP^{Total\text{-}DTT}$. Carbon analysis (EC/OC) was performed on a 1.5 cm^2 punch from the quartz filters using Interagency Monitoring of Protected Visual Environments (IMPROVE) thermal optical reflectance (TOR) protocol (Chow et al., 1993).

Total and water-soluble metals were determined by inductively coupled plasma-mass spectrometry (ICP-MS) (Agilent 7500a series, Agilent Technologies, Inc., CA, USA) using EPA method 6020, again from sections of the same HiVol quartz filters. The elements of interest included species that possibly play a role in ROS generation (Fe, Mn, Cu;

Schoonen et al., 2006) and K, a marker of biomass burning (Artaxo et al., 1994). For the determination of concentrations of total metals, acid digestion was carried out on a 1.5 cm^2 filter punch using nitro hydrochloric acid (HNO_3 + 3HCl). The acid-digested sample was then diluted in DI water, filtered with a 0.45 μm PTFE syringe filter. No digestion was required prior to the analysis of water-soluble metals. A 1.5 cm^2 punch from the quartz filter was sonicated in DI for 30 minutes. After sonication, the extract was filtered using a 0.45 μm PTFE syringe filter, and then acid-preserved by adding concentrated nitric acid (70 %) to a final concentration of 2 % (v/v). A set of mixed calibration standard solutions were prepared by diluting the stock standard solutions and treated with the same procedures as samples. Internal standards including lithium (^{6}Li) and scandium (^{45}Sc), were added to all calibration standards and samples to monitor instrumental drift. DI blank and field blank which consist of same concentrations of acid and internal standards were used to monitor for possible contamination resulting from the sample preparation procedures. This was critical since in this case no special care was taken to pre-acid wash the quartz filters or syringe filters used in the water-soluble metals analysis. The method detection limits are defined here as three times the standard deviation of blanks, which for water-soluble metal method were 0.03 mg L^{-1} for K, 0.00007 mg L^{-1} for Mn, 0.009 mg L^{-1} for Fe, 0.0002 mg L^{-1} for Cu, and for the total metal method were 0.03 mg L^{-1} for K, 0.0002 mg L^{-1} for Mn, 0.02 mg L^{-1} for Fe, and 0.002 mg L^{-1} for Cu.

3.3.4 Data analysis

Linear regression was applied to the experimental data in order to assess relationships between measurements. Since the data was normally distributed (shown in Fig. B-6), the Pearson correlation coefficients were calculated to further demonstrate the strength and the

direction of a linear relationship between two measurements. A correlation coefficient greater than 0.7 with a low p-value (<0.05) was generally described as strong.

The paired t-tests were used to determine whether there was a significant difference in OP measurements between two methods. Each $OP^{Total\text{-}DTT}$ was measured using three methods, resulting in pairs of observations. The null hypothesis of the paired t-test assumed that the mean difference between the paired observations was zero. p-value of the test gave the probability of observing the test results under the null hypothesis. p-values less than 0.05 rejected the null hypothesis at the 5 % significance level.

The F-tests in one-way analysis of Variance (ANOVA) were employed to evaluate the impact of filter type (i.e., quartz vs. Teflon filters) on the PM OP measurements for a given site. The F-statistic is the ratio of between-group variability to within-group variability, which followed an F-distribution under the null hypothesis. In this paper, the null hypothesis assumed that there was no significant OP difference between Teflon and quartz filters. If the F calculated from the data was smaller than the critical F-value of the F-distribution for significance level α=0.05, then the null hypothesis would be true with 95 % confidence.

The spatial variability of OP (Table B-6) was assessed by the coefficients of divergence (CODs) (Pinto et al., 2004; Wilson et al., 2005).

$$COD = \sqrt{\frac{1}{N}\sum_{i=1}^{N}\left(\frac{c_{ij} - c_{ik}}{c_{ij} + c_{ik}}\right)^2} \quad (1)$$

where c_{ij} and c_{ik} were $OP^{WS\text{-}DTT}$ or $OP^{Total\text{-}DTT}$ measured at site j and k, respectively, and N was the number of observations. A COD close to zero implied spatial uniformity, while a value approaching unity indicated absolute heterogeneity.

3.4 Results and discussion

First we discuss the performance of the automated system for measuring $OP^{Total\text{-}DTT}$ where filters were extracted by method 3 (Fig. 3-1), and then compare the results of the three differing methods for measuring $OP^{Total\text{-}DTT}$ at the two sampling sites. The system performance was assessed by only method 3 since these samples were easiest to prepare and this is the final approach of the three methods tested that was extensively utilized. Finally, we compare results from method 3 using quartz filters to a later study using Teflon filters. All OP^{DTT} results were blank-corrected.

3.4.1 Automated $OP^{Total\text{-}DTT}$ system performance

The performance of the automated system was assessed in terms of the system response, accuracy and precision. 9,10-phenanthraquinone (PQN), a quinone that has been identified to be DTT-active (Kumagai et al., 2002) and often utilized as a positive control (Fang et al., 2015), was used to test the system response. A highly linear relationship (R^2=0.97) was found between PQN concentration in the incubation vial and the DTT consumption rate measured by the system (shown in Fig. 3-3). This linear relationship is consistent with the results shown in Fang et al. (2015) and Charrier et al. (2016).

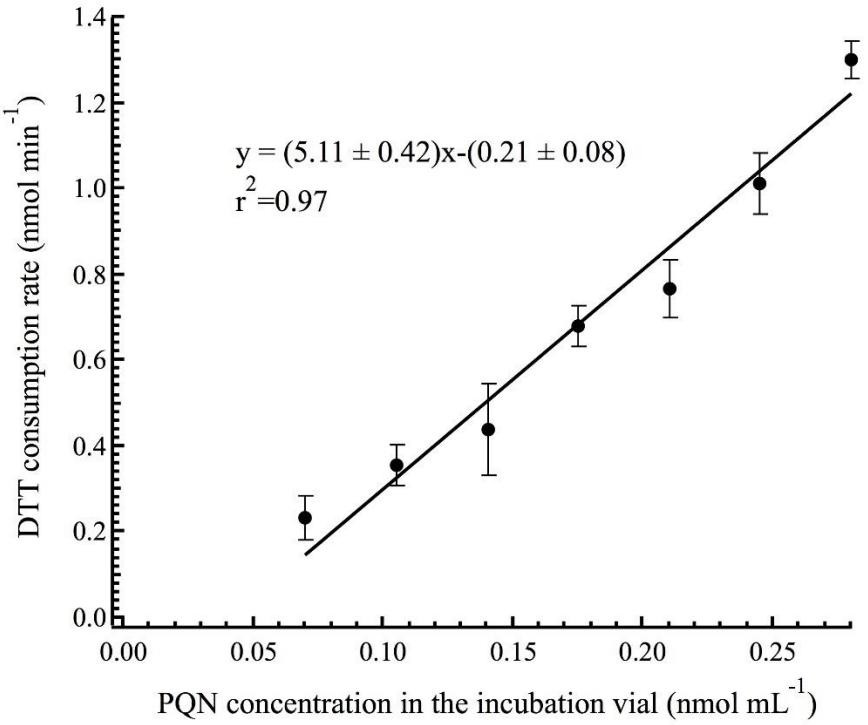

Figure 3-3. Blank-corrected DTT consumption rate as a function of PQN showing linearity between PQN concentrations and DTT consumption rate for the total analytical system (for PQN levels shown in the range above). Error bar represents the standard deviation of three independent DTT measurements on each concentration.

The accuracy of measurements given by the $OP^{Total\text{-}DTT}$ system was further assessed by comparing the DTT consumption rate obtained by the system to that following the manual DTT analysis approach of Cho et al. (2005). Seven PQN solutions of various concentrations were tested by both the automated system and manual approach. As shown in Fig. 3-4, a bivariate linear regression was applied and yielded a slope near unity (0.99 ± 0.06), intercept close to zero (0.04 ± 0.04), and correlation of determination (R^2) of 0.98. For further validation, five ambient samples, which in this case would include insoluble species, were extracted by method 3 and analyzed using both the automated and manual methods (see Supplement Fig. B-7). The ratio of automated-to-manual DTT consumption

rate was 0.98 ± 0.05. These tests illustrate the validity of the $OP^{Total\text{-}DTT}$ system as an alternative to the manual DTT assay.

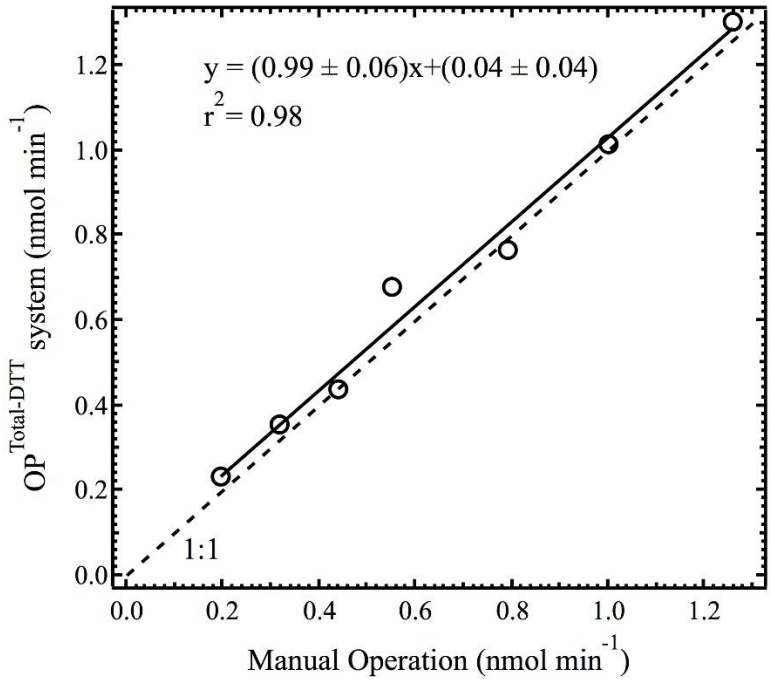

Figure 3-4. DTT consumption rate (blank-corrected) comparison of the automated system for measuring $OP^{Total\text{-}DTT}$ (shown in Fig. 3-2) to a manual analysis using PQN. Slope (± 1 standard deviation) and intercept (± 1 standard deviation) are based on orthogonal regression.

To assess the precision of the automated $OP^{Total\text{-}DTT}$ system, the DTT consumption rates of identical concentrations of several PQN solutions were repeatedly measured. The $OP^{Total\text{-}DTT}$ system produced consistent results for the PQN replicates (blank-corrected DTT consumption rate of 0.76 ± 0.05 nmol min^{-1} for 0.21 nmol mL^{-1} of PQN in the incubation vial, coefficient of variation (CV) = 6 %, N=7), suggesting good precision of the system.

We conclude that most variability in the analysis of samples will be introduced in the extraction process and not the DTT analysis.

3.4.2 Precisions of various methods

To test the precision of the complete approach for measurement of $OP^{Total\text{-}DTT}$ (i.e., extraction and analysis), measurements of $OP^{Total\text{-}DTT}$ were repeated three times using three separate punches from the same Hivol quartz filter. This was done for all three $OP^{Total\text{-}DTT}$ methods. The coefficient of variation (CV) for replicates is used to assess the precision of each method. The results are summarized in Table 3-1. CV ranged from 3 % to 6 % for method 1, which may result from the combined uncertainties of the two respective steps (i.e., extraction and analysis). The range of CV for method 2 was from 5 % to 12 %. The root of this variability may arise from the insoluble material remaining in the reaction suspension that was difficult to reproduce from run-to-run. In contrast, lower CV (1 %~5 %) was observed for method 3, possibly because it involved the least steps in the filter extraction.

Table 3-1. Coefficient of variation (CV) of $OP^{Total\text{-}DTT}$ for three extraction methods.

	Method 1	Method 2	Method 3
Coefficient of variation (CV) from triplicate	3–6 % N=10	5–12 % N=7	1–5 % N=12

*N is the number of HiVol filters tested.

3.4.3 Comparison of methods for measuring total oxidative potential ($OP^{Total\text{-}DTT}$)

3.4.3.1 Comparison of oxidative potential

In the following, OP^{DTT} m^{-3} determined by the three methods for simultaneously collected HiVol quartz filters at the GT and RS sites are compared. Since no standard method is available for assessing the ability to measure OP^{DTT} m^{-3}, we simply compare the various methods and assume that the highest measurement represents the most comprehensive analytical method for measuring total oxidative potential. No HiVol conversion factors were applied to the OP data as the three methods were all performed on filters collected using the same HiVol sampler at each site.

Figure 3-5 shows the OP^{DTT} m^{-3} comparison between method 1 and 3 at both GT and RS sites. In general, the response of the DTT assay of method 3 was significantly higher than that of method 1 at the 95 % confidence level (paired t-test: $p = 0.028$ at GT, N=35; $p<0.001$ at RS, N=31). The results are expected since in method 1, both the water and methanol liquid extracts are filtered, potentially removing species that could have been DTT-active but remained attached to solid particles. A few observations where $OP^{Total\text{-}DTT\text{-}3}$ is less than $OP^{Total\text{-}DTT\text{-}1}$ are likely due to propagation of errors for the summation method (method 1) combined with variability in the extraction process for each method. The mean $OP^{Total\text{-}DTT\text{-}1}$ to $OP^{Total\text{-}DTT\text{-}3}$ ratio at GT was close to 1 (ratio = 0.95) and also higher than that at RS (ratio = 0.85). The lower $OP^{Total\text{-}DTT\text{-}1}$ may be due to liquid filtration after water extraction. The ratios of $OP^{sM\text{-}DTT}$ to $OP^{WS\text{-}DTT}$ are 0.34 ± 0.14 (N=35) at GT and 0.37 ± 0.12 (N=31) at RS, which are consistent with the ratios from SCAPE data (0.27 ± 0.08, N=198; unpublished data) and fall into the typical range of ambient samples. The water-insoluble

OP determined by the difference in $OP^{Total\text{-}DTT\text{-}3}$ (which includes solid particles) and $OP^{WS\text{-}DTT}$ ($OP^{WI\text{-}DTT\text{-}3} = OP^{Total\text{-}DTT\text{-}3} - OP^{WS\text{-}DTT}$) to $OP^{WS\text{-}DTT}$ ratio, by contrast, is 0.45 ± 0.25 at GT (N=35) and 0.67 ± 0.35 at RS (N=31). There was very little correlation between the $OP^{WI\text{-}DTT\text{-}3}$ and $OP^{WS\text{-}DTT}$ with Pearson correlations of r = -0.23 and -0.51 at GT and RS sites, respectively (see Supplement Table B-1), which further indicates the importance of water-insoluble compounds to a total OP measurement. Additionally, $OP^{WI\text{-}DTT\text{-}3}$ was weakly correlated with $OP^{sM\text{-}DTT}$ (Pearson correlation: r = 0.31 at GT; r = 0.04 at RS). Based on these data, it is clear that there were species associated with water-insoluble OP^{DTT} not extracted by methanol and that remain attached to solid particles. This analysis shows that filtering the liquid extract, even if methanol solvent is used, will result in a substantial underestimation of $OP^{Total\text{-}DTT}$. Therefore, in terms of the OP response, method 3 is preferred to method 1. Furthermore, the comparison between these two methods can provide insights into the water-insoluble components that contribute to PM OP.

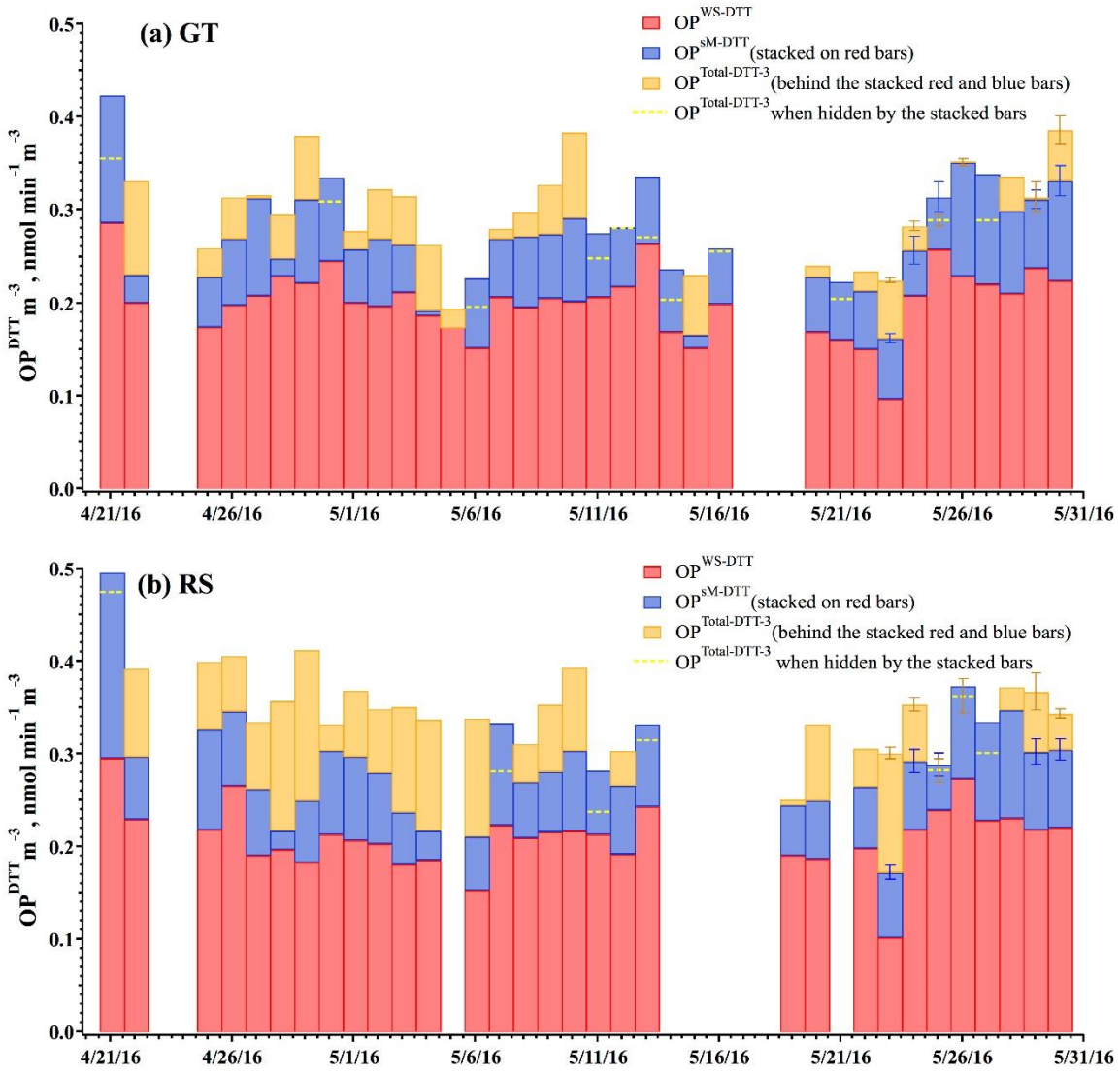

Figure 3-5. Comparison of OP^{DTT} m^{-3} between extraction methods 1 and 3 at (a) GT (N=35) and (b) RS (N=31). Error bars denote 1 standard deviation in OP^{DTT} m^{-3} from repeated measurements and are propagated in calculating $OP^{Total\text{-}DTT\text{-}1}$.

Figure 3-6 shows the OP^{DTT} m^{-3} comparison between method 2 and 3 at both GT and RS sites. At the GT site, method 3 generally yielded higher OP responses compared to method 2 with mean $OP^{Total\text{-}DTT\text{-}2}$ to $OP^{Total\text{-}DTT\text{-}3}$ ratio of 0.90 ($p<0.001$ for a paired t-test (N=35)). For the RS site, however, method 2 was able to produce comparable ($p=0.060$ for a paired

t-test, N=31) or even higher OP responses, at times, than method 3 with a $OP^{Total\text{-}DTT\text{-}2}$ to $OP^{Total\text{-}DTT\text{-}3}$ ratio of 0.94, which may imply that method 2, in some cases, might be more efficient in extracting DTT-active species from the unique RS sources such as vehicular emissions.

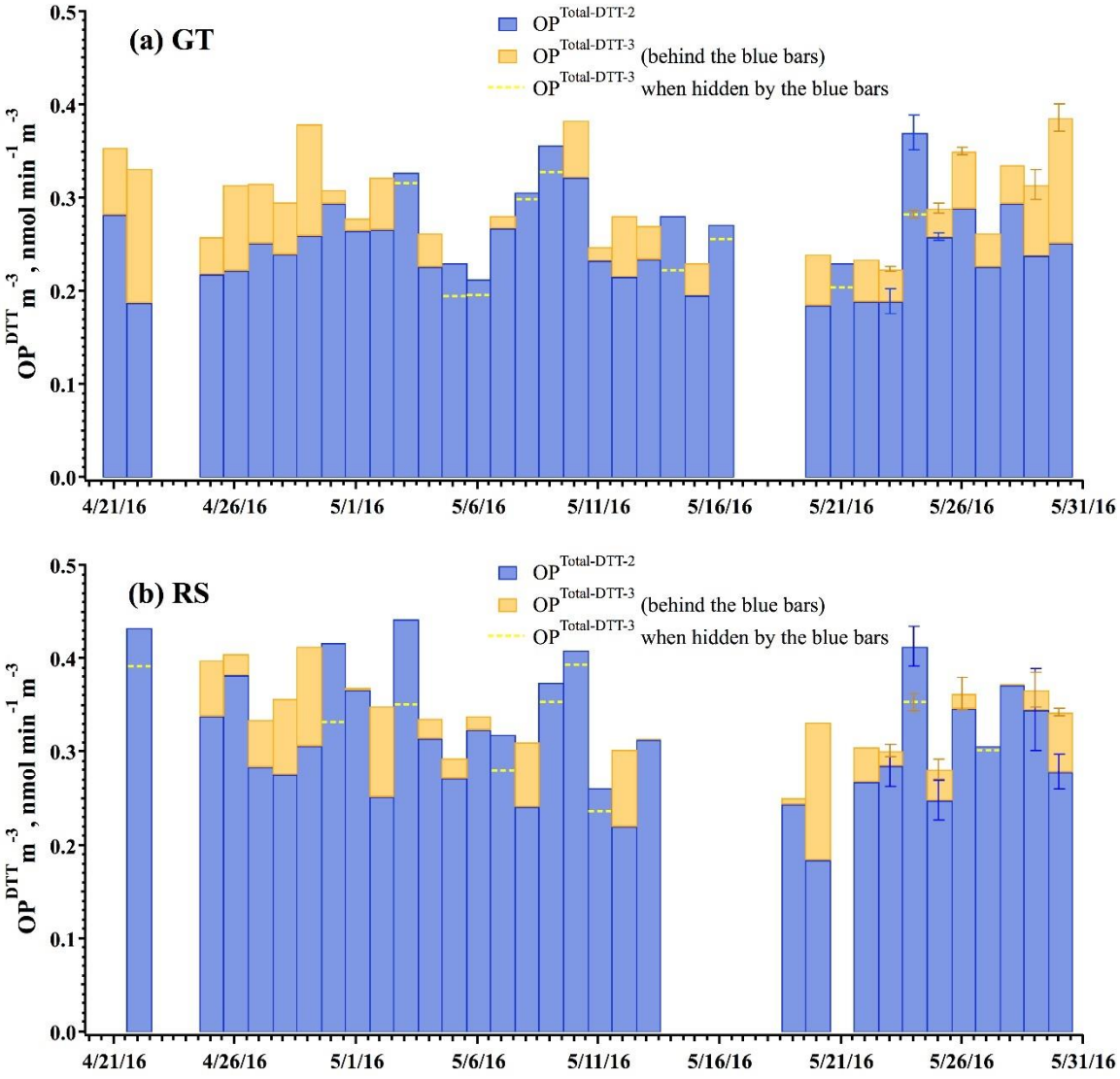

Figure 3-6. Comparison of OP^{DTT} m^{-3} between extraction methods 2 and 3 at (a) GT (N=35) and (b) RS (N=31). Error bars denote 1 standard deviation in OP^{DTT} m^{-3} from repeated measurements.

From the perspective of OP response, method 3 generally produced the highest signals compared to the other two methods, in both the urban (GT) and near-road (RS) sites.

3.4.3.2 Association between OP^{DTT} and PM composition

A correlation analysis was performed between measured $PM_{2.5}$ chemical constituents and OP^{DTT} determined by the three methods. Figure 3-7 shows the correlation results (detailed values are provided in Table B-2). It is seen that $OP^{Total\text{-}DTT\text{-}3}$ is better correlated with the measured species than $OP^{Total\text{-}DTT\text{-}1}$ and $OP^{Total\text{-}DTT\text{-}2}$. Compared with $OP^{WS\text{-}DTT}$, the stronger correlations between $OP^{Total\text{-}DTT\text{-}1}$ and PM species suggests that $OP^{Total\text{-}DTT\text{-}1}$ captures more chemical components contributing to DTT than $OP^{WS\text{-}DTT}$. In contrast, $OP^{Total\text{-}DTT\text{-}2}$ is correlated with the least number of measured PM species.

By subtracting $OP^{WS\text{-}DTT}$ from $OP^{Total\text{-}DTT}$, $OP^{WI\text{-}DTT}$ is determined for the three methods. In general, the correlations between $OP^{WI\text{-}DTT}$ and PM species are mediocre for all three methods, with a slightly better performance of method 1. The water-insoluble OP^{DTT} determined by method 1, i.e. $OP^{sM\text{-}DTT}$, has good correlation with OC at GT and OC, EC and water-soluble Fe at RS. Verma et al. (2012) also showed good correlations between OP^{DTT} of filtered methanol extracts and OC and EC, and attributed this association to water-insoluble organic carbon species (WIOC) that dissolve in methanol. Thus, $OP^{sM\text{-}DTT}$ in method 1 is likely attributed to some fraction of the WIOC. $OP^{WI\text{-}DTT}$ obtained in method 1 is determined from the direct measure of $OP^{sM\text{-}DTT}$, whereas $OP^{WI\text{-}DTT}$ is determined by difference for method 2 and 3, which leads to larger uncertainty and more scatter associated with these data.

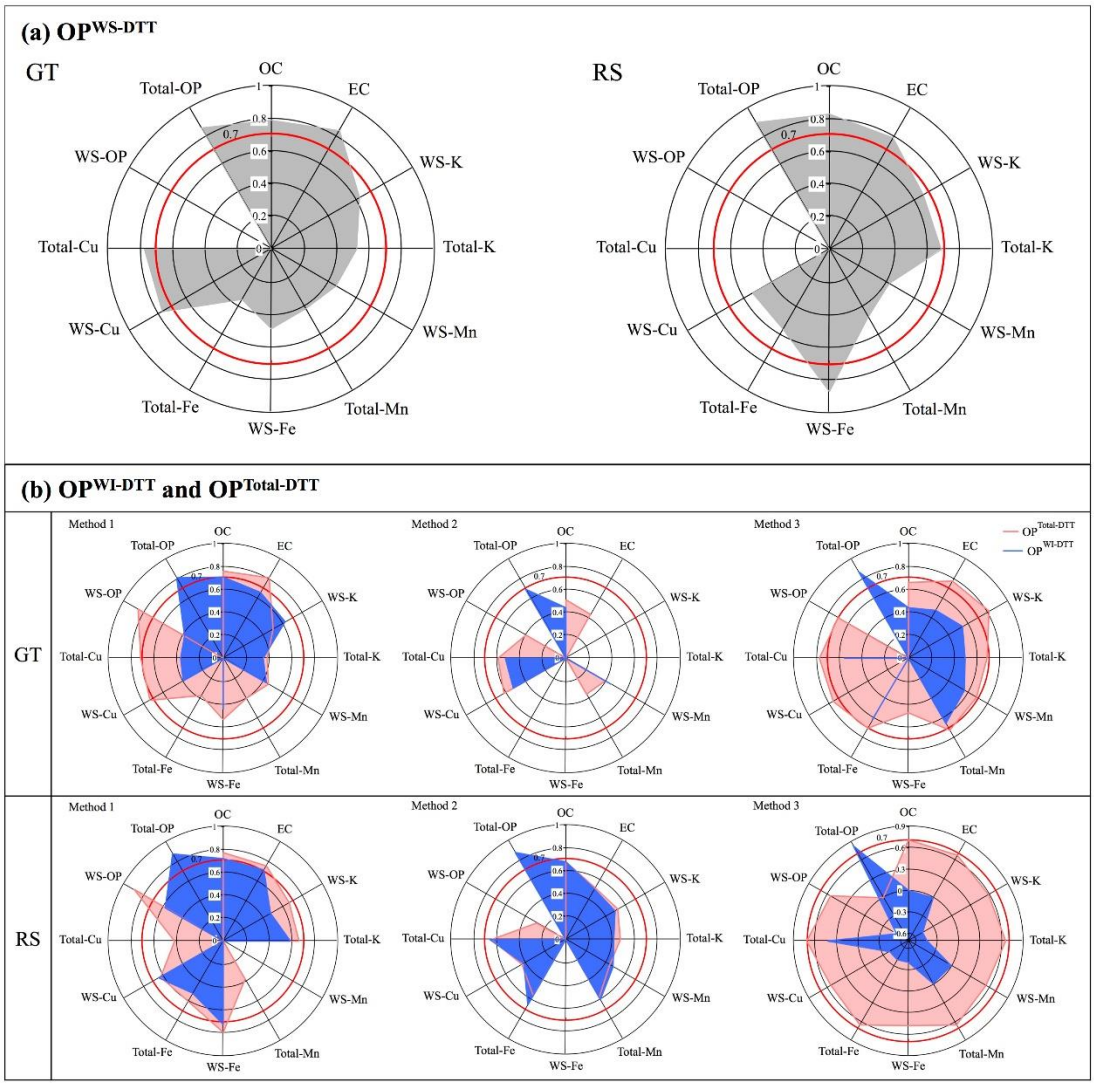

Figure 3-7. Polar plots comparing Pearson correlation coefficients (r) between various forms of OP^{DTT} m^{-3} (a $OP^{WS\text{-}DTT}$, b $OP^{WI\text{-}DTT}$ and $OP^{Total\text{-}DTT}$; red: $OP^{Total\text{-}DTT}$; blue: $OP^{WI\text{-}DTT}$ ($OP^{WI\text{-}DTT}$ = $OP^{Total\text{-}DTT}$ - $OP^{WS\text{-}DTT}$ for methods 2 and 3)) and PM chemical components at GT (N=34) and RS (N=29) sites. Correlations not statistically significant (p-value > 0.05) are not shown on the plots but can be found in Table B-2. The red line indicates r = 0.7. Note: the scales for method 3 RS are different from those for the other methods.

The overall assessment of the three methods is summarized in Table 3-2. By comparison, it is found that method 3 has better precision, more comprehensive response (i.e., generally highest $OP^{Total\text{-}DTT}$), stronger correlations with PM components, and easiest filter preparation (extraction) process, all of which provide an efficient way for $OP^{Total\text{-}DTT}$ determination. The other two methods have some value owing to their insights into the attributes of water-insoluble OP contributors. In a subsequent study, discussed next, only Method 3 was utilized to measure $OP^{Total\text{-}DTT}$ of PM for Teflon filters.

Table 3-2. Comparison of methods for measuring $OP^{Total\text{-}DTT}$.

		Method 1	Method 2	Method 3
Description		Measured: • $OP^{WS\text{-}DTT}$ • $OP^{WI\text{-}DTT\text{-}1}$($OP^{sM\text{-}DTT}$): OP of water-insoluble but only methanol-extractable species $OP^{Total\text{-}DTT\text{-}1} = OP^{WS\text{-}DTT} + OP^{sM\text{-}DTT}$	Measured: • $OP^{Total\text{-}DTT\text{-}2}$: OP of methanol-extractable species and some methanol-insoluble solids $OP^{WI\text{-}DTT\text{-}2} = OP^{Total\text{-}DTT\text{-}2} - OP^{WS\text{-}DTT}$	Measured: • $OP^{Total\text{-}DTT\text{-}3}$: OP of water-soluble and -insoluble species, solids. $OP^{WI\text{-}DTT\text{-}3} = OP^{Total\text{-}DTT\text{-}3} - OP^{WS\text{-}DTT}$
Comparison	Ease of operation	Method 3 > Method 2 > Method 1		
	Precision	Method 3 > Method 1 > Method 2		
	OP magnitude	At GT: Method 3 > Method 1 > Method 2 At RS: Method 3 ≈ Method 2 > Method 1		
	Correlations with PM components	Number of correlations of $OP^{Total\text{-}DTT}$ with various species: Method 3 > Method 1 > Method 2 $OP^{WI\text{-}DTT}$: poor or mediocre correlations for all three methods.		

3.4.4 *$OP^{WS\text{-}DTT}$ and $OP^{Total\text{-}DTT}$ measurements on quartz versus Teflon filters and their spatial distributions.*

The time series of volume-normalized water-soluble and total OP^{DTT} via method 3 are shown in Fig. 3-8 for two different sample time periods using HiVol samplers with quartz filters (21 April 2016–30 May 2016; HiVol conversion factors of 1.00 and 1.10 were applied to GT $OP^{WS\text{-}DTT}$ and $OP^{Total\text{-}DTT}$ data, respectively.) and PCMs with Teflon filters (26 July 2016–21 August 2016). A summary of the average OP data is given in Supplement Table B-3. The ANOVA results (Supplement Table B-4) indicate negligible difference between types of filter (i.e., quartz versus Teflon) on OP^{DTT} measurements.

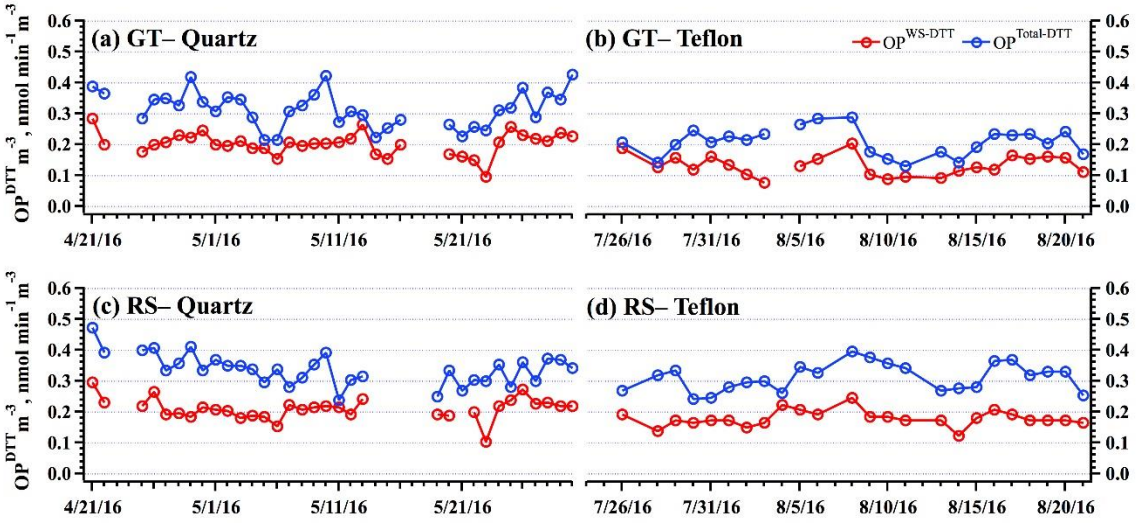

Figure 3-8. Volume-normalized OP^{DTT} of ambient $PM_{2.5}$ particles collected on quartz and Teflon filters at GT and RS sites for two different sampling time periods. Red lines indicate volume-normalized $OP^{WS\text{-}DTT}$, and blue lines denote volume-normalized $OP^{Total\text{-}DTT}$.

Figure 3-8 shows that, as expected, $OP^{Total\text{-}DTT}$ is always higher than $OP^{WS\text{-}DTT}$. The ratios of $OP^{WS\text{-}DTT}$ to $OP^{Total\text{-}DTT}$ were on average 65 ± 10 % (insoluble accounts for 35 ± 10 %) and 65 ± 14 % at GT, compared to 62 ± 12 % and 58 ± 10 % at RS, for quartz and Teflon PM samples, respectively. Thus, $OP^{Total\text{-}DTT}$ of $PM_{2.5}$ contained on average 35 to 42 % insoluble species. The correlation coefficients between $OP^{WI\text{-}DTT}$ and $OP^{Total\text{-}DTT}$ were 0.87 and 0.84 for quartz filters at GT and RS, respectively (Table B-1), which reflects the contribution of insoluble species to total OP as well.

Spatial distributions in OP^{DTT} can also be investigated. As discussed above, the water-soluble fraction of total OP ($OP^{WS\text{-}DTT}$ to $OP^{Total\text{-}DTT}$ ratio) was fairly similar at the two sites, which means that the insoluble fraction was not vastly different between the two sites. Figure 3-9 shows a summary of daily concentration ratios between the sites. EC, a marker for incomplete combustion, and so associated with vehicle emissions, was much higher at the RS site; the ratio of RS to GT was 3.2 on average. OC was only slightly elevated, as expected, since OC is largely secondary in Atlanta (Xu et al., 2015) and so more spatially uniform (i.e., primary OC is a small fraction of total OC, even at RS). Both $OP^{WS\text{-}DTT}$ and $OP^{Total\text{-}DTT}$ were spatially uniform with daily RS-to-GT OP ratios close to one. CODs were also calculated to further assess the spatial variability of OP (Table B-6). The low COD values (COD<0.08 for the quartz filters and <0.23 for the Teflon filters) between RS and GT site indicate spatial homogeneity of OP during the sampling periods. This was found for both quartz and Teflon filters. The homogenous distributions of OP are very similar to that of OC (COD=0.18) and in contrast to EC (COD=0.52). Note that both $OP^{WS\text{-}DTT}$ and $OP^{Total\text{-}DTT}$ were slightly higher at the RS site, possibly indicating a linkage to RS emissions. Uniformity of $OP^{WS\text{-}DTT}$ is consistent with the results shown in the study of Fang

et al. (2015), but similar uniformity in $OP^{Total\text{-}DTT}$ may seem somewhat unexpected since water-insoluble aerosol components are often associated with primary species. These data show the importance of secondary atmospheric processes $OP^{WI\text{-}DTT}$. The results are consistent with studies that have found water-insoluble DTT-active constituents could be secondary quinones from oxidized PAHs that remain bound to the surface of soot particles associated with traffic emissions (Antinolo et al., 2015; Li et al., 2013b; Shiraiwa et al., 2012). This means that although roadway emissions are a source for components that contribute to OP, some form of processing is needed to convert the roadway emissions to species with measurable oxidative potential for both $OP^{Total\text{-}DTT}$ and $OP^{WS\text{-}DTT}$. Size distributions of $OP^{WI\text{-}DTT}$ (Fang et al., 2017) suggest that $OP^{WI\text{-}DTT}$ is composed of different types of insoluble species, OP from oxidized aromatic species (e.g., quinones) may be mainly associated with smaller sized insoluble soot particles, and at the large end of the $PM_{2.5}$ size range, transition metal ions (i.e., water-soluble Cu) associated with road and brake dust may be the main source.

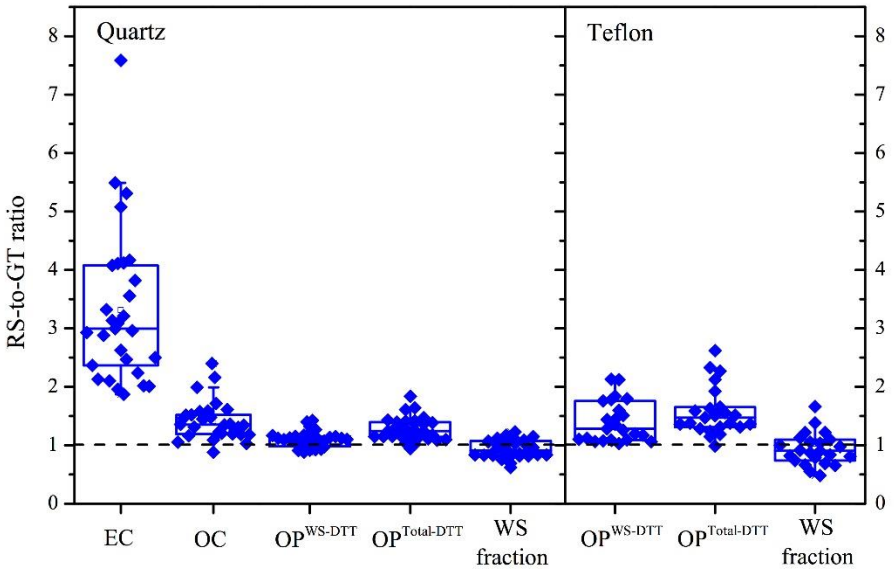

Figure 3-9. Comparison of simultaneous measurements at GT and RS sites based on daily RS-to-GT concentration ratios. The bottom and top of the box are the first (Q1) and third quartiles (Q3), and the band inside the box is the median. The lowest and highest ends of whisker are (Q1-1.5IQR) and (Q3+1.5IQR), where the interquartile range IQR=Q3-Q1.

3.5 Conclusions

An automated analytical system was developed for quantifying total aerosol oxidative potential with the DTT assay ($OP^{Total\text{-}DTT}$) from filter sample extracts. The method is based on modifying an automated analytical system developed by Fang et al (2015) for measuring water-soluble oxidative potential ($OP^{WS\text{-}DTT}$). Three methods for including the contribution of water-insoluble components to oxidative potential of PM ($OP^{WI\text{-}DTT}$), for a measurement of $OP^{Total\text{-}DTT}$ were tested: 1) Extracting filter punches in deionized water (DI), filtering the extract and measuring $OP^{WS\text{-}DTT}$, followed by methanol extraction on the same filter, filtering the extract and removing most methanol by evaporation, then reconstituting in

water and summing with $OP^{WS\text{-}DTT}$ to obtain $OP^{Total\text{-}DTT}$; 2) Extracting filter punches in methanol, reconstituting the unfiltered methanol extracts with DI after evaporation of methanol, and performing the DTT assay on the DI-reconstituted suspension; 3) Extracting filter punches in a vial with DI and then performing the DTT assay in the vial containing the filter. Method 3 generally yielded higher DTT responses with higher precision (coefficient of variation of 1~5 %), and was highly correlated with more aerosol species, including OC, EC and various water-soluble and total elements. Because this method requires no use of organic solvents that must be mostly eliminated prior to DTT analysis, it is the easiest to automate. The automated system for measuring $OP^{WS\text{-}DTT}$ (Fang et al., 2015) was modified to follow method 3 and the system performance was tested.

An ambient study was conducted to contrast measures of $OP^{Total\text{-}DTT}$ and $OP^{WS\text{-}DTT}$ for $PM_{2.5}$ collected at a roadside (RS) site (highway with restricted heavy duty diesel access) and a site more representative of overall average urban Atlanta air quality (GT). Simultaneous daily filter samples were collected during two separate one-month periods and comparisons were made using quartz and Teflon filters. At the representative urban site (GT), the ratio of $OP^{WS\text{-}DTT}$ to $OP^{Total\text{-}DTT}$ was 65 % for both types of filters. At the roadside site (RS) the ratio was only slightly lower, 62 % for quartz filters, 58 % for Teflon filters. $OP^{WS\text{-}DTT}$ and $OP^{Total\text{-}DTT}$ were moderately correlated with Pearson Product correlation coefficients between 0.56 (roadside) and 0.71 (urban). Simultaneous measures of $OP^{WS\text{-}DTT}$ and $OP^{Total\text{-}DTT}$ at the GT and RS site showed only slightly higher levels of both at the RS site, indicating both $OP^{WS\text{-}DTT}$ and $OP^{Total\text{-}DTT}$ were spatially homogeneous. The results are consistent with roadway emissions as sources of OP, but that $PM_{2.5}$ OP was largely secondary for both soluble and insoluble aerosol components contributing to OP.

CHAPTER 4. CHARACTERIZATION OF WATER-INSOLUBLE OXIDATIVE POTENTIAL OF PM2.5 USING THE DITHIOTHREITOL ASSAY

Dong Gao, James A. Mulholland, Armistead G. Russell, Rodney J. Weber

Atmos Environ, in review, 2019

4.1 Abstract

Both water-soluble and insoluble components of ambient particulate matter (PM) have been shown to contribute to the oxidative potential (OP) of PM. In this study, we used the dithiothreitol (DTT) assay to assess the water-soluble ($OP^{WS\text{-}DTT}$) and total OP ($OP^{total\text{-}DTT}$) of ambient fine particles ($PM_{2.5}$), with water-insoluble OP ($OP^{WI\text{-}DTT}$) determined by difference. Ambient $PM_{2.5}$ filter samples were collected daily during 2017 in urban Atlanta and were analyzed for OP and major PM components. Results from measurements suggested a measurable contribution of water-insoluble components to OP^{DTT}, which comprised on average 20% of total PM OP. Strong seasonal trends were observed in both volume- and mass-normalized $OP^{total\text{-}DTT}$ and $OP^{WI\text{-}DTT}$, with higher values in the winter than in the summer, possibly driven by biomass burning emission seasonality. Correlation analysis indicated that all forms of OP^{DTT} measurements were related to organic species and metals. $OP^{total\text{-}DTT}$ and $OP^{WI\text{-}DTT}$ were correlated with brown carbon (BrC) and total metals, especially total crustal elements. A multivariate regression model was developed for $OP^{total\text{-}DTT}$ based on particle composition data. The model suggested that the variability

of $OP^{total\text{-}DTT}$ was primarily affected by BrC, followed by EC, total Cu and an antagonistic interaction between BrC and total Cu.

4.2 Introduction

Extensive studies have associated adverse health effects with ambient particulate pollution (Brook et al., 2010; Gauderman et al., 2007; Hoek et al., 2002; Hoek et al., 2013). Oxidative stress, an imbalance wherein the level of reactive oxygen species (ROS) overwhelms the biological system's antioxidant defenses, has been suggested as a key mechanism underlying the toxic effects of exposure to particulate matter (PM) (Esposito et al., 2014; Lodovici and Bigagli, 2011). Inhaled PM can induce oxidative stress by transporting ROS on particles into the respiratory system, or by introducing redox-active PM components which are capable of catalytically generating ROS *in vivo* with simultaneous depletion of antioxidants (Netto and Stadtman, 1996; Squadrito et al., 2001; Venkatachari and Hopke, 2008). The resulting oxidative stress can further cause oxidative damage to biomolecules (e.g., proteins, lipids, and DNA), eventually leading to both acute and chronic diseases (Li et al., 2003b; Pizzino et al., 2017; Prahalad et al., 2001; Tao et al., 2003). The ability of PM to generate ROS, defined as oxidative potential (OP), integrates different physiochemical properties of PM, including size, surface area and chemical composition (Delfino et al., 2011; Zielinski et al., 1999), and thus has been proposed as a more biologically relevant exposure metric than PM mass.

A variety of methods have been developed to evaluate PM OP both in purely chemical as well as cell-based assays (Ayres et al., 2008; Bates et al., 2019). The dithiothreitol (DTT) assay, a widely used chemical assay, was applied in this study. This assay is based on the

ability of redox-active compounds associated with PM to catalyze the electron transfer from DTT, a surrogate of biological reducing agent, to dissolved oxygen, with the rate of DTT consumption a measure of the PM OP (i.e., OP^{DTT}) (Cho et al., 2005; Kumagai et al., 2002). OP^{DTT} has been found to be sensitive to a wide range of PM components, including organics (e.g. quinones) and soluble transition metals (e.g. copper and manganese) (Charrier and Anastasio, 2012; Kumagai et al., 2002; Verma et al., 2015a). OP^{DTT} has also been linked with several biological end points, including hemeoxygenase-1 (HO-1) expression (Li et al., 2003b), fractional exhaled nitric oxide (Delfino et al., 2013), and increased relative risk for asthma and congestive heart failure (Bates et al., 2015; Fang et al., 2016). A detailed review of the relationship between health end points and OP^{DTT} is given by Bates et al. (Bates et al., 2019).

The solubility of PM components is one of the crucial factors affecting PM OP. The focus of most studies applying OP assays has generally been to characterize OP of the water-soluble fraction of PM, which is considered more readily bioavailable than the water-insoluble fraction. However, studies have shown that insoluble fraction of PM also plays an important role in generating oxidative stress (Knaapen et al., 2002; Sorensen et al., 2003; Yi et al., 2014). Efforts have been made to evaluate the contribution of insoluble aerosol species to the overall redox activity of PM. In the studies of Daher et al. (Daher et al., 2011) and Wang et al. (Wang et al., 2013), ambient particles were collected directly into an aqueous suspension using a BioSampler, and the redox activity of the unfiltered suspension was substantially higher than that of the particle-free extracts, underscoring the OP contribution of insoluble species. Organic solvents have been used in other studies to extract water-insoluble species, where the solvents were removed by evaporation and the

samples were reconstituted in water prior to the OP analysis. Verma et al. (Verma et al., 2012) attempted to dissolve water-insoluble aerosol species by methanol extraction, and found high correlation between OP^{DTT} of the reconstituted methanol extracts and water-insoluble organic carbon contents of PM. However, McWhinney et al. (McWhinney et al., 2013) found that the redox active species in diesel exhaust particles could be strongly bound to black carbon, and was not extractable by water and moderately polar and nonpolar organic solvents. In our previous study (Gao et al., 2017), we compared three commonly used extraction methods for measuring total PM OP, and found that performing the OP assay on the extraction liquid that still contained the particle-laden filter was a more effective way to capture water-insoluble OP compared to organic solvent extraction. This extraction method was further employed in the study of Fang et al. (Fang et al., 2017b) to investigate the size distribution of water-insoluble OP^{DTT}.

Studies show that the effects of water-insoluble OP may be mediated by chemical species adsorbed to the soot surface. It has been found that the soot surface is coated with sulfates and condensed organic matter, and the presence of various organic functional groups allows complex chemistry to occur on the surface of soot particles (Jacobson et al., 2000). Antinolo et al. (Antinolo et al., 2015) have connected the increased OP^{DTT} to the oxidation of soot-surface polycyclic aromatic hydrocarbons (PAHs). In the study of Fang et al. (Fang et al., 2017b), the size distribution of water-insoluble OP^{DTT} has been found to be related to a surface property of EC and mineral dust.

In this study, we used two semi-automated DTT systems to assess the water-soluble and total OP^{DTT} of over 300 $PM_{2.5}$ filter samples collected from urban Atlanta. Water-insoluble OP^{DTT} was determined by difference (i.e., $OP^{WI\text{-}DTT} = OP^{Total\text{-}DTT} - OP^{WS\text{-}DTT}$). The large

data set on $OP^{Total\text{-}DTT}$ and $OP^{WI\text{-}DTT}$ allowed us to investigate the temporal variability and chemical determinants of $OP^{Total\text{-}DTT}$ and $OP^{Total\text{-}DTT}$. Associations between PM chemical speciation data and OP^{DTT} measurements were explored to identify potential major drivers of $OP^{Total\text{-}DTT}$ and $OP^{WI\text{-}DTT}$. A multivariate regression model was developed for $OP^{Total\text{-}DTT}$ to predict $OP^{Total\text{-}DTT}$ from the species data and to further assess the relative importance of specific PM species on $OP^{Total\text{-}DTT}$ activity.

4.3 Methods

4.3.1 Sampling

Sampling was conducted for one year, from January 2017 to December 2017 (a total of 349 samples) at the Jefferson Street Southeastern Aerosol Research and Characterization (SEARCH) site in Atlanta (Hansen et al., 2003). The site is located near the city center, representative of urban Atlanta. Aged urban vehicular and industrial emissions are presumably the major sources contributing to this site. Ambient data collected from this site has been the basis for many health studies from the Atlanta metropolitan area (Darrow et al., 2014; Sarnat, 2008; Strickland et al., 2010; Ye et al., 2017; Ye et al., 2018).

Ambient $PM_{2.5}$ was collected using high-volume samplers (HiVol, Thermo Anderson, nominal flow rate 1.13 m^3 min^{-1}, $PM_{2.5}$ impactor). The 24-hr integrated samples (from midnight to midnight) were collected daily on prebaked 8×10 in. quartz filters (Pallflex Tissuquartz, Pall Life Sciences). Field blanks were collected once per month. All samples were wrapped in prebaked aluminum foil and stored in freezer (-18 °C) until analyses. $PM_{2.5}$ mass was measured at the sampling site with a tapered element oscillating microbalance (TEOM, Thermo Scientific TEOM 1400a). Continuous measurements for

organic carbon (OC) and elemental carbon (EC) of $PM_{2.5}$ were also obtained using a Sunset semi-continuous OC-EC field analyzer (Sunset Laboratory).

4.3.2 Chemical analysis on PM filters

The bulk and specific chemical components, i.e., water-soluble organic carbon (WSOC), water-soluble brown carbon (BrC), inorganic anions, and various transition metals, were analyzed on the collected HiVol filters.

For WSOC and BrC (latter used as a combustion source tracer) measurements, two 1.5 cm^2 filter punches from the HiVol filter were extracted in 15 mL deionized water (DI, Milli-Q; >18 MΩ) in a pre-baked glass vial via 30 min of sonication. The extracts were then filtered using PTFE 0.45 μm pore syringe filter (Fisher Scientific) and transferred into another pre-baked glass vial for analysis. For BrC determination, a fraction of the filter extracts (~6 mL) was passed through a 2.5-m path length liquid waveguide capillary cell (LWCC; World Precision Instruments, Inc., FL, USA), where absorbance at 365 nm wavelength (BrC) was measured using an online spectrophotometer (Ocean Optics, Inc., Dunedin, FL, USA). The remaining extracts were conducted to a total organic carbon (TOC) analyzer (Model 900, GE Analytical Instruments, Boulder, CO, USA) for WSOC determination (Hecobian et al., 2010; Zhang et al., 2010).

A wide range of elements were measured using inductively coupled plasma-mass spectrometry (ICP-MS; Agilent 7500a series, Agilent Technologies, Inc., CA, USA), including magnesium (Mg), aluminum (Al), potassium (K), calcium (Ca), chromium (Cr), manganese (Mn), iron (Fe), copper (Cu) and zinc (Zn). Both total and water-soluble metal

concentrations were determined. Details of the method are described in Gao et al. (Gao et al., 2017) and in the Supplement.

Inorganic anions (SO_4^{2-}, NO_3^- and Cl^-) were measured on the filtered water extracts which were prepared by extracting 1.5 cm^2 filter punch in 10 mL DI via 30-min sonication. An automated system, which included an automated sampler (Dionex AS40, Thermo Fisher Scientific, Waltham, MA) and ion chromatography (IC) (Metrosep A Supp 5- 150/4.0 anion separation column), was used for the determination of anion concentrations.

4.3.3 Oxidative potential measurements

4.3.3.1 Water-soluble OP^{DTT} ($OP^{WS\text{-}DTT}$)

One circular punch (diameter of 1 in.) was extracted in 4.9 mL of DI via 30-min sonication. The extracts were filtered using 0.45 μm PTFE syringe filters to remove insoluble materials and then analyzed using a semi-automated system developed by Fang et al. (Fang et al., 2015b). This semi-automated system is based on the protocol adopted from Cho et al. (Cho et al., 2005). In brief, DTT oxidation was carried out by incubating the mixture of DTT (1 mM; 0.5 mL), PM extract (3.5 mL) and potassium phosphate buffer (pH~7.4, Chelex-resin treated; 1 mL) at 37°C. At designated time intervals (0, 4, 13, 23, 31 and 41 min), an aliquot (100 μL) of mixture was withdrawn and mixed with trichloroacetic acid (TCA, 1 % w/v) to quench the DTT reactions. 0.5 mL of 5,5'-dithiobis-(2-nitrobenzoic acid) (DTNB) and 1 mL of Tris buffer (pH ~8.9) were added to form 5-thio-2-nitrobenzoic acid (TNB) by reacting with the remaining DTT. Light absorption of this product was measured at 412 nm using an online spectrometer (Ocean Optics, Inc., Dunedin, FL, USA) to quantify the concentration of residual DTT. Linear regression was applied to the data points measured

at various time points, and the slope was used to estimate the overall DTT consumption rate. Multiple field blanks and positive controls (9,10-phenanthraquinone) were also analyzed along with the samples. The final OP measure was blank corrected and normalized by the volume of sampled air (OPv, expressed in units of nmol min^{-1} m^{-3}). This measure is therefore analogous to ambient concentrations of PM expressed as $\mu g/m^3$, and can be used to assess the human exposure to DTT-active species. Mass-normalized OP^{DTT} (OPm) was further obtained by dividing OPv by the particulate mass concentration, expressed in units of nmol min^{-1} μg^{-1}. OPm represents the intrinsic property of particles linked to PM composition and sources.

4.3.3.2 Total OP^{DTT} ($OP^{Total\text{-}DTT}$)

A semi-automated system developed by Gao et al. (Gao et al., 2017) was used to quantify $OP^{Total\text{-}DTT}$, following the same protocol as in $OP^{WS\text{-}DTT}$ measurement. The main difference between $OP^{Total\text{-}DTT}$ and $OP^{WS\text{-}DTT}$ measurements was that the PM extracts for $OP^{Total\text{-}DTT}$ measurement were not filtered, and the filter punch was also left in the extracts. In this case, the insoluble PM components suspended in the extracts or attached to the filter surface could also be in contact with DTT and participate in DTT oxidation. At different time intervals, a small aliquot of PM-DTT mixture was withdrawn and passed through an in-line syringe filter (0.45 μm Polypropylene (PP) filter media, Whatman) to prevent the insoluble material from clogging tubing and interfering the light absorption. The filtered aliquot was then used to determine the concentration of remaining DTT. Field blanks and positive controls were analyzed in parallel with each sample run to evaluate the consistency of the system performance. $OP^{Total\text{-}DTT}$ is reported in units of nmol min^{-1} per m^3 of air and nmol min^{-1} per µg of particles.

The relative uncertainties of the OP measures were within 5% of the measurements, as reported in Fang et al. (2015) and Gao et al. (2017).

4.3.4 Multivariate regression

Multivariate linear regression was implemented using OP^{DTT} as the dependent variable and the other PM species measurements as candidate independent variables. All the measured data were approximately normally distributed, which were examined with histograms. Linear regression was performed between OP^{DTT} and PM components, and the species correlated with OP^{DTT} ($r>0.4$, $p<0.01$) were used as the independent variables. A stepwise regression was conducted using Matlab R2016a to build a multivariate regression model. 5-fold cross validation was performed to avoid overfitting.

4.4 Results and discussion

4.4.1 Seasonal variability of OP^{DTT}

The time series of OP^{DTT} (both OPv and OPm), along with the annual average levels, is shown in Fig. 4-1. As shown in Fig. 4-1a and 1c, there was no significant seasonal variation observed for either volume or mass-normalized $OP^{WS\text{-}DTT}$. In contrast, both volume and mass-normalized $OP^{Total\text{-}DTT}$ (and thus $OP^{WI\text{-}DTT}$) varied substantially between seasons, with higher levels in the cold months than in summer. The two-sample t-test was used to assess the differences between winter and summer in OP^{DTT} levels, and the test results (Table C-1) also validated the pronounced seasonal difference in $OP^{Total\text{-}DTT}$ and $OP^{WI\text{-}DTT}$ (both OPv and OPm).

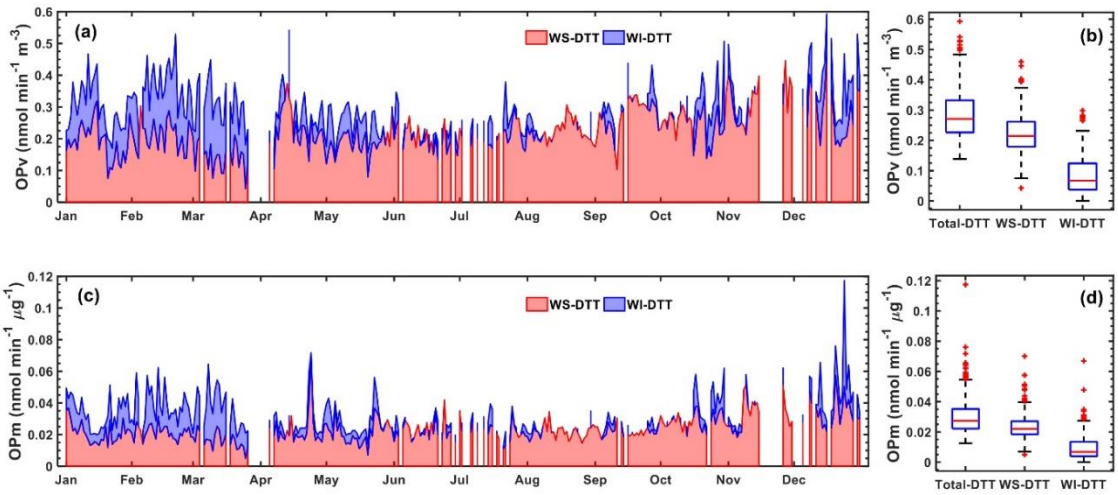

Figure 4-1. Time series (left panels) of (a) volume- (OPv) and (c) mass-normalized (OPm) OP^{DTT} (red area: $OP^{WS\text{-}DTT}$; stacked blue area: $OP^{WI\text{-}DTT}$; total area: $OP^{Total\text{-}DTT}$. $OP^{Total\text{-}DTT}$ lower than $OP^{WS\text{-}DTT}$ is not shown), and annual averages (right panels) of (b) OPv and (d) OPm.

The annual averages of $OP^{WS\text{-}DTT}$ were 0.22±0.07 nmol min^{-1} m^{-3} and 0.024±0.008 nmol min^{-1} μg^{-1} for OPv and OPm, respectively, within the typical range (0.1-1.0 nmol min^{-1} m^{-3} for OPv and 0.005-0.1 nmol min^{-1} μg^{-1} for OPm) measured at this site previously (Fang et al., 2015b). The levels of $OP^{Total\text{-}DTT}$ were generally higher than $OP^{WS\text{-}DTT}$, consistent with our previous study (Gao et al., 2017), clearly demonstrating a measurable contribution of insoluble species to overall PM OP. Compared to $OP^{WI\text{-}DTT}$, $OP^{WS\text{-}DTT}$ accounted for a larger fraction of $OP^{Total\text{-}DTT}$ (81±22 %), and the contribution of $OP^{WS\text{-}DTT}$ increased during summer (94±16 %) and diminished in winter (65±13 %). The proximity of $OP^{WS\text{-}DTT}$ to $OP^{Total\text{-}DTT}$ in summer may be attributed to the stronger secondary oxidation processes which have been found to play an important role in aging aerosols and enhancing the water-soluble OP^{DTT} (Li et al., 2009; Verma et al., 2009a; Verma et al., 2015b). Our previous

findings demonstrated a slightly lower water-soluble OP fraction (or higher insoluble fraction) at a site closer to a highway, with $OP^{WS\text{-}DTT}$ to $OP^{Total\text{-}DTT}$ ratios of 62% (adjacent to 75/85 interstate highway) and 65% (Georgia Tech campus, 430 m from highway) (Gao et al., 2017). This may suggest that the Jefferson Street site is more affected by secondary aerosols with increased solubility in water than the near highway sites. The level of $OP^{WI\text{-}DTT}$ in winter (0.12±0.06 nmol min^{-1} m^{-3} for OPv and 0.014±0.009 nmol min^{-1} μg^{-1} for OPm) was much higher than the level in summer (0.04±0.03 nmol min^{-1} m^{-3} for OPv and 0.004±0.003 nmol min^{-1} μg^{-1} for OPm), indicating sources more associated with the cold season, such as biomass burning, may be a major source for $OP^{WI\text{-}DTT}$ in winter.

4.4.2 Correlations of OP^{DTT} with PM chemical composition

Pearson's correlation coefficients for the linear regression between OP^{DTT} and select chemical components were calculated and are discussed in the subsections below. In this analysis, we present only the relevant species which are either used as specific emission markers (Ca, Mg and Al, mineral dust; BrC and K, biomass burning; WSOC and SO_4^{2-}, secondary processes) or possibly play a role in ROS generation (Fe, Cu, Mn, Zn). The regression was conducted on both OPv and OPm.

4.4.2.1 Volume-normalized OP with PM species concentrations

Pearson's correlation coefficients between volume-normalized OP^{DTT} and the ambient concentrations of select chemical components are shown graphically in Fig. 4-2. A detailed correlation table is given in Table C-2. For the sake of clarity, all types of OP^{DTT} mentioned in this subsection are volume-normalized OP.

Generally, both $OP^{WS\text{-}DTT}$ and $OP^{WI\text{-}DTT}$ were correlated with $OP^{Total\text{-}DTT}$ (Table C-2), but there was no correlation (r = -0.07) between $OP^{WS\text{-}DTT}$ and $OP^{WI\text{-}DTT}$, suggesting differing chemical determinants of $OP^{WS\text{-}DTT}$ and $OP^{WI\text{-}DTT}$. Both $OP^{WS\text{-}DTT}$ and $OP^{Total\text{-}DTT}$ showed correlations with $PM_{2.5}$ mass concentration, with r=0.55 and 0.43, respectively. The correlations of $OP^{WS\text{-}DTT}$ and $OP^{Total\text{-}DTT}$ with PM species were in general similar, both broadly correlated with aerosol species, ranging from metals to EC and OC. These results are in agreement with our previous study conducted in Atlanta during springtime (Gao et al., 2017), though the correlations reported here were less strong, possibly due to seasonality in emission sources and weather conditions. BrC, of which biomass burning is by far the largest source (Hecobian et al., 2010; Zhang et al., 2011), was highly correlated with $OP^{Total\text{-}DTT}$ (r=0.74), but its correlation with $OP^{WS\text{-}DTT}$ was weaker (r=0.41). $OP^{WI\text{-}DTT}$, determined by the difference between $OP^{Total\text{-}DTT}$ and $OP^{WS\text{-}DTT}$, was also observed to be correlated with BrC with Pearson's r=0.56. The concurrent correlation of $OP^{Total\text{-}DTT}$ with BrC and K (r=0.54 and 0.43 for WS-K and Total-K, respectively) reflects the contribution of biomass burning to $OP^{Total\text{-}DTT}$. As for the correlations of OPv with metals, $OP^{WS\text{-}DTT}$ had better correlations with water-soluble metals, such as water-soluble K, Fe, and Cu, than with total metals. However, $OP^{Total\text{-}DTT}$ was more correlated with total metals, including total K, Mn and Fe (r=0.43–0.50), suggesting possible OP contributions of species on the surfaces of these water-insoluble metals. $OP^{WI\text{-}DTT}$ was moderately correlated with total Mg (r=0.45) and weakly correlated with other total metals (r<0.30).

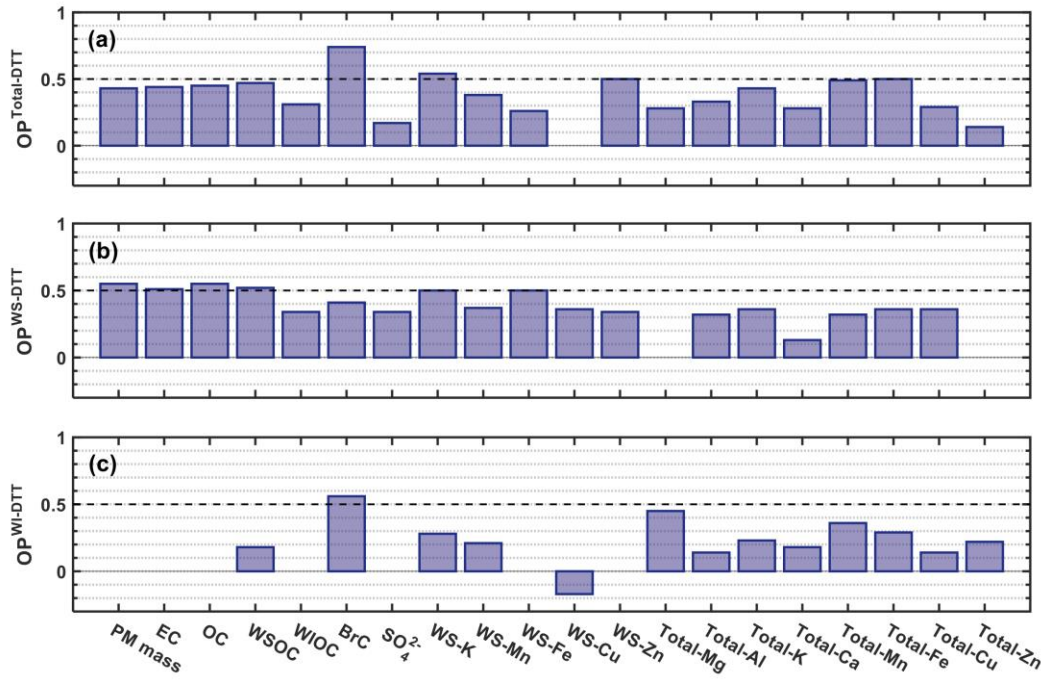

Figure 4-2. Correlation coefficients (Pearson's r) of volume-normalized (a) $OP^{Total\text{-}DTT}$, (b) $OP^{WS\text{-}DTT}$, and (c) $OP^{WI\text{-}DTT}$ with ambient concentrations of select PM components. The correlations not statistically significant (p>0.05) are omitted from the graph.

4.4.2.2 Mass-normalized OP with PM species mass fractions

The correlations of mass-normalized measures of OP^{DTT} (intrinsic OP^{DTT}) with mass fractions of chemical species were used to evaluate variation in OP^{DTT} resulting from differences in PM chemical composition. The correlation coefficients are graphically shown in Fig. 4-3, with detailed correlation table provided in Table C-3. Compared to OPv, OPm displayed different associations with PM species. The correlations of the intrinsic $OP^{WS\text{-}DTT}$ with OC and WIOC mass fractions were not significant, and only a weak correlation with WSOC (r=0.2) was observed. Studies have shown diverse intrinsic $OP^{WS\text{-}}$

^{DTT} for organic aerosol components linked to different emission sources and atmospheric conditions (Tuet et al., 2017; Verma et al., 2015a; Verma et al., 2015b). OC (or WSOC), as an aggregate measure of PM organic compounds, may mask the variability in concentrations of individual organic compounds with varying intrinsic redox activity, leading to poor correlations observed between intrinsic $OP^{WS\text{-}DTT}$ and OC. The intrinsic $OP^{WS\text{-}DTT}$ was mainly associated with Cu (r=0.30 and 0.41 for water-soluble and total Cu, respectively) and total mineral dust constituents, such as total Al and Ca (r=0.57 and 0.55, respectively). The water-soluble metals exhibited a weak linear relationship with the intrinsic $OP^{WS\text{-}DTT}$, consistent with the nonlinear behavior of water-soluble metals with DTT oxidation (Charrier and Anastasio, 2012) and the synergistic or antagonistic interactions between water-soluble organic compounds and metals (Yu et al., 2018), but in contrast to a number of previous studies (Hu et al., 2008; Verma et al., 2009b; Yang et al., 2014) where good correlations between intrinsic $OP^{WS\text{-}DTT}$ and water-soluble metals were found, possibly due to common origins of transition metals with other redox-active species.

As for the intrinsic $OP^{Total\text{-}DTT}$ and $OP^{WI\text{-}DTT}$, both had relatively strong positive correlations with mass-normalized BrC, suggesting the contribution of incomplete combustion to $OP^{Total\text{-}DTT}$ and $OP^{WI\text{-}DTT}$. Total metals, especially total crustal elements, such as total Mg, Al, and Ca, and two DTT-active metals, Mn and Cu, appear to be contributing factors to both intrinsic $OP^{Total\text{-}DTT}$ and $OP^{WI\text{-}DTT}$, as indicated from the moderate correlations (r=0.29-0.62 for $OP^{Total\text{-}DTT}$ and r=0.39-0.54 for $OP^{WI\text{-}DTT}$). The correlations with mineral dust may be attributed to the surface properties of dust. Studies have found that organic compounds could be absorbed on the surface of mineral dust (Falkovich et al., 2004), and the reactive surface property of mineral aerosol could accelerate the heterogeneous

nitration of dust-bound PAHs and enhance the toxicity of aerosol (Kameda et al., 2016). In the study of Fang et al. (2017), the coarse-mode water-insoluble OP^{DTT} has been found to match well with the mineral dust surface area distribution, also suggesting a connection between $OP^{WI\text{-}DTT}$ and dust surface property.

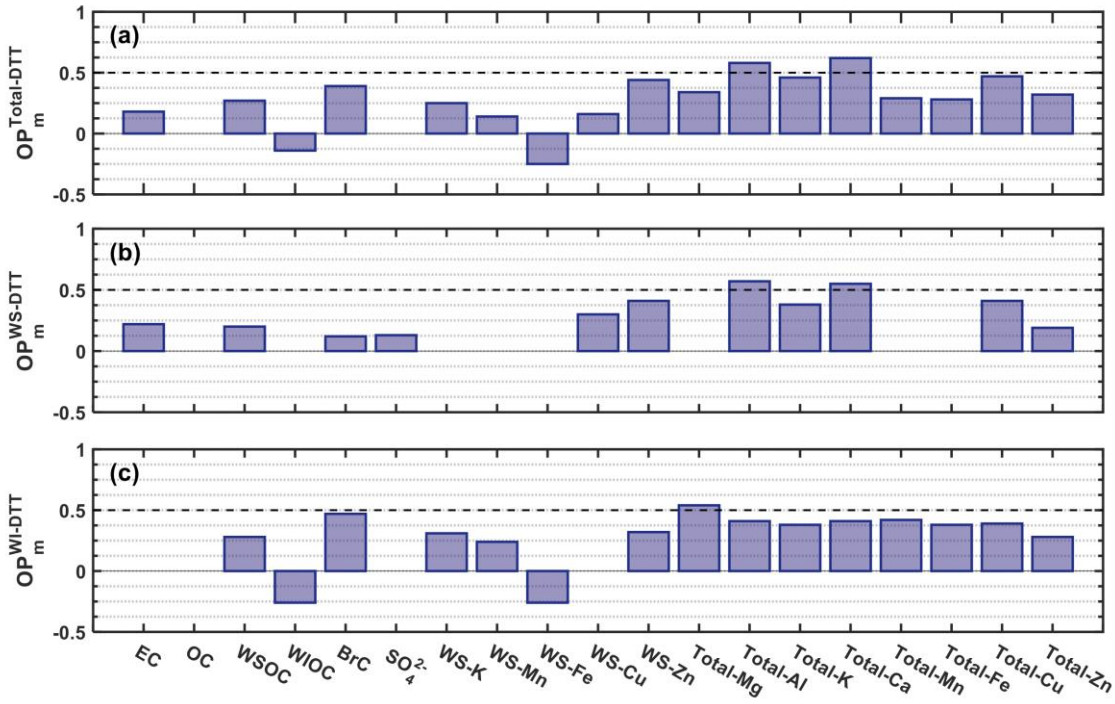

Figure 4-3. Correlation coefficients (Pearson's r) of mass-normalized (a) $OP^{Total\text{-}DTT}$, (b) $OP^{WS\text{-}DTT}$, and (c) $OP^{WI\text{-}DTT}$ with select PM components. The correlations not statistically significant ($p>0.05$) are omitted from the graph. To be distinguished from Fig. 4-2, a subscript "m" was used to denote mass-normalized OP.

4.4.3 Multivariate regression model

4.4.3.1 General regression model

We used multivariate stepwise linear regression to identify the most significant observed variables accounting for the variation in the volume-normalized OP^{DTT} measurements. The regression for the $OP^{WS\text{-}DTT}$ measurements has been discussed elsewhere (Gao et al., 2019). In this analysis, considering the large uncertainties associated with $OP^{WI\text{-}DTT}$, multivariate regression analysis was limited only to $OP^{Total\text{-}DTT}$.

PM components most correlated with $OP^{Total\text{-}DTT}$ (Fig. 4-2 and Table C-2) were used as independent variables to develop the multivariate model, including EC, BrC, total K, total Fe, and total Mn. Total Cu, though weakly correlated with $OP^{Total\text{-}DTT}$ (r=0.29), was also included due to the redox activity of Cu in DTT oxidation (Charrier and Anastasio, 2012). The final regression for $OP^{Total\text{-}DTT}$ is

$$OP^{Total\text{-}DTT} = 4.2E\text{-}2*EC + 1.1E\text{-}1*BrC + 9.9E\text{-}1*TotalCu - 6.5E\text{-}1*(BrC*TotalCu) + 0.17$$

All species except BrC are in units of μg m^{-3}; the unit for BrC is Mm^{-1}. The regression model explained 55% variance in $OP^{Total\text{-}DTT}$, and the mean squared error was 0.0031 nmol min^{-1} m^{-3} (1.1% of $OP^{Total\text{-}DTT}$ mean of measurements).

The $OP^{WS\text{-}DTT}$ regression model obtained from our previous work suggested that the variability of $OP^{WS\text{-}DTT}$ was related to water-soluble metals (Fe and Cu), organic species correlated with BrC (e.g., incomplete combustion products), and the antagonistic interactions between BrC and water-soluble Cu and between water-soluble Fe and Cu (Gao et al., 2019). Similar to $OP^{WS\text{-}DTT}$, the regression model for $OP^{Total\text{-}DTT}$ captures the

contributions from BrC, Cu, and the interaction between BrC and Cu. Note that the $OP^{WS\text{-}DTT}$ model was related to water-soluble Cu, whereas the $OP^{Total\text{-}DTT}$ model involved total Cu. The presence of total Cu in the $OP^{Total\text{-}DTT}$ model may suggest the contribution from both water-soluble and a surface property of insoluble Cu. In the study of Zhou et al. (Zhou et al., 2003), a synergistic interaction between soot and insoluble iron particles was observed for the induction of oxidative stress in the lungs of rats. It was postulated that soot could convert insoluble iron particles to more biologically active form, and could also allow particle solubilization by impeding clearance of iron particles from the lungs. It is reasonable to hypothesize that water-insoluble Cu could contribute OP^{DTT} by participating in similar processes and getting solubilized gradually during the DTT measurement. The presence of BrC in the $OP^{Total\text{-}DTT}$ model is as expected. Studies have shown that the humic-like substances (HULIS), especially quinones, was the major group of water-soluble organic components driving the ROS generation mechanism (Lin and Yu, 2011; Verma et al., 2015a; Verma et al., 2015b). BrC, which has been found to predominantly represent HULIS fraction of PM extracts (Verma et al., 2012), indicates the contribution of HULIS in $OP^{Total\text{-}DTT}$. The interaction term between total Cu and BrC is consistent with the antagonistic effect of Cu with HULIS compounds in oxidizing DTT observed by Yu et al. (Yu et al., 2018), and may be explained by the binding between Cu and organics (Wang et al., 2018).

Compared to $OP^{WS\text{-}DTT}$, the variability of $OP^{Total\text{-}DTT}$ was related to EC, one of the insoluble species in PM, rather than water-soluble Fe, a species with low intrinsic redox activity. As discussed in our previous work, the water-soluble Fe in the $OP^{WS\text{-}DTT}$ model may be a surrogate measure of co-emitted redox-active species that was not quantified. EC, in this

case, may also be a representative of incomplete combustion products, such as the products from vehicular emissions. Moreover, the EC term is also consistent with the observed OP contribution resulting from EC-surface-bound organic species, such as quinones (Antinolo et al., 2015).

The time series of reconstituted $OP^{Total\text{-}DTT}$, along with the relative contribution of each model variable to the estimated $OP^{Total\text{-}DTT}$, is shown in Fig. 4-4. Overall, compared to the other species, BrC was the dominant contributor to the estimated $OP^{Total\text{-}DTT}$. The relative contribution of BrC to $OP^{Total\text{-}DTT}$ was higher in winter, consistent with biomass burning being a strong source in winter. In summer, total Cu contributed a relatively large fraction of $OP^{Total\text{-}DTT}$, possibly due to the enhanced metal dissolution resulting from the strong secondary oxidation processes (Fang et al., 2017b). Even though the relative contribution of EC was also higher in summer, the absolute EC contribution to $OP^{Total\text{-}DTT}$ remained stable throughout the year, which is because of little seasonal variability in EC.

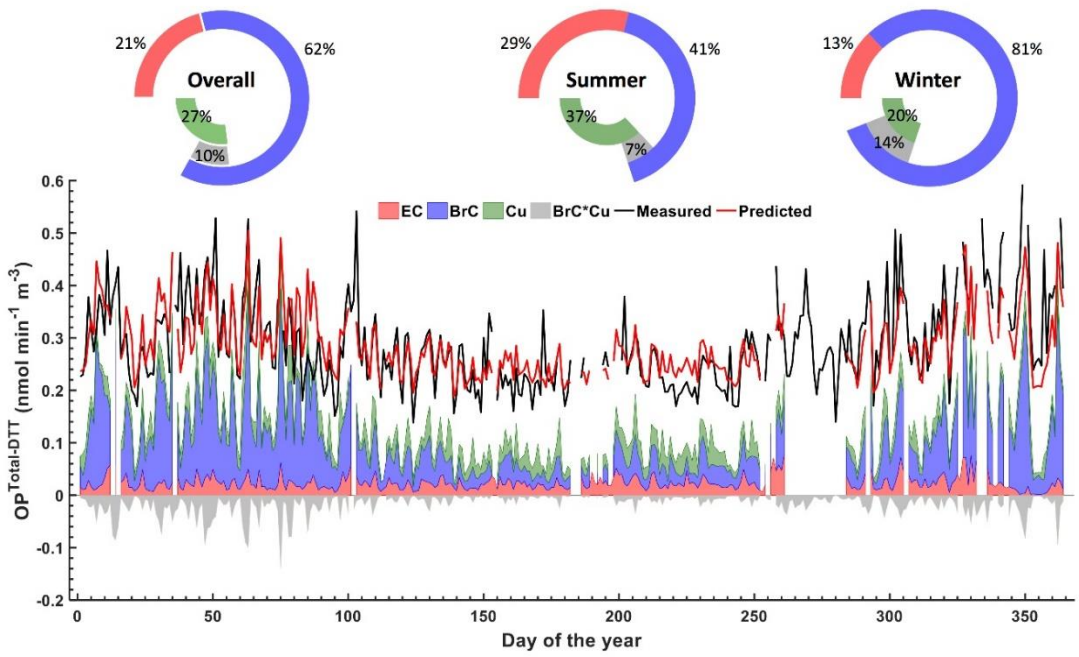

Figure 4-4. Time series of measured and predicted $OP^{Total\text{-}DTT}$ and the contribution of specific species to daily estimated $OP^{Total\text{-}DTT}$ (intercept not shown). The multi-level pie charts show the relative contribution of each model variable to the estimated $OP^{Total\text{-}DTT}$ during the whole sampling period, summer and winter. The Cu in the graph is total Cu.

4.4.3.2 Seasonal analysis

Multivariate regression was conducted for $OP^{Total\text{-}DTT}$ measured in different seasons, and the results are given in Table 4-1. In summer, EC and water-soluble Fe explained 27.7% of the variability in $OP^{Total\text{-}DTT}$. Since EC and water-soluble Fe were highly inter-correlated in summer (Pearson's r = 0.67; Table A-2), the presence of these two terms may suggest the contributions from the common origins of these two species, such as vehicular emissions. Moreover, water-soluble Fe has been found to be a dominant species driving the variability of water-soluble OP^{DTT} (Gao et al., 2019), and thus water-soluble Fe in $OP^{Total\text{-}DTT}$ summer model may result from the large fraction of $OP^{WS\text{-}DTT}$ in $OP^{Total\text{-}DTT}$

(94±16 %) in summer (Fig. 4-1). In winter, the variability of $OP^{Total\text{-}DTT}$ was driven by BrC, suggesting the strong impact of biomass burning.

Table 4-1. Multivariate regression models for $OP^{Total\text{-}DTT}$ in summer and winter.

	summer			winter	
	EC	WS-Fe	intercept	BrC	intercept
coef	5.2E-2	1.2	1.8E-1	9.5E-2	2.2E-1
SD	2.5E-2	4.8E-1	1.1E-2	1.4E-2	2.0E-2
R^2	0.277			0.434	

Note: The values represent the coefficients for variables. The units of EC and water-soluble Fe are μg m^{-3}; the unit of BrC is Mm^{-1}.

The coefficients of the regression models may provide information about the intrinsic property of the specific aerosol species. However, due to the inter-correlation between the predictor variables, the coefficients cannot be compared directly between models without eliminating the collinearity.

4.4.3.3 Uncertainty analysis

If the $OP^{Total\text{-}DTT}$ model coefficients are assumed to be known exactly, the uncertainty of the overall $OP^{Total\text{-}DTT}$ model can be evaluated based upon uncertainty of independent variables. The regression model of $OP^{Total\text{-}DTT}$ shows that the dependent variable is a function of aerosol species (EC, BrC and total Cu). That is

$$y = f(x_1, x_2, \ldots x_n) \qquad (2)$$

where y represents the dependent variable (i.e., $OP^{Total\text{-}DTT}$), x_i denotes the aerosol species.

The combined uncertainty is calculated as follows,

$$\Delta y = \sqrt{\sum_{i=1}^{n} (\frac{\partial f}{\partial x_i} \Delta x_i)^2} \qquad (3)$$

Specifically, for $y = a \cdot EC + b \cdot BrC + c \cdot TotalCu + d \cdot (BrC * TotalCu) + e$, where a–e are the model coefficients,

$$\Delta y = \sqrt{\left(\frac{\partial f}{\partial EC} \Delta EC\right)^2 + \left(\frac{\partial f}{\partial BrC} \Delta BrC\right)^2 + \left(\frac{\partial f}{\partial TotalCu} \Delta TotalCu\right)^2} =$$

$$\sqrt{(a \cdot \Delta EC)^2 + [(b + d \cdot TotalCu) \cdot \Delta BrC]^2 + [(c + d \cdot BrC) \cdot \Delta TotalCu]^2} \qquad (4)$$

According to the measurements, the relative uncertainty of EC was within 10 %. Based on the relative uncertainty in sample handling and blank correction, the relative uncertainty of BrC was approximately 12 %. Similarly, the uncertainty of total Cu concentration was determined based on uncertainty in sampling, extraction and calibration, which was on average 1.28 ng m^{-3} (~6.6 % of the measurements). The overall combined uncertainty of modeled $OP^{Total\text{-}DTT}$ was calculated using equation (4), and the relative uncertainty was (33 ± 14) %. The uncertainty of the direct OP measures, on the other hand, was calculated using the uncertainty of replicate measurements which was within 5% (Gao et al., 2017) and uncertainty in field blanks (0.07 nmol min^{-1} m^{-3}). The final relative uncertainty of measured $OP^{Total\text{-}DTT}$ was (26 ± 7) %. Therefore, the precision of the estimated $OP^{Total\text{-}DTT}$ is very close to that of the measured $OP^{Total\text{-}DTT}$. However, considering the statistical uncertainties associated with the variable coefficients, the regression model is less precise compared to the direct OP measurements.

4.4.3.4 Sensitivity analysis

Standardized regression was used to rescale the variables measured in different units and eliminate the collinearity among the independent variables. The standardized coefficients are interpreted as the change in OP for one-unit change in predictor variable. The absolute values of standardized regression coefficients indicate the relative importance of these variables, and they are comparable not only across different variables but also between models. Table 4-2 shows the standardized coefficients for the $OP^{Total\text{-}DTT}$ model, and the standardized regression results for $OP^{WS\text{-}DTT}$ were also included for comparison.

Table 4-2. Regression coefficients for each variable in the $OP^{Total\text{-}DTT}$ and $OP^{WS\text{-}DTT}$ regression with standardized data

$OP^{Total\text{-}DTT}$		$OP^{WS\text{-}DTT}$	
Variable	Standardized coef	Variable	Standardized coef
EC	0.17±0.05	WS-Fe	0.46±0.06
BrC	0.66±0.04	BrC	0.35±0.05
Total-Cu	0.10±0.04	WS-Cu	0.12±0.05
Metal-organic	-0.08±0.04	Metal-organic	-0.11±0.06
		Metal-metal	-0.10±0.05

Note: WS-Fe and WS-Cu represent water-soluble iron and water-soluble copper, respectively. The $OP^{WS\text{-}DTT}$ results were discussed in detail in Gao et al. (2019).

As shown in Table 4-2, $OP^{Total\text{-}DTT}$ was most sensitive to the change in BrC, followed by EC, total Cu and metal-organic interaction. The sensitivity of $OP^{Total\text{-}DTT}$ to BrC was almost

twice the $OP^{WS\text{-}DTT}$ sensitivity, suggesting that BrC or related sources may drive the variation in water-insoluble fraction of OP^{DTT}. This is consistent with the moderate correlation observed between BrC and $OP^{WI\text{-}DTT}$. The standardized coefficients of the Cu terms in the two models were close to each other. However, considering that water-soluble Cu only accounts for 51±22 % of the total Cu concentration, one-unit change in total Cu would lead to a greater change in $OP^{Total\text{-}DTT}$ than in $OP^{WS\text{-}DTT}$. This may imply the effects of water-insoluble Cu on $OP^{WI\text{-}DTT}$.

4.5 Conclusions

We employed the DTT assay to quantify the oxidative potential of total $PM_{2.5}$ ($OP^{Total\text{-}DTT}$), water-soluble $PM_{2.5}$ fraction ($OP^{WS\text{-}DTT}$), and water-insoluble $PM_{2.5}$ fraction ($OP^{WI\text{-}DTT}$). Approximately 350 $PM_{2.5}$ filter samples collected from urban Atlanta were analyzed for OP^{DTT} and aerosol species. The results illustrated that both water-soluble and insoluble portions of PM play important roles in PM OP, with water-soluble species contributing a large fraction of $OP^{Total\text{-}DTT}$ (81±22 %). Seasonal differences are discernible in both volume- and mass-normalized $OP^{Total\text{-}DTT}$ and $OP^{WI\text{-}DTT}$, but not $OP^{WS\text{-}DTT}$, with higher levels in the winter than in the summer. Linear regression between PM components and OP^{DTT} indicated that all volume-normalized OP^{DTT} were correlated with organic species and metals, and the intrinsic $OP^{Total\text{-}DTT}$ and $OP^{WI\text{-}DTT}$ were mainly associated with BrC and total metals (especially the total crustal elements). A multivariate regression model was derived for $OP^{Total\text{-}DTT}$, showing that the variability of $OP^{Total\text{-}DTT}$ was attributed to BrC, EC, total Cu and the antagonistic interaction between BrC and total Cu. By comparing with the $OP^{WS\text{-}DTT}$ model, it was found that BrC and water-insoluble Cu contributed to $OP^{WI\text{-}DTT}$.

$OP^{WS\text{-}DTT}$ has been linked with various cardiorespiratory end points in multiple studies (Bates et al., 2015; Fang et al., 2016). $OP^{Total\text{-}DTT}$ also appears to be a health-relevant OP measure as it has been found to be correlated with $OP^{WS\text{-}DTT}$. Nevertheless, $OP^{Total\text{-}DTT}$, which captures the OP contribution from both water-soluble and insoluble PM components, may be closer to the actual PM exposure compared to $OP^{WS\text{-}DTT}$, and thus may better explain the health effects related to PM exposure. In addition, previous studies have associated organic compounds in PM with respiratory and systemic inflammation (Delfino et al., 2010a; Delfino et al., 2010b). $OP^{Total\text{-}DTT}$, as demonstrated in our results, is primarily dominated by BrC, therefore, an association between $OP^{Total\text{-}DTT}$ and these organics-driven health effects could be expected.

It should be noted that the water-insoluble OP in this study is operationally defined by the OP analysis method and very likely cannot fully characterize the oxidative properties of all water-insoluble species. For example, PAHs adsorbed onto particles can undergo biotransformation into quinones *in vivo*, inducing oxidative stress (Kelly, 2003). However, we are unable to quantify the OP formed through this route using the DTT assay since PAHs are not DTT-active. Nonetheless, the DTT assay tends to provide a more comprehensive measure of aerosol oxidative potential than many other currently available OP assays (Bates et al., 2019).

CHAPTER 5. CONCLUSIONS AND FUTURE WORK

5.1 Summary of findings

PM oxidative potential has been proposed as a health-related exposure metric for air quality assessment. The findings from previous and current studies conducted in Atlanta region are briefly summarized in Fig. 5-1c. In previous studies (Fig. 5-1a), the ambient PM data collected at the JST site have been extensively used to investigate the sources, associated PM species and health effects of OP. Water-soluble OP measured by the DTT assay was the focus of the past studies.

As shown in Fig. 5-1b, the water-soluble OP assessment in this dissertation was extended to include the RTLF assay, providing a contrast to the DTT assay. This dissertation shows that antioxidants in the DTT and the RTLF assay responded to different OP components. OP^{DTT} and OP^{AA} were more chemically integrative OP measures, which were associated with organic species, transition metal ions, and the interactions among the species. OP^{GSH} was predominantly sensitive to water-soluble Cu. AA response in the RTLF assay was affected by the composition of synthetic lung fluid, emphasizing the importance of developing a "standard" method. Due to little seasonality in the combined PM constituents, no substantial temporal variation was observed for these OP measures.

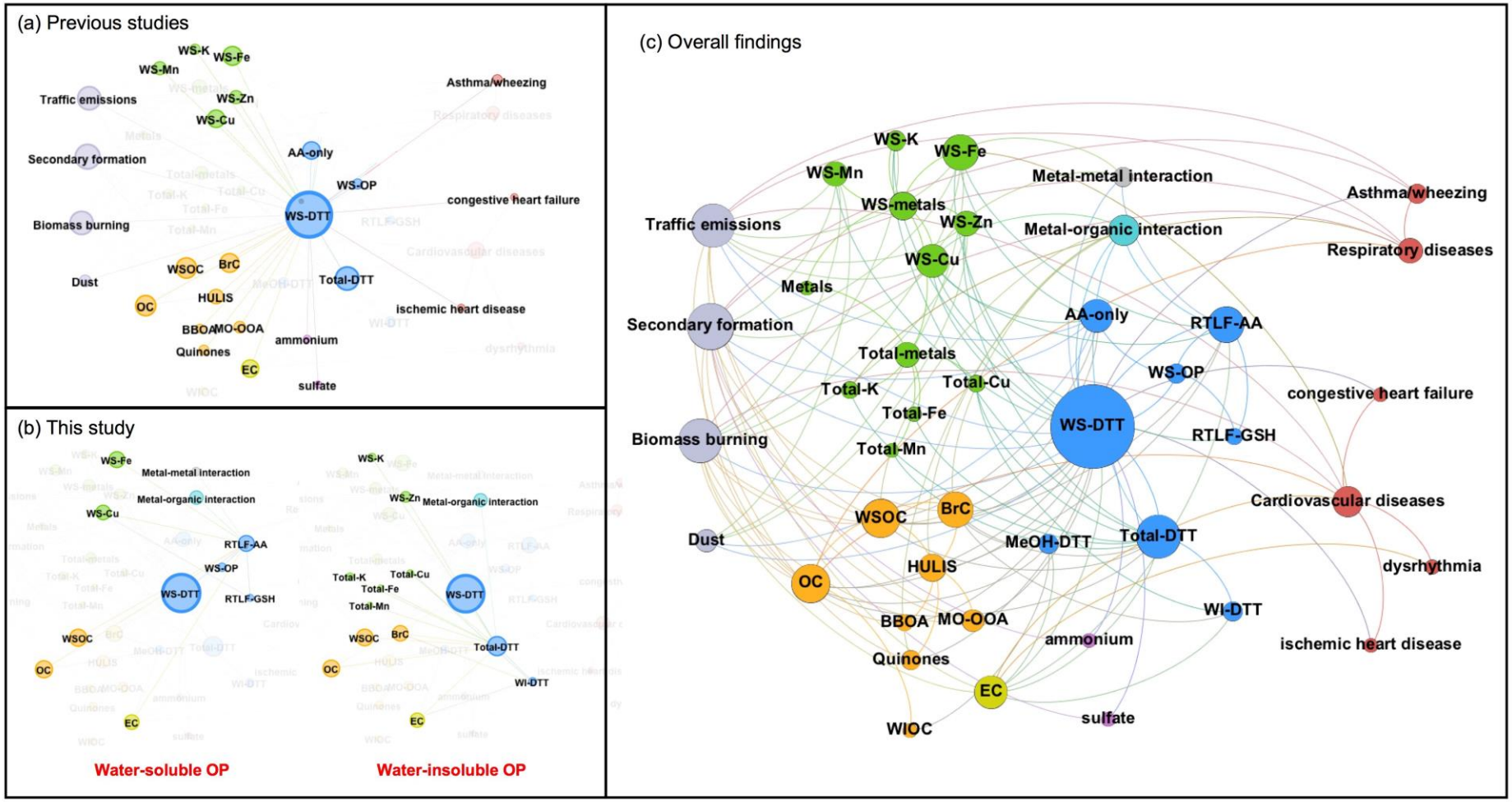

Figure 5-1. Network graphs summarizing the connections found in (a) previous and (b) current studies using the JST data among the OP measures (blue nodes), PM species, emission sources (light purple nodes) and health effects (red nodes). The overall

findings are shown in (c). Green nodes represent trace metals in PM; yellow nodes are PM organic components; other PM species, such as EC and inorganic ions, are presented using different colors. The size of a node is proportional to its degree of freedom.

In this dissertation, water-insoluble OP assessed using the DTT assay was also evaluated and characterized. The commonly used extraction methodologies (water vs. methanol, filtered extracts vs. unfiltered suspensions) were evaluated and compared. It was found that compared to organic solvent extraction, performing the DTT assay directly on the water extracts with filter remaining in the incubation vial could capture more water-insoluble OP contribution. An automated analytical DTT system was further developed to automate and facilitate water-insoluble OP measurement. The results demonstrate that water-insoluble PM contributed a significant fraction (20–35 %) of overall PM OP. Compared to an urban site, the site by the roadside which was heavily affected by primary vehicular emissions did not display higher OP levels, either for total or water-soluble OP, suggesting that insoluble OP contributors are largely secondary. Total and water-insoluble OP exhibited evident temporal variations, higher in winter and lower in warm seasons, indicating biomass burning emissions may play an important role in generating water-insoluble OP. Univariate and multivariate analyses suggested that water-insoluble OP was related to incomplete combustion products and surface properties of soot and water-insoluble metals.

To sum up, the studies conducted in Atlanta found linkages among the OP measures, PM species, emission sources, and respiratory and cardiovascular diseases. The overall findings (Fig. 5-1c) show that WSOC, especially the hydrophobic organic fraction (HULIS), and water-soluble Cu and Fe are the most important PM constituents related to PM OP. These species may be either redox active or serve as surrogate measures of unquantified redox-active species. Sources, including biomass burning, secondary processing and traffic emissions, play important roles in producing OP or OP-related

species, and thus need to be paid attention to when developing air quality control strategies aiming to protect human health.

5.2 Future work

OP measurements

In this dissertation, we assessed the relation between different OP metrics and PM chemical composition, which highlights the various sensitivities of OP assays to PM species. These OP assays may provide complementary information in elucidating health risks related to PM exposure. Therefore, in future studies, incorporating the OP responses from different assays may provide a more comprehensive picture of PM toxicity. In addition, effects of interactions among the species are identified in this work, which suggests that OP studies should not only focus on the bulk concentrations of species but also pay attention to the relative fraction of species in PM, especially the relative fraction of organic species and metals.

This thesis demonstrates that the water-insoluble OP fraction is not negligible, and biomass burning is an important source of water-insoluble OP. Therefore, including the contribution of water-insoluble species in OP assessment would be closer to actual OP exposure, especially when biomass burning is a dominant source of PM. It is necessary to measure total PM OP instead of water-soluble OP when attempting to link aerosols to adverse health effects. Measuring total OP may also be helpful in exploring the health impacts of biomass burning such as wildfires and prescribed burning.

In this thesis, we assessed the OP of ambient particles collected from a single stationary air monitoring site. The human health risks depend on personal exposure—that is, the exposures received by people in the various specific places where they spend time. The indoor environment is an important microenvironment in which people spend a large part of their time each day. In many cases, indoor exposure can considerably differ from ambient air because of various types of indoor sources of pollution, different atmospheric chemistry of the two environments, and various types of ventilation. As a result, characterization of the OP of indoor aerosol is another topic that needs extensive research.

OP modeling

This thesis and some previous studies (Bates et al., 2015; Verma et al., 2015a) have used multivariate regression models to reconstruct OP measures based on sources and species concentrations. However, as shown in this thesis, the OP responses are affected by interactions among PM species and composition of antioxidant solutions, which makes it difficult to extend, or to generalize, the results to other datasets. Several investigations are underway to predict OP based on kinetic models of biological system. Lakery et al. (2016) have developed a kinetic model of surface and bulk chemistry in the epithelial lining fluid. In a recent study (Fang et al., 2019), this model has been combined with a human respiratory tract model to investigate ROS generation induced by PM inhalation. In future studies, the kinetic model that simulates the complex physiological processes in human body could be useful for OP prediction, which would also enable implementation of large population-based investigations of PM OP.

APPENDIX A. SUPPLEMENTAL MATERIAL FOR CHAPTER 2

Table A-1. Correlation matrix for various PM components and OP metrics over the one-year sampling period.

	DTT	AA	GSH	WSOC	BrC	SO4	WS-K	WS-Mn	WS-Fe	WS-Cu	WS-Zn	OC	EC
AA	**0.606**												
GSH	0.455	**0.669**											
WSOC	0.524	0.551	0.190										
BrC	0.408	0.357	0.045	**0.602**									
SO4	0.343	0.413	0.374	0.370	0.093								
WS-K	0.174	0.486	0.304	0.071	0.042	0.482							
WS-Mn	0.387	0.377	0.191	0.553	0.380	0.404	0.363						
WS-Fe	0.502	0.472	0.169	0.483	0.137*	0.377	-0.007	0.461					
WS-Cu	0.341	0.500	**0.740**	0.203	-0.078	0.426	0.533	0.294	0.176				
WS-Zn	0.343	0.309	0.314	0.191	0.137*	0.450	**0.907**	0.483	0.179	0.510			
OC	0.546	0.497	0.105	**0.774**	0.426	0.245	0.054	0.437	0.599	0.143	0.223		
EC	0.513	0.488	0.126*	0.584	0.392	0.184	0.093	0.434	0.552	0.173	0.312	**0.833**	
PM mass	0.552	0.555	0.239	**0.747**	0.414	0.554	0.314	0.539	0.511	0.313	0.418	**0.774**	**0.639**

Note: r>0.6 are highlighted. Black without superscript: p-value<0.01; *p-value<0.05; grey: not statistically significant.

Table A-2. Correlation matrix for PM components and OP metrics (Summer, Jun-Aug/2017).

Summer	DTT	AA	GSH	WSOC	BrC	SO4	WS-K	WS-Mn	WS-Fe	WS-Cu	WS-Zn	OC	EC
AA	**0.656**												
GSH	**0.695**	**0.784**											
WSOC	0.412	0.244*	0.202										
BrC	0.510	0.330	0.137	**0.818**									
SO4	0.477	0.425	0.350	0.479	0.323								
WS-K	0.464	0.322	0.085	**0.708**	0.566	0.442							
WS-Mn	**0.611**	0.345	0.134	0.457	0.410	0.319	**0.616**						
WS-Fe	0.587	0.428	0.212	**0.683**	**0.762**	0.395	0.500	0.428					
WS-Cu	**0.648**	0.515	**0.791**	0.400	0.300	0.479	0.220	0.312	0.418				
WS-Zn	0.457	0.326	0.110	0.526	0.518	0.168	0.426	0.518	0.573	0.262*			
OC	0.400	0.161	0.030	**0.810**	**0.761**	0.405	**0.643**	0.418	**0.730**	0.266*	**0.624**		
EC	0.386	0.114	0.007	0.442	0.540	0.082	0.233*	0.284	**0.668**	0.197	**0.678**	**0.640**	
PM mass	0.486	0.229*	0.188	**0.606**	0.459	0.578	0.451	0.384	0.455	0.264*	0.312	**0.728**	0.368

Note: r>0.6 are highlighted. Black without superscript: p-value<0.01; *p-value<0.05; grey: not statistically significant.

Table A-3. Correlation matrix for PM components and OP metrics (Winter, Jan-Feb/2017 and Dec/2017).

Winter	DTT	AA	GSH	WSOC	BrC	SO4	WS-K	WS-Mn	WS-Fe	WS-Cu	WS-Zn	OC	EC
AA	0.534												
GSH	0.498	**0.616**											
WSOC	0.538	**0.659**	0.383										
BrC	**0.689**	0.514	0.332	**0.758**									
SO4	0.183*	0.332	0.268	0.275	0.067								
WS-K	0.563	0.523	0.333	**0.779**	**0.682**	0.288							
WS-Mn	0.373	0.492	0.284	0.589	0.540	0.220	**0.651**						
WS-Fe	0.483	0.518	0.239	0.422	0.213*	0.294	0.259	0.429					
WS-Cu	0.308	**0.601**	**0.776**	0.437	0.209*	0.339	0.343	0.227	0.294				
WS-Zn	0.309	0.414	0.140	0.461	0.450	0.016	0.368	0.524	0.495	0.185*			
OC	0.501	**0.613**	0.256	**0.748**	0.506	0.152	0.456	0.433	0.508	0.346	0.549		
EC	0.439	0.600	0.282	0.574	0.380	0.110	0.347	0.403	0.481	0.370	**0.667**	**0.874**	
PM mass	0.542	**0.701**	0.361	**0.825**	**0.645**	0.397	**0.720**	0.499	0.513	0.385	0.540	**0.789**	**0.670**

Note: r>0.6 are highlighted. Black without superscript: p-value<0.01; *p-value<0.05; grey: not statistically significant.

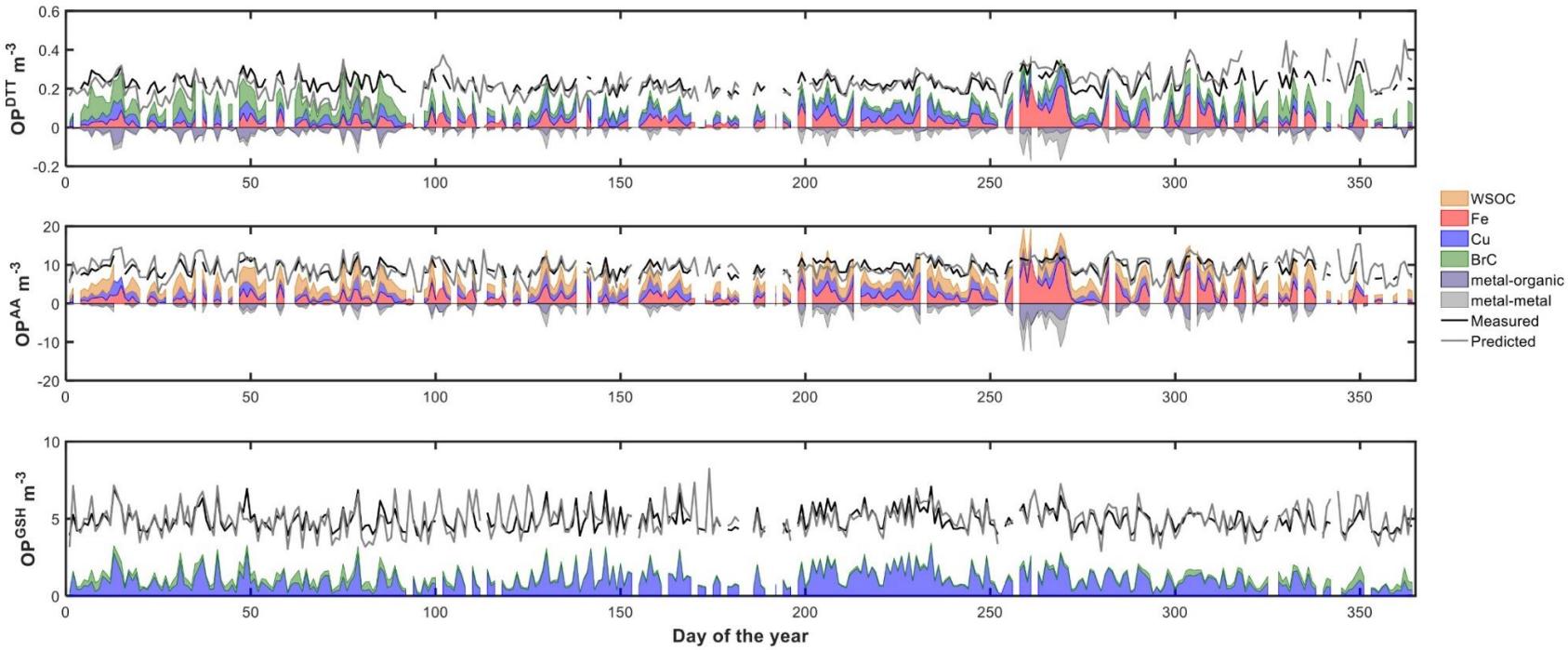

Figure A-1. Time series of measured and predicted OP measures and the contributions of model variables to OPs (intercepts are not shown).

APPENDIX B. SUPPLEMENTAL MATERIAL FOR CHAPTER 3

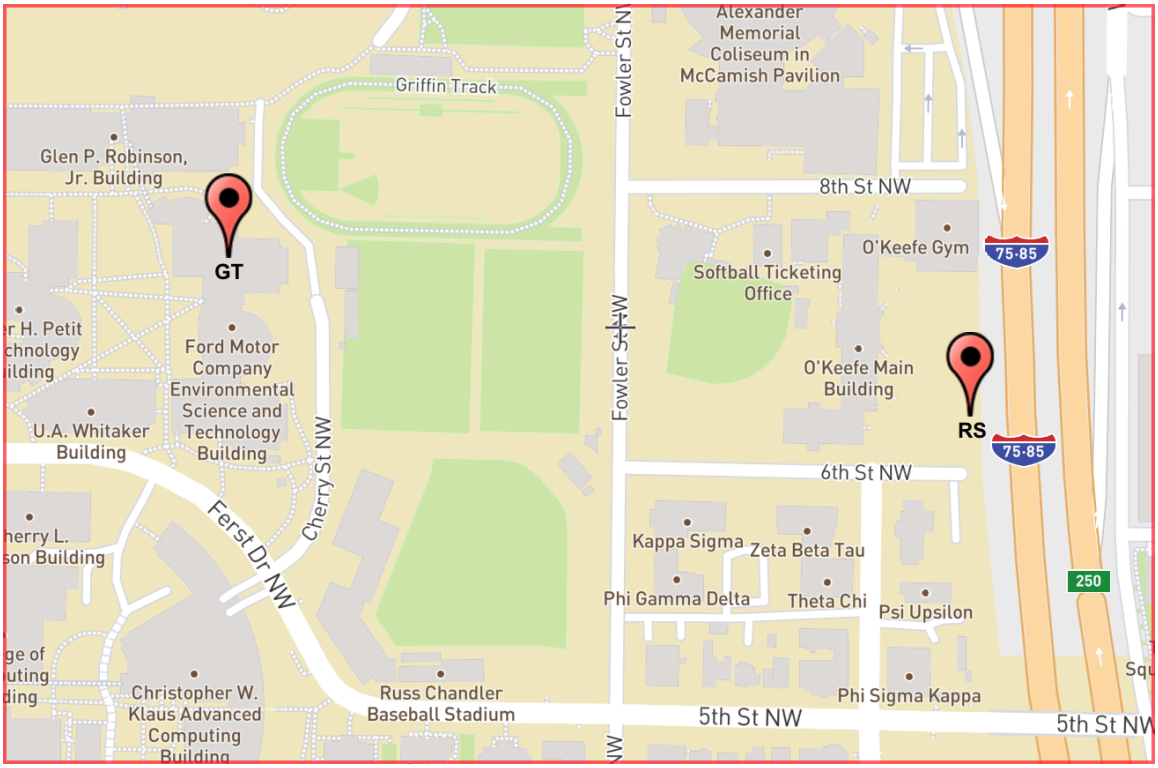

Figure B-1. Map of sampling sites (Scale is 1:5000). (Map data ©2016 Google Imagery ©2016, DigitalGlobe, Sanborn, U.S. Geological Survey, USDA Farm Service Agency.)

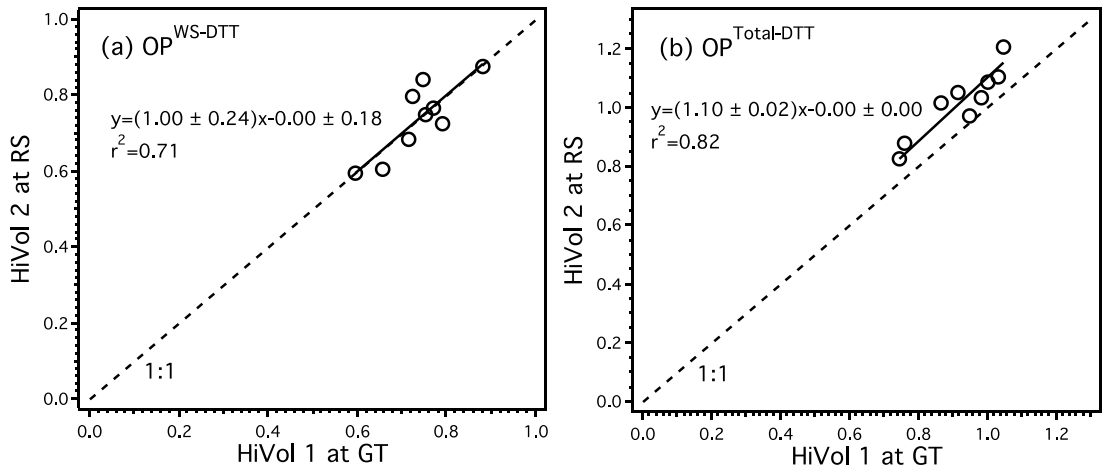

Figure B-2. (a) $OP^{WS\text{-}DTT}$ (N=9) and (b) $OP^{Total\text{-}DTT}$ (N=9) comparisons for PM samples collected simultaneously at GT using two HiVol sampler. Regression analysis was done by orthogonal regression. The dotted line is 1:1.

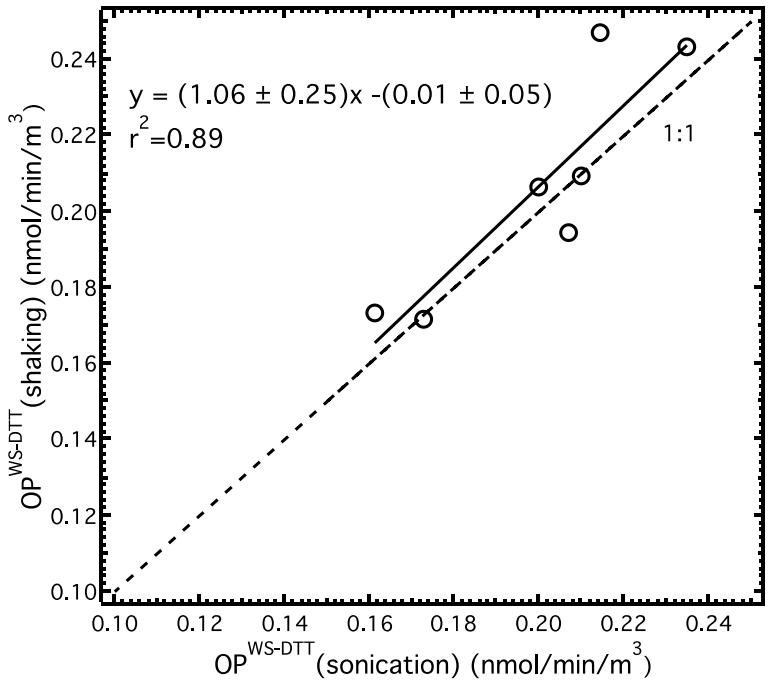

Figure B-3. 30-minute sonication vs. 2.5-hour shaking comparison for $OP^{WS\text{-}DTT}$ measurements (N=7). Regression analysis was done by orthogonal regression. The dotted line is 1:1.

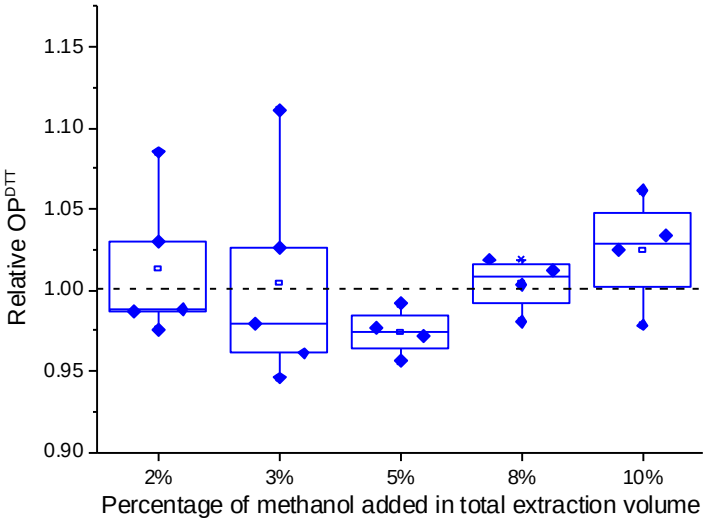

Figure B-4. The relative OP^{DTT} response (the ratio of OP^{DTT} extracted by methanol-containing solvent to OP^{DTT} extracted by DI only) to adding small amount of methanol into extraction solvent.

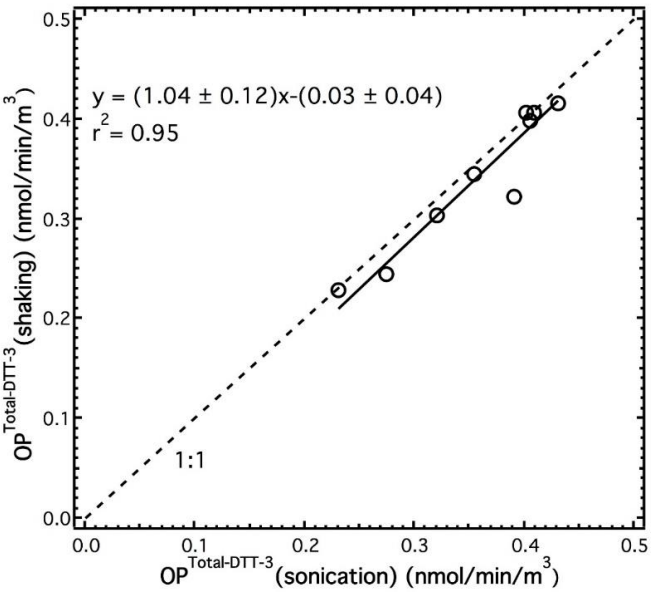

Figure B-5. 30-minute sonication vs. 2.5-hour shaking comparison for $OP^{Total\text{-}DTT\text{-}3}$ measurements (N=9). Regression analysis was done by orthogonal regression. The dotted line is 1:1.

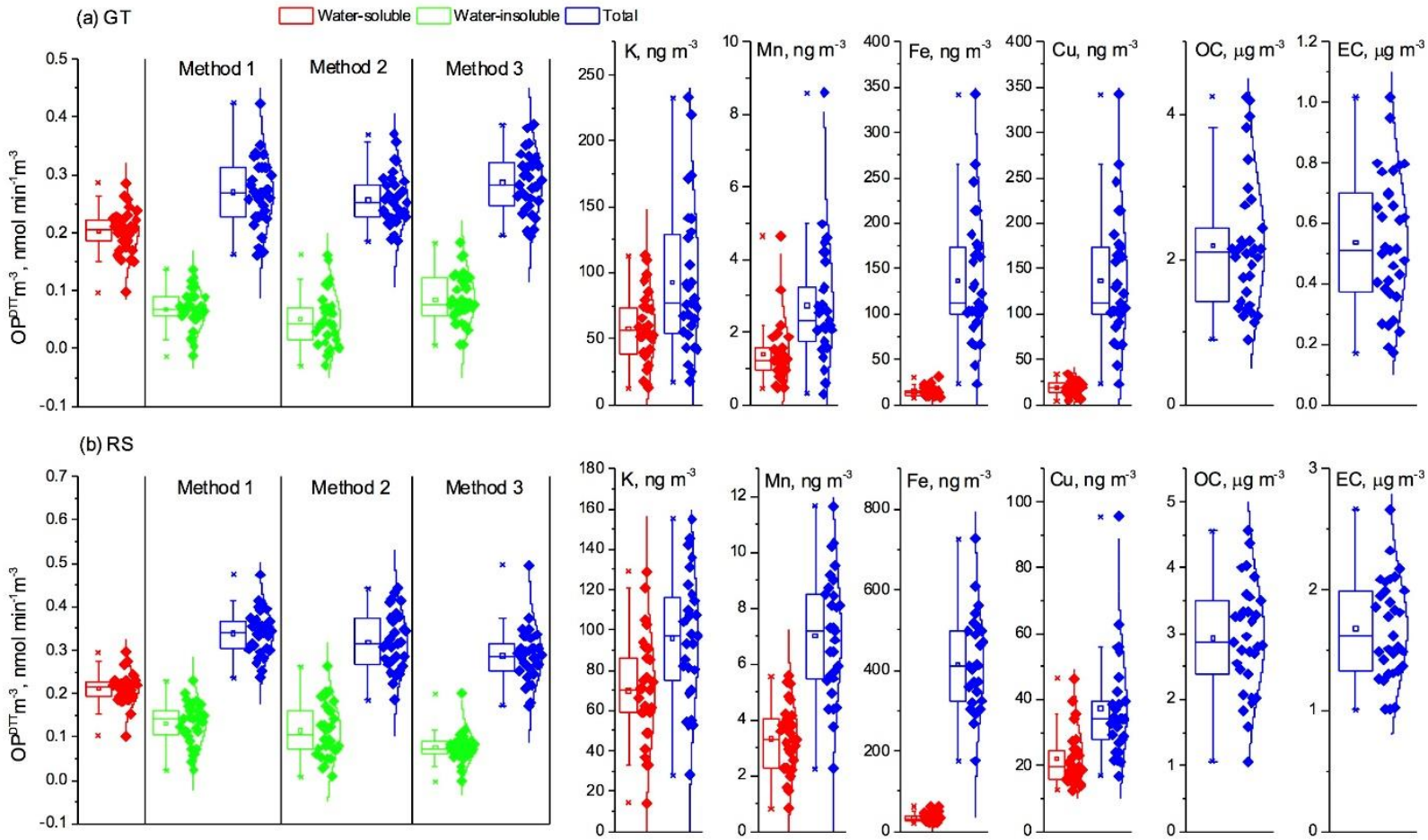

Figure B-6. Graphical assessment of data normality.

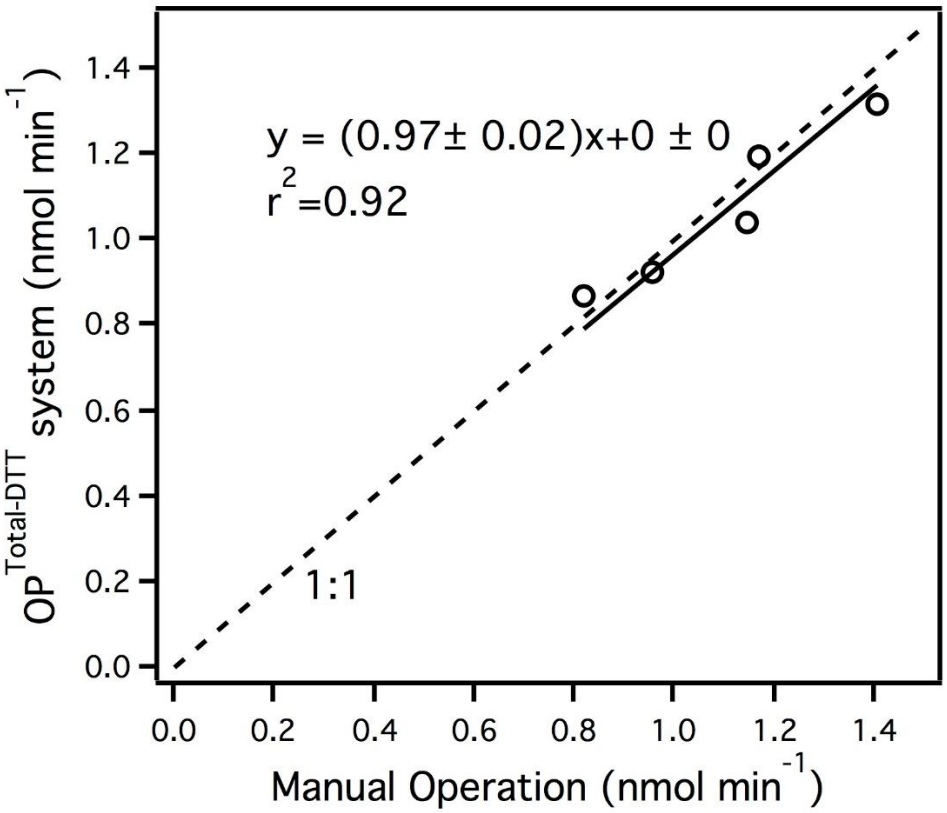

Figure B-7. Blank-corrected DTT consumption rate comparison of the automated system to a manual analysis using ambient samples (N=5).

Table B-1. Correlation matrix for the various metals and OP^{DTT} obtained by method 3

GT				Water-soluble					Total					Water-insoluble				
N=35		OC	EC	DTT	K	Mn	Fe	Cu	DTT	K	Mn	Fe	Cu	DTT	K	Mn	Fe	Cu
	EC	**0.83****	**1**															
Water-soluble	DTT	**0.79****	**0.84****	**1**														
	K	0.6**	**0.88****	0.63**	**1**													
	Mn	**0.86****	**0.7****	0.46*	0.54**	**1**												
	Fe	**0.8****	**0.82****	0.49*	0.62**	**0.82****	**1**											
	Cu	**0.7****	**0.78****	**0.77****	**0.71****	**0.72****	0.64**	**1**										
Total	DTT	0.66**	**0.78****	**0.71****	**0.82****	0.69**	0.48*	**0.76****	**1**									
	K	0.67**	**0.84****	0.53**	**0.82****	**0.7****	0.59**	0.52**	0.69**	**1**								
	Mn	0.67**	0.66**	0.43*	0.51**	**0.94****	0.61**	0.65**	**0.73****	**0.7****	**1**							
	Fe	0.53**	0.58**	0.36	0.51**	**0.86****	0.6**	0.62**	**0.71****	0.56**	**0.97****	**1**						
	Cu	**0.72****	**0.78****	**0.78****	0.62**	**0.87****	0.54**	**0.97****	**0.78****	**0.7****	**0.88****	**0.84****	**1**					
Water-insoluble	DTT	0.44*	0.48**	-0.23	0.55**	0.57**	0.26	0.38	**0.87****	0.50*	0.66**	0.63**	0.56**	**1**				
	K	0.6**	0.6**	0.42*	0.61**	**0.76****	0.54**	0.3	0.66**	**0.94****	**0.74****	0.69**	0.61**	0.50*	**1**			
	Mn	0.43*	0.66**	0.31	0.37	**0.79****	0.64**	0.43*	0.62**	0.62**	**0.96****	**0.95****	**0.75****	0.59**	**0.7****	**1**		
	Fe	0.49*	0.57**	0.35*	0.49*	**0.86****	0.57**	0.59**	**0.7****	0.55**	**0.96****	**0.9995****	**0.84****	0.64**	0.69**	**0.95****	**1**	
	Cu	**0.72****	**0.78****	**0.78****	0.61**	**0.88****	0.54**	**0.97****	**0.78****	**0.7****	**0.89****	**0.85****	**0.9999****	0.56**	0.63**	**0.76****	**0.84****	**1**

Note: r>0.70 are bold.

**p<0.01. *p<0.05. Correlation not statistically significant is without superscript.

RS				Water-soluble					Total					Water-insoluble				
		OC	EC	DTT	K	Mn	Fe	Cu	DTT	K	Mn	Fe	Cu	DTT	K	Mn	Fe	Cu
	EC	**0.75****	**1**															
Water-soluble	DTT	**0.83****	**0.79****	**1**														
	K	**0.86****	0.68**	0.67**	**1**													
	Mn	**0.79****	0.63**	0.43*	0.56**	**1**												
	Fe	**0.8****	**0.8****	**0.88****	0.66**	0.45*	**1**											
	Cu	0.64**	**0.78****	0.54**	**0.77****	0.36	0.63**	**1**										
Total	DTT	**0.71****	0.68**	0.56**	0.6**	0.56**	0.49*	0.55**	**1**									
	K	**0.88****	**0.71****	0.69**	**0.9****	0.65**	**0.72****	0.51*	0.67**	**1**								
	Mn	**0.86****	0.69**	0.48*	0.53**	**0.95****	0.56**	0.56**	0.66**	0.61**	**1**							
	Fe	**0.79****	**0.75****	0.57**	0.55**	**0.72****	**0.72****	**0.71****	0.66**	0.6**	**0.9****	**1**						
	Cu	0.66**	**0.72****	0.4	**0.78****	0.65**	0.56**	**0.93****	**0.72****	0.57**	**0.79****	**0.84****	**1**					
Water-insoluble	DTT	-0.34	-0.37	-0.51**	-0.47*	-0.37	-0.40*	-0.40*	**0.84****	-0.43*	0.31	-0.39*	0.43*	**1**				
	K	0.6**	0.47*	0.37	0.4	0.56**	**0.73****	0.28	0.47*	**0.7****	0.63**	0.62**	0.24*	-0.27	**1**			
	Mn	**0.77****	**0.72****	0.42*	0.44*	**0.81****	0.62**	0.65**	0.67**	0.49*	**0.95****	**0.96****	**0.82****	0.31	0.57**	**1**		
	Fe	**0.74****	**0.71****	0.47*	0.49*	**0.71****	0.66**	**0.7****	0.66**	0.54**	**0.9****	**0.998****	**0.84****	-0.36	0.59**	**0.97****	**1**	
	Cu	0.67**	**0.73****	0.25	**0.79****	0.65**	0.56**	**0.92****	**0.73****	0.59**	**0.79****	**0.84****	**0.9996****	0.44*	0.14	**0.82****	**0.84****	**1**

Note: r>0.70 are bold.

**p<0.01. *p<0.05. Correlation not statistically significant is without superscript.

N=31 for corrletions between OP^{DTT}, N=29 for correlations between OP^{DTT} and PM components.

Table B-2. Pearson's r between OP^{DTT} m^{-3} and PM chemical components at GT (N=34) and RS (N=29) sites.

GT		OC	EC	WS				Total			
				K	Mn	Fe	Cu	K	Mn	Fe	Cu
Method1	$OP^{WS\text{-}DTT}$	**0.79****	**0.84****	0.63**	0.46*	0.49*	**0.77****	0.53**	0.43*	0.36	**0.78****
	$OP^{sM\text{-}DTT}$	**0.71****	0.66**	0.28*	0.44**	0.45**	0.4*	0.35*	0.38	0.2	0.37*
	$OP^{Total\text{-}DTT\text{-}1}$	**0.76****	**0.81****	0.51**	0.46*	0.54**	**0.74****	0.39*	0.41*	0.38*	**0.72****
Method2	$OP^{Total\text{-}DTT\text{-}2}$	0.51**	0.44*	0.27	0.40*	0.09	0.62**	0.15	0.37*	0.23	0.59**
	$OP^{WI\text{-}DTT\text{-}2}$	0.44*	0.25	-0.31	0.46*	-0.39	0.53**	-0.28	0.32	0.13	0.53**
Method3	$OP^{Total\text{-}DTT\text{-}3}$	0.66**	**0.78****	**0.82****	0.69**	0.48*	**0.76****	0.69**	**0.73****	**0.71****	**0.78****
	$OP^{WI\text{-}DTT\text{-}3}$	0.44*	0.48**	0.55**	0.57**	0.26	0.38	0.50*	0.66**	0.63**	0.56**
RS											
Method1	$OP^{WS\text{-}DTT}$	**0.83****	**0.79****	0.67**	0.43*	**0.88****	0.54**	0.69**	0.48*	0.57**	0.40
	OP^{sM_DTT}	**0.72****	**0.72****	0.48**	0.13	**0.73****	0.65**	0.59**	0.18	0.53**	0.38
	$OP^{Total\text{-}DTT\text{-}1}$	**0.77****	**0.76****	0.67**	0.28	**0.80****	0.63**	0.67**	0.39*	0.61**	0.42*
Method2	$OP^{Total\text{-}DTT\text{-}2}$	0.68**	0.52**	0.53**	0.45*	0.09	0.44*	0.48*	0.59**	0.57**	0.65**
	$OP^{WI\text{-}DTT\text{-}2}$	0.68**	0.51**	0.50*	0.48*	0.07	0.42*	0.42*	0.61**	0.66**	0.66**
Method3	$OP^{Total\text{-}DTT\text{-}3}$	**0.71****	0.68**	0.6**	0.56**	0.49*	0.55**	0.67**	0.66**	0.66**	**0.72****
	$OP^{WI\text{-}DTT\text{-}3}$	-0.34	-0.37	-0.47*	-0.37	-0.40*	-0.40*	-0.43*	0.31	-0.39*	0.43*

Note: Water-insoluble $OP^{WI\text{-}DTT}$ obtained by method 2 and 3 is calculated by $OP^{WI\text{-}DTT} = OP^{Total\text{-}DTT} - OP^{WS\text{-}DTT}$.
r>0.70 are bold.
**p-value<0.01. *p-value<0.05. The correlation not statistically significant is without superscript and greyed out.

Table B-3. $OP^{WS\text{-}DTT}$ m^{-3} and $OP^{Total\text{-}DTT}$ m^{-3} (nmol min^{-1} m^{-3})

Filter type	GT			RS		
	$OP^{WS\text{-}DTT}$	$OP^{Total\text{-}DTT}$	$\frac{OP^{WS-DTT}}{OP^{Total-DTT}}$	$OP^{WS\text{-}DTT}$	$OP^{Total\text{-}DTT}$	$\frac{OP^{WS-DTT}}{OP^{Total-DTT}}$
Quartz	0.20 ± 0.04 N=35	0.32 ± 0.06 N=35	$65 \pm 10\%$ N=35	0.21 ± 0.03 N=32	0.34 ± 0.05 N=33	$62 \pm 12\%$ N=32
Teflon	0.13 ± 0.03 N=23	0.21 ± 0.04 N=23	$65 \pm 14\%$ N=23	0.18 ± 0.02 N=24	0.31 ± 0.04 N=24	$58 \pm 10\%$ N=24

Table B-4. The OP variance on Teflon versus quartz filters assessed by the F-test in ANOVA.

	F	$F_{critical}$ for $\alpha = 0.05$
GT-$OP^{WS\text{-}DTT}$	2.082	4.013
RS-$OP^{WS\text{-}DTT}$	0.499	4.020
GT-$OP^{Total\text{-}DTT}$	2.084	4.013
RS-$OP^{Total\text{-}DTT}$	0.159	4.016

*Null hypothesis assumes that there is no significant difference between Teflon and quartz filters.

*$F < F_{critical}$ when the null hypothesis is true with significance level of 0.05.

Table B-5. Summary of concentrations of measured PM components.

	Water-soluble		Total	
	GT	RS	GT	RS
K, ng/m^3	57.49±28.08 N=28	69.79±26.56 N=29	92.54±56.05 N=28	95.97±31.63 N=28
Mn, ng/m^3	1.40±0.85 N=29	3.32±1.20 N=29	2.73±1.64 N=29	7.02±2.21 N=29
Fe, ng/m^3	13.94±5.04 N=29	33.25±11.36 N=29	136.69±70.72 N=29	414.41±116.54 N=29
Cu, ng/m^3	18.17±7.27 N=28	22.03±8.29 N=28	35.23±18.40 N=29	37.20±15.94 N=29
OC, µg/m^3	-	-	2.19±0.90 N=33	2.92±0.82 N=31
EC, µg/m^3	-	-	0.54±0.22 N=32	1.68±0.41 N=31

Table B-6. Coefficients of divergence (CODs) for the paired GT-RS site.

	Quartz filters				Teflon filters	
	EC	OC	$OP^{WS\text{-}DTT}$	$OP^{Total\text{-}DTT}$	$OP^{WS\text{-}DTT}$	$OP^{Total\text{-}DTT}$
Coefficients of divergence (CODs)	0.52	0.18	0.06	0.08	0.19	0.23

APPENDIX C. SUPPLEMENTAL MATERIAL FOR CHAPTER 4

C.1 Elemental analysis procedures

Both total and water-soluble trace metals were determined by inductively coupled plasma-mass spectrometry (ICP-MS) (Agilent 7500a series, Agilent Technologies). The elements of interest included magnesium (Mg), aluminum (Al), potassium (K), calcium (Ca), chromium (Cr), manganese (Mn), iron (Fe), copper (Cu) and zinc (Zn).

Sample preparation: For the determination of concentrations of total metals, a 1.5 cm^2 filter punch from the HiVol quartz filter was acid-digested for 20 min using aqua regia (HNO_3+3HCl). The acid-digested sample was then diluted in deionized water (DI, >18MΩ cm^{-1}) to 10 mL, filtered with a 0.45 μm PTFE syringe filter (Fisher Scientific).

For the analysis of water-soluble metals, no digestion was required. One circular punch (diameter of 1 in.) was extracted in 5 mL of DI via 30-min sonication. The extract was filtered using a 0.45 μm PTFE syringe filter, and then acid-preserved by adding concentrated nitric acid (70%) to a final concentration of 2% (v/v).

Analytical quality control and LOD: A set of mixed calibration standard solutions were prepared by diluting the stock standard solutions and treated with the same procedures as samples. Internal standards including lithium (^{6}Li) and scandium (^{45}Sc), were added to all calibration standards and samples to monitor instrumental drift. DI blank and field blank which consist of same concentrations of acid and internal standards were used to monitor for possible contamination resulting from the sample preparation procedures. The method detection limits were defined as three times the standard deviation of blanks.

Table C-1. The difference in OP^{DTT} between summer (Jun-Aug) and winter (Jan-Feb, Dec) assessed by two-sample t-test

		t-value	df	p-value	t_critical (α<0.01)
OPv	$OP^{WS\text{-}DTT}$	1.27	159	0.21	2.60
	$OP^{Total\text{-}DTT}$	10.76	162	1.0E-20	
	$OP^{WI\text{-}DTT}$	9.89	131	1.4E-17	
OPm	$OP^{WS\text{-}DTT}$	2.45	156	0.02	2.60
	$OP^{Total\text{-}DTT}$	8.08	159	1.5E-13	
	$OP^{WI\text{-}DTT}$	7.61	128	5.2E-12	

Note: df is degree of freedom.

Table C-2. Pearson's r between volume-normalized OP and PM species ambient concentrations

	$OP^{WS\text{-}DTT}$	$OP^{Total\text{-}DTT}$	$OP^{WI\text{-}DTT}$
$OP^{Total\text{-}DTT}$	0.58**		
$OP^{WI\text{-}DTT}$	-0.07	**0.66****	
PM mass	0.55**	0.43**	0.03
EC	0.51**	0.44**	0.10
OC	0.55**	0.45**	0.05
WSOC	0.52**	0.47**	0.18**
WIOC	0.34**	0.31**	-0.06
BrC	0.41**	**0.74****	0.56**
SO_4^{2-}	0.34**	0.17**	-0.04
WS-K	0.50**	0.54**	0.28**
WS-Mn	0.37**	0.38**	0.21**
WS-Fe	0.50**	0.26**	-0.10
WS-Cu	0.36**	0.07	-0.17**
WS-Zn	0.34**	0.50**	0.05
Total-Mg	-0.02	0.28**	0.45**
Total-Al	0.32**	0.33**	0.14*
Total-K	0.36**	0.43**	0.23**
Total-Ca	0.13**	0.28**	0.18**
Total-Mn	0.32**	0.49**	0.36**
Total-Fe	0.36**	0.50**	0.29**
Total-Cu	0.36**	0.29**	0.14*
Total-Zn	-0.09	0.14*	0.22**

Note: **p-value<0.01; *p-value<0.05. Correlations not statistically significant (p>0.05) are in grey. r>0.65 are bold.

Table C-3. Pearson's r between mass-normalized OP and mass fraction of PM species.

	$OP^{WS\text{-}DTT}$	$OP^{Total\text{-}DTT}$	$OP^{WI\text{-}DTT}$
$OP^{Total\text{-}DTT}$	**0.76****		
$OP^{WI\text{-}DTT}$	0.31**	**0.79****	
EC	0.22**	0.18**	0.09
OC	0.07	-0.02	-0.07
WSOC	0.20**	0.27**	0.28**
WIOC	-0.02	-0.14*	-0.26**
BrC	0.12*	0.39**	0.47**
SO_4^{2-}	0.13*	0.11	0.11
WS-K	0.11	0.25**	0.31**
WS-Mn	0.01	0.14**	0.24**
WS-Fe	-0.07	-0.25**	-0.26**
WS-Cu	0.30**	0.16**	0.02
WS-Zn	0.41**	0.44**	0.32**
Total-Mg	-0.05	0.34**	0.54**
Total-Al	0.57**	0.58**	0.41**
Total-K	0.38**	0.46**	0.38**
Total-Ca	0.55**	0.62**	0.41**
Total-Mn	0.03	0.29**	0.42**
Total-Fe	0.05	0.28**	0.38**
Total-Cu	0.41**	0.47**	0.39**
Total-Zn	0.19**	0.32**	0.28**

Note: **p-value<0.01; *p-value<0.05. Correlations not statistically significant (p>0.05) are in grey. r>0.65 are bold.

REFERENCES

Abrams, J. Y., Weber, R. J., Klein, M., Sarnat, S. E., Chang, H. H., Strickland, M. J., Verma, V., Fang, T., Bates, J. T., Mulholland, J. A., Russell, A. G., and Tolbert, P. E.: Associations between Ambient Fine Particulate Oxidative Potential and Cardiorespiratory Emergency Department Visits (vol 125, 2017), Environ Health Persp, 125, 2017.

Akhtar, U. S., McWhinney, R. D., Rastogi, N., Abbatt, J. P. D., Evans, G. J., and Scott, J. A.: Cytotoxic and proinflammatory effects of ambient and source-related particulate matter (PM) in relation to the production of reactive oxygen species (ROS) and cytokine adsorption by particles, Inhal Toxicol, 22, 37-47, 2010.

Aliaga, M. E., Carrasco-Pozo, C., Lopez-Alarcon, C., and Speisky, H.: The Cu(I)-glutathione complex: factors affecting its formation and capacity to generate reactive oxygen species, Transit Metal Chem, 35, 321-329, 2010.

Anderson, J. O., Thundiyil, J. G., and Stolbach, A.: Clearing the Air: A Review of the Effects of Particulate Matter Air Pollution on Human Health, J Med Toxicol, 8, 166-175, 2012.

Antinolo, M., Willis, M. D., Zhou, S. M., and Abbatt, J. P. D.: Connecting the oxidation of soot to its redox cycling abilities, Nat Commun, 6, 2015.

Atkinson, R. W., Anderson, H. R., Sunyer, J., Ayres, J., Baccini, M., Vonk, J. M., Boumghar, A., Forastiere, F., Forsberg, B., Touloumi, G., Schwartz, J., and Katsouyanni, K.: Acute effects of particulate air pollution on respiratory admissions - Results from APHEA 2 project, Am J Resp Crit Care, 164, 1860-1866, 2001.

Atkinson, R. W., Samoli, E., Analitis, A., Fuller, G. W., Green, D. C., Anderson, H. R., Purdie, E., Durister, C., Aitlhadj, L., Kelly, F. J., and Mudway, I. S.: Short-term associations between particle oxidative potential and daily mortality and hospital admissions in London, Int J Hyg Envir Heal, 219, 566-572, 2016.

Ayres, J. G., Borm, P., Cassee, F. R., Castranova, V., Donaldson, K., Ghio, A., Harrison, R. M., Hider, R., Kelly, F., Kooter, I. M., Marano, F., Maynard, R. L., Mudway, I., Nel, A., Sioutas, C., Smith, S., Baeza-Squiban, A., Cho, A., Duggan, S., and Froines, J.: Evaluating the toxicity of airborne particulate matter and nanoparticles

by measuring oxidative stress potential - A workshop report and consensus statement, Inhal Toxicol, 20, 75-99, 2008.

Baker, M. A., Cerniglia, G. J., and Zaman, A.: Microtiter Plate Assay for the Measurement of Glutathione and Glutathione Disulfide in Large Numbers of Biological Samples, Anal Biochem, 190, 360-365, 1990.

Bates, J. T., Fang, T., Verma, V., Zeng, L. H., Weber, R. J., Tolbert, P. E., Abrams, J. Y., Sarnat, S. E., Klein, M., Mulholland, J. A., and Russell, A. G.: Review of Acellular Assays of Ambient Particulate Matter Oxidative Potential: Methods and Relationships with Composition, Sources, and Health Effects, Environ Sci Technol, 53, 4003-4019, 2019.

Bates, J. T., Weber, R. J., Abrams, J., Verma, V., Fang, T., Klein, M., Strickland, M. J., Sarnat, S. E., Chang, H. H., Mulholland, J. A., Tolbert, P. E., and Russell, A. G.: Reactive Oxygen Species Generation Linked to Sources of Atmospheric Particulate Matter and Cardiorespiratory Effects, Environ Sci Technol, 49, 13605-13612, 2015.

Birch, M. E. and Cary, R. A.: Elemental carbon-based method for monitoring occupational exposures to particulate diesel exhaust, Aerosol Sci Tech, 25, 221-241, 1996.

Brook, R. D., Rajagopalan, S., Pope, C. A., 3rd, Brook, J. R., Bhatnagar, A., Diez-Roux, A. V., Holguin, F., Hong, Y., Luepker, R. V., Mittleman, M. A., Peters, A., Siscovick, D., Smith, S. C., Jr., Whitsel, L., Kaufman, J. D., American Heart Association Council on, E., Prevention, C. o. t. K. i. C. D., Council on Nutrition, P. A., and Metabolism: Particulate matter air pollution and cardiovascular disease: An update to the scientific statement from the American Heart Association, Circulation, 121, 2331-2378, 2010.

Brunekreef, B. and Holgate, S. T.: Air pollution and health, Lancet, 360, 1233-1242, 2002.

Calas, A., Uzu, G., Kelly, F. J., Houdier, S., Martins, J. M. F., Thomas, F., Molton, F., Charron, A., Dunster, C., Oliete, A., Jacob, V., Besombes, J. L., Chevrier, F., and Jaffrezo, J. L.: Comparison between five acellular oxidative potential measurement assays performed with detailed chemistry on PM10 samples from the city of Chamonix (France), Atmos Chem Phys, 18, 7863-7875, 2018.

Calas, A., Uzu, G., Martins, J. M. F., Voisin, D., Spadini, L., Lacroix, T., and Jaffrezo, J. L.: The importance of simulated lung fluid (SLF) extractions for a more relevant evaluation of the oxidative potential of particulate matter, Sci Rep-Uk, 7, 2017.

Campen, M. J., Nolan, J. P., Schladweiler, M. C. J., Kodavanti, U. P., Costa, D. L., and Watkinson, W. P.: Cardiac and thermoregulatory effects of instilled particulate matter-associated transition metals in healthy and cardiopulmonary-compromised rats, J Toxicol Env Heal A, 65, 1615-1631, 2002.

Canova, C., Minelli, C., Dunster, C., Kelly, F., Shah, P. L., Caneja, C., Tumilty, M. K., and Burney, P.: PM10 Oxidative Properties and Asthma and COPD, Epidemiology, 25, 467-468, 2014.

Charrier, J. G. and Anastasio, C.: Impacts of antioxidants on hydroxyl radical production from individual and mixed transition metals in a surrogate lung fluid, Atmos Environ, 45, 7555-7562, 2011.

Charrier, J. G. and Anastasio, C.: On dithiothreitol (DTT) as a measure of oxidative potential for ambient particles: evidence for the importance of soluble transition metals, Atmospheric Chemistry and Physics, 12, 9321-9333, 2012.

Charrier, J. G., McFall, A. S., Vu, K. K. T., Baroi, J., Olea, C., Hasson, A., and Anastasio, C.: A bias in the "mass-normalized" DTT response - An effect of non-linear concentration-response curves for copper and manganese, Atmos Environ, 144, 325-334, 2016.

Cho, A. K., Sioutas, C., Miguel, A. H., Kumagai, Y., Schmitz, D. A., Singh, M., Eiguren-Fernandez, A., and Froines, J. R.: Redox activity of airborne particulate matter at different sites in the Los Angeles Basin, Environ Res, 99, 40-47, 2005.

Chow, J. C., Watson, J. G., Pritchett, L. C., Pierson, W. R., Frazier, C. A., and Purcell, R. G.: The Dri Thermal Optical Reflectance Carbon Analysis System - Description, Evaluation and Applications in United-States Air-Quality Studies, Atmos Environ a-Gen, 27, 1185-1201, 1993.

Cohen, A. J., Brauer, M., Burnett, R., Anderson, H. R., Frostad, J., Estep, K., Balakrishnan, K., Brunekreef, B., Dandona, L., Dandona, R., Feigin, V., Freedman, G., Hubbell, B., Jobling, A., Kan, H., Knibbs, L., Liu, Y., Martin, R., Morawska, L., Pope, C. A., Shin, H., Straif, K., Shaddick, G., Thomas, M., van Dingenen, R., van Donkelaar, A., Vos, T., Murray, C. J. L., and Forouzanfar, M. H.: Estimates and 25-year trends of the global burden of disease attributable to

ambient air pollution: an analysis of data from the Global Burden of Diseases Study 2015, Lancet, 389, 1907-1918, 2017.

Daher, N., Ning, Z., Cho, A. K., Shafer, M., Schauer, J. J., and Sioutas, C.: Comparison of the Chemical and Oxidative Characteristics of Particulate Matter (PM) Collected by Different Methods: Filters, Impactors, and BioSamplers, Aerosol Sci Tech, 45, 1294-1304, 2011.

Darrow, L. A., Klein, M., Flanders, W. D., Mulholland, J. A., Tolbert, P. E., and Strickland, M. J.: Air Pollution and Acute Respiratory Infections Among Children 0-4 Years of Age: An 18-Year Time-Series Study, Am J Epidemiol, 180, 968-977, 2014.

Das, S. K.: SPECIAL ISSUE ON "FREE RADICALS AND ANTIOXIDANTS IN HEALTH & DISEASES" Preface, Indian J Exp Biol, 54, 681-683, 2016.

Delfino, R. J., Staimer, N., Tjoa, T., Arhami, M., Polidori, A., Gillen, D. L., George, S. C., Shafer, M. M., Schauer, J. J., and Sioutas, C.: Associations of Primary and Secondary Organic Aerosols With Airway and Systemic Inflammation in an Elderly Panel Cohort, Epidemiology, 21, 892-902, 2010a.

Delfino, R. J., Staimer, N., Tjoa, T., Arhami, M., Polidori, A., Gillen, D. L., Kleinman, M. T., Schauer, J. J., and Sioutas, C.: Association of Biomarkers of Systemic Inflammation with Organic Components and Source Tracers in Quasi-Ultrafine Particles, Environ Health Persp, 118, 756-762, 2010b.

Delfino, R. J., Staimer, N., Tjoa, T., Gillen, D. L., Schauer, J. J., and Shafer, M. M.: Airway inflammation and oxidative potential of air pollutant particles in a pediatric asthma panel, J Expo Sci Env Epid, 23, 466-473, 2013.

Delfino, R. J., Staimer, N., and Vaziri, N. D.: Air pollution and circulating biomarkers of oxidative stress, Air Qual Atmos Hlth, 4, 37-52, 2011.

DiStefano, E., Eiguren-Fernandez, A., Delfino, R. J., Sioutas, C., Froines, J. R., and Cho, A. K.: Determination of metal-based hydroxyl radical generating capacity of ambient and diesel exhaust particles, Inhal Toxicol, 21, 731-738, 2009.

Donaldson, K., Stone, V., Seaton, A., and MacNee, W.: Ambient particle inhalation and the cardiovascular system: Potential mechanisms, Environ Health Persp, 109, 523-527, 2001.

Edgerton, E. S., Hartsell, B. E., Saylor, R. D., Jansen, J. J., Hansen, D. A., and Hidy, G. M.: The Southeastern Aerosol Research and Characterization Study, part 3: Continuous measurements of fine particulate matter mass and composition, J Air Waste Manage, 56, 1325-1341, 2006.

Edgerton, E. S., Hartsell, B. E., Saylor, R. D., Jansen, J. J., Hansen, D. A., and Hidy, G. M.: The southeastern aerosol research and characterization study: Part II. Filter-based measurements of fine and coarse particulate matter mass and composition, J Air Waste Manage, 55, 1527-1542, 2005.

Esposito, S., Tenconi, R., Lelii, M., Preti, V., Nazzari, E., Consolo, S., and Patria, M. F.: Possible molecular mechanisms linking air pollution and asthma in children, Bmc Pulm Med, 14, 2014.

Falkovich, A. H., Schkolnik, G., Ganor, E., and Rudich, Y.: Adsorption of organic compounds pertinent to urban environments onto mineral dust particles, J Geophys Res-Atmos, 109, 2004.

Fang, T., Guo, H., Verma, V., Peltier, R. E., and Weber, R. J.: PM2.5 water-soluble elements in the southeastern United States: automated analytical method development, spatiotemporal distributions, source apportionment, and implications for heath studies, Atmos Chem Phys, 15, 11667-11682, 2015a.

Fang, T., Guo, H. Y., Zeng, L. H., Verma, V., Nenes, A., and Weber, R. J.: Highly Acidic Ambient Particles, Soluble Metals, and Oxidative Potential: A Link between Sulfate and Aerosol Toxicity, Environ Sci Technol, 51, 2611-2620, 2017a.

Fang, T., Lakey, P. S. J., Weber, R. J., and Shiraiwa, M.: Oxidative Potential of Particulate Matter and Generation of Reactive Oxygen Species in Epithelial Lining Fluid, Environ Sci Technol, doi: 10.1021/acs.est.9b03823, 2019. 2019.

Fang, T., Verma, V., Bates, J. T., Abrams, J., Klein, M., Strickland, M. J., Sarnat, S. E., Chang, H. H., Mulholland, J. A., Tolbert, P. E., Russell, A. G., and Weber, R. J.: Oxidative potential of ambient water-soluble PM2.5 in the southeastern United States: contrasts in sources and health associations between ascorbic acid (AA) and dithiothreitol (DTT) assays, Atmos Chem Phys, 16, 3865-3879, 2016.

Fang, T., Verma, V., Guo, H., King, L. E., Edgerton, E. S., and Weber, R. J.: A semi-automated system for quantifying the oxidative potential of ambient particles in aqueous extracts using the dithiothreitol (DTT) assay: results from the

Southeastern Center for Air Pollution and Epidemiology (SCAPE), Atmospheric Measurement Techniques, 8, 471-482, 2015b.

Fang, T., Zeng, L. H., Gao, D., Verma, V., Stefaniak, A. B., and Weber, R. J.: Ambient Size Distributions and Lung Deposition of Aerosol Dithiothreitol-Measured Oxidative Potential: Contrast between Soluble and Insoluble Particles, Environ Sci Technol, 51, 6802-6811, 2017b.

Frampton, M. W., Ghio, A. J., Samet, J. M., Carson, J. L., Carter, J. D., and Devlin, R. B.: Effects of aqueous extracts of PM(10) filters from the Utah Valley on human airway epithelial cells, Am J Physiol-Lung C, 277, L960-L967, 1999.

Gao, D., Fang, T., Verma, V., Zeng, L., and Weber, R. J.: A method for measuring total aerosol oxidative potential (OP) with the dithiothreitol (DTT) assay and comparisons between an urban and roadside site of water-soluble and total OP, Atmos Meas Tech, 10, 2821-2835, 2017.

Gao, D., Pollitt, K. J., Mulholland, J. A., Russell, A. G., and Weber, R. J.: Characterization and comparison of PM2.5 oxidative potential assessed by two acellular assays, Atmos. Chem. Phys. Discuss., http://doi.org/10.5194/acp-2019-941, in review, 2019.

Gauderman, W. J., Vora, H., McConnell, R., Berhane, K., Gilliland, F., Thomas, D., Lurmann, F., Avol, E., Kunzli, N., Jerrett, M., and Peters, J.: Effect of exposure to traffic on lung development from 10 to 18 years of age: a cohort study, Lancet, 369, 571-577, 2007.

Ghio, A. J., Stoneheurner, J., McGee, J. K., and Kinsey, J. S.: Sulfate content correlates with iron concentrations in ambient air pollution particles, Inhal Toxicol, 11, 293-307, 1999.

Godri, K. J., Duggan, S. T., Fuller, G. W., Baker, T., Green, D., Kelly, F. J., and Mudway, I. S.: Particulate Matter Oxidative Potential from Waste Transfer Station Activity, Environ Health Persp, 118, 493-498, 2010.

Godri, K. J., Harrison, R. M., Evans, T., Baker, T., Dunster, C., Mudway, I. S., and Kelly, F. J.: Increased Oxidative Burden Associated with Traffic Component of Ambient Particulate Matter at Roadside and Urban Background Schools Sites in London, Plos One, 6, 2011.

Halliwell, B.: Free-Radicals, Antioxidants, and Human-Disease - Curiosity, Cause, or Consequence, Lancet, 344, 721-724, 1994.

Hansen, D. A., Edgerton, E., Hartsell, B., Jansen, J., Burge, H., Koutrakis, P., Rogers, C., Suh, H., Chow, J., Zielinska, B., McMurry, P., Mulholland, J., Russell, A., and Rasmussen, R.: Air quality measurements for the aerosol research and inhalation epidemiology study, J Air Waste Manage, 56, 1445-1458, 2006.

Hansen, D. A., Edgerton, E. S., Hartsell, B. E., Jansen, J. J., Kandasamy, N., Hidy, G. M., and Blanchard, C. L.: The southeastern aerosol research and characterization study: Part 1-overview, J Air Waste Manage, 53, 1460-1471, 2003.

Harrison, R. M., Jones, A. M., and Lawrence, R. G.: A pragmatic mass closure model for airborne particulate matter at urban background and roadside sites, Atmospheric Environment, 37, 4927-4933, 2003.

Heal, M. R., Hibbs, L. R., Agius, R. M., and Beverland, L. J.: Total and water-soluble trace metal content of urban background PM10, PM2.5 and black smoke in Edinburgh, UK, Atmos Environ, 39, 1417-1430, 2005.

Hecobian, A., Zhang, X., Zheng, M., Frank, N., Edgerton, E. S., and Weber, R. J.: Water-Soluble Organic Aerosol material and the light-absorption characteristics of aqueous extracts measured over the Southeastern United States, Atmos Chem Phys, 10, 5965-5977, 2010.

Hoek, G., Brunekreef, B., Goldbohm, S., Fischer, P., and van den Brandt, P. A.: Association between mortality and indicators of traffic-related air pollution in the Netherlands: a cohort study, Lancet, 360, 1203-1209, 2002.

Hoek, G., Krishnan, R. M., Beelen, R., Peters, A., Ostro, B., Brunekreef, B., and Kaufman, J. D.: Long-term air pollution exposure and cardio- respiratory mortality: a review, Environ Health-Glob, 12, 2013.

Hu, S., Polidori, A., Arhami, M., Shafer, M. M., Schauer, J. J., Cho, A., and Sioutas, C.: Redox activity and chemical speciation of size fractioned PM in the communities of the Los Angeles-Long Beach harbor, Atmos Chem Phys, 8, 6439-6451, 2008.

Huang, W., Zhang, Y. X., Zhang, Y., Fang, D. Q., and Schauer, J. J.: Optimization of the Measurement of Particle-Bound Reactive Oxygen Species with 2 ',7 '-dichlorofluorescin (DCFH), Water Air Soil Poll, 227, 2016.

Janssen, N. A. H., Strak, M., Yang, A., Hellack, B., Kelly, F. J., Kuhlbusch, T. A. J., Harrison, R. M., Brunekreef, B., Cassee, F. R., Steenhof, M., and Hoek, G.: Associations between three specific a-cellular measures of the oxidative potential of particulate matter and markers of acute airway and nasal inflammation in healthy volunteers, Occup Environ Med, 72, 49-56, 2015.

Kameda, T., Azumi, E., Fukushima, A., Tang, N., Matsuki, A., Kamiya, Y., Toriba, A., and Hayakawa, K.: Mineral dust aerosols promote the formation of toxic nitropolycyclic aromatic compounds, Sci Rep-Uk, 6, 2016.

Kelly, F., Anderson, H. R., Armstrong, B., Atkinson, R., Barratt, B., Beevers, S., Derwent, D., Green, D., Mudway, I., Wilkinson, P., and Committee, H. E. I. H. R.: The impact of the congestion charging scheme on air quality in London. Part 2. Analysis of the oxidative potential of particulate matter, Res Rep Health Eff Inst, 2011. 73-144, 2011.

Kelly, F. J.: Oxidative stress: Its role in air pollution and adverse health effects, Occup Environ Med, 60, 612-616, 2003.

Kelly, F. J., Cotgrove, M., and Mudway, I. S.: Respiratory tract lining fluid antioxidants: the first line of defence against gaseous pollutants, Cent Eur J Public Health, 4 Suppl, 11-14, 1996.

Kelly, F. J. and Fussell, J. C.: Size, source and chemical composition as determinants of toxicity attributable to ambient particulate matter, Atmospheric Environment, 60, 504-526, 2012.

Knaapen, A. M., Shi, T. M., Borm, P. J. A., and Schins, R. P. F.: Soluble metals as well as the insoluble particle fraction are involved in cellular DNA damage induced by particulate matter, Mol Cell Biochem, 234, 317-326, 2002.

Kumagai, Y., Koide, S., Taguchi, K., Endo, A., Nakai, Y., Yoshikawa, T., and Shimojo, N.: Oxidation of proximal protein sulfhydryls by phenanthraquinone, a component of diesel exhaust particles, Chem Res Toxicol, 15, 483-489, 2002.

Kunzli, N., Mudway, I. S., Gotschi, T., Shi, T. M., Kelly, F. J., Cook, S., Burney, P., Forsberg, B., Gauderman, J. W., Hazenkamp, M. E., Heinrich, J., Jarvis, D., Norback, D., Payo-Losa, F., Poli, A., Sunyer, J., and Borm, P. J. A.: Comparison of oxidative properties, light absorbance, and total and elemental mass concentration of ambient PM2.5 collected at 20 European sites, Environ Health Persp, 114, 684-690, 2006.

Lakey, P. S. J., Berkemeier, T., Tong, H. J., Arangio, A. M., Lucas, K., Poschl, U., and Shiraiwa, M.: Chemical exposure-response relationship between air pollutants and reactive oxygen species in the human respiratory tract, Sci Rep-Uk, 6, 2016.

Landreman, A. P., Shafer, M. M., Hemming, J. C., Hannigan, M. P., and Schauer, J. J.: A macrophage-based method for the assessment of the reactive oxygen species (ROS) activity of atmospheric particulate matter (PM) and application to routine (daily-24 h) aerosol monitoring studies, Aerosol Science and Technology, 42, 946-957, 2008.

Li, N., Hao, M. Q., Phalen, R. F., Hinds, W. C., and Nel, A. E.: Particulate air pollutants and asthma - A paradigm for the role of oxidative stress in PM-induced adverse health effects, Clin Immunol, 109, 250-265, 2003a.

Li, N., Sioutas, C., Cho, A., Schmitz, D., Misra, C., Sempf, J., Wang, M. Y., Oberley, T., Froines, J., and Nel, A.: Ultrafine particulate pollutants induce oxidative stress and mitochondrial damage, Environ Health Persp, 111, 455-460, 2003b.

Li, Q., Shang, J., and Zhu, T.: Physicochemical characteristics and toxic effects of ozone-oxidized black carbon particles, Atmos Environ, 81, 68-75, 2013.

Li, Q. F., Wyatt, A., and Kamens, R. M.: Oxidant generation and toxicity enhancement of aged-diesel exhaust, Atmos Environ, 43, 1037-1042, 2009.

Lim, S. S., Vos, T., and Flaxman, A. D.: A comparative risk assessment of burden of disease and injury attributable to 67 risk factors and risk factor clusters in 21 regions, 1990-2010: a systematic analysis for the Global Burden of Disease Study 2010 (vol 380, pg 2224, 2012), Lancet, 381, 1276-1276, 2013.

Lin, P. and Yu, J. Z.: Generation of Reactive Oxygen Species Mediated by Humic-like Substances in Atmospheric Aerosols, Environmental Science & Technology, 45, 10362-10368, 2011.

Lippmann, M.: Toxicological and epidemiological studies of cardiovascular effects of ambient air fine particulate matter (PM2.5) and its chemical components: Coherence and public health implications, Crit Rev Toxicol, 44, 299-347, 2014.

Lodovici, M. and Bigagli, E.: Oxidative Stress and Air Pollution Exposure, J Toxicol, doi: Artn 48707410.1155/2011/487074, 2011. 2011.

Maikawa, C. L., Weichenthal, S., Wheeler, A. J., Dobbin, N. A., Smargiassi, A., Evans, G., Liu, L., Goldberg, M. S., and Pollitt, K. J. G.: Particulate Oxidative Burden as a Predictor of Exhaled Nitric Oxide in Children with Asthma, Environ Health Persp, 124, 1616-1622, 2016.

McWhinney, R. D., Badali, K., Liggio, J., Li, S. M., and Abbatt, J. P. D.: Filterable Redox Cycling Activity: A Comparison between Diesel Exhaust Particles and Secondary Organic Aerosol Constituents, Environ Sci Technol, 47, 3362-3369, 2013.

McWhinney, R. D., Gao, S. S., Zhou, S. M., and Abbatt, J. P. D.: Evaluation of the Effects of Ozone Oxidation on Redox-Cycling Activity of Two-Stroke Engine Exhaust Particles, Environ Sci Technol, 45, 2131-2136, 2011.

Meyer, M. B., Patashnick, H., Ambs, J. L., and Rupprecht, E.: Development of a sample equilibration system for the TEOM continuous PM monitor, J Air Waste Manage, 50, 1345-1349, 2000.

Miljevic, B., Hedayat, F., Stevanovic, S., Fairfull-Smith, K. E., Bottle, S. E., and Ristovski, Z. D.: To Sonicate or Not to Sonicate PM Filters: Reactive Oxygen Species Generation Upon Ultrasonic Irradiation, Aerosol Sci Tech, 48, 1276-1284, 2014.

Mudway, I. S., Stenfors, N., Duggan, S. T., Roxborough, H., Zielinski, H., Marklund, S. L., Blomberg, A., Frew, A. J., Sandstrom, T., and Kelly, F. J.: An in vitro and in vivo investigation of the effects of diesel exhaust on human airway lining fluid antioxidants, Arch Biochem Biophys, 423, 200-212, 2004.

Nel, A.: Air pollution-related illness: effects of particles (vol 308, pg 804, 2005), Science, 309, 1326-1326, 2005.

Netto, L. E. S. and Stadtman, E. R.: The iron-catalyzed oxidation of dithiothreitol is a biphasic process: Hydrogen peroxide is involved in the initiation of a free radical chain of reactions, Arch Biochem Biophys, 333, 233-242, 1996.

Norris, G., YoungPong, S. N., Koenig, J. Q., Larson, T. V., Sheppard, L., and Stout, J. W.: An association between fine particles and asthma emergency department visits for children in Seattle, Environ Health Persp, 107, 489-493, 1999.

Ovrevik, J.: Oxidative Potential Versus Biological Effects: A Review on the Relevance of Cell-Free/Abiotic Assays as Predictors of Toxicity from Airborne Particulate Matter, Int J Mol Sci, 20, 2019.

Pietrogrande, M. C., Bertoli, I., Manarini, F., and Russo, M.: Ascorbate assay as a measure of oxidative potential for ambient particles: Evidence for the importance of cell-free surrogate lung fluid composition, Atmos Environ, 211, 103-112, 2019.

Pinto, J. P., Lefohn, A. S., and Shadwick, D. S.: Spatial variability of PM2.5 in urban areas in the United States, J Air Waste Manage, 54, 440-449, 2004.

Pizzino, G., Irrera, N., Cucinotta, M., Pallio, G., Mannino, F., Arcoraci, V., Squadrito, F., Altavilla, D., and Bitto, A.: Oxidative Stress: Harms and Benefits for Human Health, Oxid Med Cell Longev, doi: Artn 841676310.1155/2017/8416763, 2017. 2017.

Pope, C. A.: Particulate Air-Pollution and Human Health - Assessment of the Epidemiology, Inhal Toxicol, 7, 749-752, 1995.

Pope, C. A. and Dockery, D. W.: Health effects of fine particulate air pollution: Lines that connect, J Air Waste Manage, 56, 709-742, 2006.

Pope, C. A., Burnett, R. T., Thurston, G. D., Thun, M. J., Calle, E. E., Krewski, D., and Godleski, J. J.: Cardiovascular mortality and long-term exposure to particulate air pollution - Epidemiological evidence of general pathophysiological pathways of disease, Circulation, 109, 71-77, 2004.

Prahalad, A. K., Inmon, J., Dailey, L. A., Madden, M. C., Ghio, A. J., and Gallagher, J. E.: Air pollution particles mediated oxidative DNA base damage in a cell free system and in human airway epithelial cells in relation to particulate metal content and bioreactivity, Chem Res Toxicol, 14, 879-887, 2001.

Samet, J. M., Dominici, F., Curriero, F. C., Coursac, I., and Zeger, S. L.: Fine particulate air pollution and mortality in 20 US Cities, 1987-1994., New Engl J Med, 343, 1742-1749, 2000.

Sarnat, J. A.: Fine Particle Sources and Cardiorespiratory Morbidity: An Application of Chemical Mass Balance and Factor Analytical Source Apportionment Methods, Epidemiology, 19, S44-S44, 2008.

Schwarze, P. E., Ovrevik, J., Lag, M., Refsnes, M., Nafstad, P., Hetland, R. B., and Dybing, E.: Particulate matter properties and health effects: consistency of epidemiological and toxicological studies, Hum Exp Toxicol, 25, 559-579, 2006.

Shi, T., Knaapen, A. M., Begerow, J., Birmili, W., Borm, P. J. A., and Schins, R. P. F.: Temporal variation of hydroxyl radical generation and 8-hydroxy-2 '-deoxyguanosine formation by coarse and fine particulate matter, Occup Environ Med, 60, 315-321, 2003a.

Shi, T. M., Schins, R. P. F., Knaapen, A. M., Kuhlbusch, T., Pitz, M., Heinrich, J., and Borm, P. J. A.: Hydroxyl radical generation by electron paramagnetic resonance as a new method to monitor ambient particulate matter composition, J Environ Monitor, 5, 550-556, 2003b.

Shiraiwa, M., Selzle, K., and Poschl, U.: Hazardous components and health effects of atmospheric aerosol particles: reactive oxygen species, soot, polycyclic aromatic compounds and allergenic proteins, Free Radical Res, 46, 927-939, 2012.

Sorensen, M., Daneshvar, B., Hansen, M., Dragsted, L. O., Hertel, O., Knudsen, L., and Loft, S.: Personal PM2.5 exposure and markers of oxidative stress in blood, Environ Health Persp, 111, 161-165, 2003.

Squadrito, G. L., Cueto, R., Dellinger, B., and Pryor, W. A.: Quinoid redox cycling as a mechanism for sustained free radical generation by inhaled airborne particulate matter, Free Radical Bio Med, 31, 1132-1138, 2001.

Strak, M., Janssen, N. A. H., Godri, K. J., Gosens, I., Mudway, I. S., Cassee, F. R., Lebret, E., Kelly, F. J., Harrison, R. M., Brunekreef, B., Steenhof, M., and Hoek, G.: Respiratory Health Effects of Airborne Particulate Matter: The Role of Particle Size, Composition, and Oxidative Potential-The RAPTES Project, Environ Health Persp, 120, 1183-1189, 2012.

Strickland, M. J., Darrow, L. A., Klein, M., Flanders, W. D., Sarnat, J. A., Waller, L. A., Sarnat, S. E., Mulholland, J. A., and Tolbert, P. E.: Short-term Associations between Ambient Air Pollutants and Pediatric Asthma Emergency Department Visits, Am J Resp Crit Care, 182, 307-316, 2010.

Sullivan, A. P. and Weber, R. J.: Chemical characterization of the ambient organic aerosol soluble in water: 1. Isolation of hydrophobic and hydrophilic fractions with a XAD-8 resin, J Geophys Res-Atmos, 111, 2006.

Sun, Q. H., Hong, X. R., and Wold, L. E.: Cardiovascular Effects of Ambient Particulate Air Pollution Exposure, Circulation, 121, 2755-2765, 2010.

Tao, F., Gonzalez-Flecha, B., and Kobzik, L.: Reactive oxygen species in pulmonary inflammation by ambient particulates, Free Radical Bio Med, 35, 327-340, 2003.

Thurston, G. D., Kipen, H., Annesi-Maesano, I., Balmes, J., Brook, R. D., Cromar, K., De Matteis, S., Forastiere, F., Forsberg, B., Frampton, M. W., Grigg, J., Heederik, D., Kelly, F. J., Kuenzli, N., Laumbach, R., Peters, A., Rajagopalan, S. T., Rich, D., Ritz, B., Samet, J. M., Sandstrom, T., Sigsgaard, T., Sunyer, J., and Brunekreef, B.: A joint ERS/ATS policy statement: what constitutes an adverse health effect of air pollution? An analytical framework, Eur Respir J, 49, 2017.

Tuet, W. Y., Chen, Y. L., Xu, L., Fok, S., Gao, D., Weber, R. J., and Ng, N. L.: Chemical oxidative potential of secondary organic aerosol (SOA) generated from the photooxidation of biogenic and anthropogenic volatile organic compounds, Atmos Chem Phys, 17, 839-853, 2017.

Tuet, W. Y., Fok, S., Verma, V., Rodriguez, M. S. T., Grosberg, A., Champion, J. A., and Ng, N. L.: Dose-dependent intracellular reactive oxygen and nitrogen species (ROS/RNS) production from particulate matter exposure: comparison to oxidative potential and chemical composition, Atmospheric Environment, 144, 335-344, 2016.

Turpin, B. J. and Lim, H. J.: Species contributions to PM2.5 mass concentrations: Revisiting common assumptions for estimating organic mass, Aerosol Sci Tech, 35, 602-610, 2001.

Venkatachari, P. and Hopke, P. K.: Development and laboratory testing of an automated monitor for the measurement of atmospheric particle-bound reactive oxygen species (ROS), Aerosol Sci Tech, 42, 629-635, 2008.

Venkatachari, P., Hopke, P. K., Grover, B. D., and Eatough, D. J.: Measurement of particle-bound reactive oxygen species in rubidoux aerosols (vol 50, pg 49, 2005), J Atmos Chem, 52, 325-326, 2005.

Verma, V., Fang, T., Guo, H., King, L., Bates, J. T., Peltier, R. E., Edgerton, E., Russell, A. G., and Weber, R. J.: Reactive oxygen species associated with water-soluble PM2.5 in the southeastern United States: spatiotemporal trends and source apportionment, Atmos Chem Phys, 14, 12915-12930, 2014.

Verma, V., Fang, T., Xu, L., Peltier, R. E., Russell, A. G., Ng, N. L., and Weber, R. J.: Organic aerosols associated with the generation of reactive oxygen species (ROS) by water-soluble PM2.5, Environ Sci Technol, 49, 4646-4656, 2015a.

Verma, V., Ning, Z., Cho, A. K., Schauer, J. J., Shafer, M. M., and Sioutas, C.: Redox activity of urban quasi-ultrafine particles from primary and secondary sources, Atmos Environ, 43, 6360-6368, 2009a.

Verma, V., Polidori, A., Schauer, J. J., Shafer, M. M., Cassee, F. R., and Sioutas, C.: Physicochemical and Toxicological Profiles of Particulate Matter in Los Angeles during the October 2007 Southern California Wildfires, Environ Sci Technol, 43, 954-960, 2009b.

Verma, V., Rico-Martinez, R., Kotra, N., King, L., Liu, J., Snell, T. W., and Weber, R. J.: Contribution of water-soluble and insoluble components and their hydrophobic/hydrophilic subfractions to the reactive oxygen species-generating potential of fine ambient aerosols, Environ Sci Technol, 46, 11384-11392, 2012.

Verma, V., Wang, Y., El-Afifi, R., Fang, T., Rowland, J., Russell, A. G., and Weber, R. J.: Fractionating ambient humic-like substances (HULIS) for their reactive oxygen species activity - Assessing the importance of quinones and atmospheric aging, Atmos Environ, 120, 351-359, 2015b.

Vidrio, E., Jung, H., and Anastasio, C.: Generation of hydroxyl radicals from dissolved transition metals in surrogate lung fluid solutions, Atmos Environ, 42, 4369-4379, 2008.

Wang, D. B., Pakbin, P., Shafer, M. M., Antkiewicz, D., Schauer, J. J., and Sioutas, C.: Macrophage reactive oxygen species activity of water-soluble and water-insoluble fractions of ambient coarse, PM2.5 and ultrafine particulate matter (PM) in Los Angeles, Atmos Environ, 77, 301-310, 2013.

Wang, S. Y., Ye, J. H., Soong, R., Wu, B., Yu, L. G., Simpson, A. J., and Chan, A. W. H.: Relationship between chemical composition and oxidative potential of secondary organic aerosol from polycyclic aromatic hydrocarbons, Atmos Chem Phys, 18, 3987-4003, 2018.

Weber, R.: Short-term temporal variation in PM2.5 mass and chemical composition during the Atlanta supersite experiment, 1999, J Air Waste Manage, 53, 84-91, 2003.

Wei, J. L., Yu, H. R., Wang, Y. X., and Verma, V.: Complexation of Iron and Copper in Ambient Particulate Matter and Its Effect on the Oxidative Potential Measured in a Surrogate Lung Fluid, Environ Sci Technol, 53, 1661-1671, 2019.

Weichenthal, S., Crouse, D. L., Pinault, L., Godri-Pollitt, K., Lavigne, E., Evans, G., van Donkelaar, A., Martin, R. V., and Burnett, R. T.: Oxidative burden of fine particulate air pollution and risk of cause-specific mortality in the Canadian Census Health and Environment Cohort (CanCHEC), Environ Res, 146, 92-99, 2016a.

Weichenthal, S., Lavigne, E., Evans, G., Pollitt, K., and Burnett, R. T.: Ambient PM2.5 and risk of emergency room visits for myocardial infarction: impact of regional PM2.5 oxidative potential: a case-crossover study, Environ Health-Glob, 15, 2016b.

Weichenthal, S. A., Lavigne, E., Evans, G. J., Pollitt, K. J. G., and Burnett, R. T.: Fine Particulate Matter and Emergency Room Visits for Respiratory Illness Effect Modification by Oxidative Potential, Am J Resp Crit Care, 194, 577-586, 2016c.

Wilson, J. G., Kingham, S., Pearce, J., and Sturman, A. P.: A review of intraurban variations in particulate air pollution: Implications for epidemiological research, Atmos Environ, 39, 6444-6462, 2005.

Xu, L., Suresh, S., Guo, H., Weber, R. J., and Ng, N. L.: Aerosol characterization over the southeastern United States using high-resolution aerosol mass spectrometry: spatial and seasonal variation of aerosol composition and sources with a focus on organic nitrates, Atmos Chem Phys, 15, 7307-7336, 2015.

Yang, A., Janssen, N. A. H., Brunekreef, B., Cassee, F. R., Hoek, G., and Gehring, U.: Children's respiratory health and oxidative potential of PM2.5: the PIAMA birth cohort study, Occup Environ Med, 73, 154-160, 2016.

Yang, A., Jedynska, A., Hellack, B., Kooter, I., Hoek, G., Brunekreef, B., Kuhlbusch, T. A. J., Cassee, F. R., and Janssen, N. A. H.: Measurement of the oxidative potential of PM2.5 and its constituents: The effect of extraction solvent and filter type, Atmospheric Environment, 83, 35-42, 2014.

Ye, D. N., Klein, M., Chang, H. H., Sarnat, J. A., Mulholland, J. A., Edgerton, E. S., Winquist, A., Tolbert, P. E., and Sarnat, S. E.: Estimating Acute Cardiorespiratory Effects of Ambient Volatile Organic Compounds, Epidemiology, 28, 197-206, 2017.

Ye, D. N., Klein, M., Mulholland, J. A., Russell, A. G., Weber, R., Edgerton, E. S., Chang, H. H., Sarnat, J. A., Tolbert, P. E., and Sarnat, S. E.: Estimating Acute Cardiovascular Effects of Ambient PM2.5 Metals, Environ Health Persp, 126, 2018.

Yi, S., Zhang, F., Qu, F., and Ding, W. J.: Water-Insoluble Fraction of Airborne Particulate Matter (PM10) Induces Oxidative Stress in Human Lung Epithelial A549 Cells, Environ Toxicol, 29, 226-233, 2014.

Yu, H. R., Wei, J. L., Cheng, Y. L., Subedi, K., and Verma, V.: Synergistic and Antagonistic Interactions among the Particulate Matter Components in Generating Reactive Oxygen Species Based on the Dithiothreitol Assay, Environ Sci Technol, 52, 2261-2270, 2018.

Zhang, X., Hecobian, A., Zheng, M., Frank, N. H., and Weber, R. J.: Biomass burning impact on PM2.5 over the southeastern US during 2007: integrating chemically speciated FRM filter measurements, MODIS fire counts and PMF analysis, Atmos Chem Phys, 10, 6839-6853, 2010.

Zhang, X. L., Lin, Y. H., Surratt, J. D., Zotter, P., Prevot, A. S. H., and Weber, R. J.: Light-absorbing soluble organic aerosol in Los Angeles and Atlanta: A contrast in secondary organic aerosol, Geophys Res Lett, 38, 2011.

Zhou, Y. M., Zhong, C. Y., Kennedy, I. M., Leppert, V. J., and Pinkerton, K. E.: Oxidative stress and NF kappa B activation in the lungs of rats: a synergistic interaction between soot and iron particles, Toxicol Appl Pharm, 190, 157-169, 2003.

Zielinski, H., Mudway, I. S., Berube, K. A., Murphy, S., Richards, R., and Kelly, F. J.: Modeling the interactions of particulates with epithelial lining fluid antioxidants, Am J Physiol-Lung C, 277, L719-L726, 1999.

Zomer, B., Colle, L., Jedynska, A., Pasterkamp, G., Kooter, I., and Bloemen, H.: Chemiluminescent reductive acridinium triggering (CRAT)-mechanism and applications, Anal Bioanal Chem, 401, 2945-2954, 2011.